# MEMBRANES FOR FLUE GAS TREATMENT

## TRANSPORT BEHAVIOR OF WATER AND GAS IN HYDROPHILIC POLYMER MEMBRANES

# DISSERTATION

to obtain
the degree of doctor at the University of Twente,
on the authority of the rector magnificus,
prof. dr. H. Brinksma,
on account of the decision of the graduation committee,
to be publicly defended
on Friday the 30$^{th}$ of January 2009 at 13.15 hrs

by

## Jens Potreck

born on the 4$^{th}$ of September 1978

in Gronau/Westfalen, Germany

This dissertation has been approved by:


Promotor:             Prof. Dr.-Ing. M. Wessling


Assistant-promotor:    Dr. Ir. D.C. Nijmeijer

"If methodical investigation within every branch of learning is carried out in accord with moral norms, it never truly conflicts with faith."

Second Vatican Council, Constitution Gaudium et Spes


"Vorausgesetzt, dass die methodische Forschung in allen Wissensbereichen in einer wirklichen wissenschaftlichen Weise und gemäß den Normen der Sittlichkeit vorgeht, wird sie niemals in einen echten Konflikt mit dem Glauben kommen."

Zweites Vatikanisches Konzil, Konstitution Gaudium et Spes


Gewidmet meiner ganzen Familie, besonders meinem Opa Bruno

**Membranes for flue gas treatment**

Transport behavior of water and gas in hydrophilic polymer membranes

Ph.D. Thesis, University of Twente

# Contents

# Chapter 1

## Introduction

Industrial plants, the chemical industry, and fossil fuel fired power plants consume enormous quantities of water for power production and steam generation. At the same time, global water resources are limited and the production of safe drinking water becomes more and more difficult. More and more the focus moves to closed water management systems to save water. Dehydration of gaseous streams has become a main focus in many industrial applications, because of the huge amounts of water present in these streams. Fossil fuel fired power plants produce extremely large amounts of flue gasses which mainly contain $N_2$, $O_2$, and $CO_2$, and also significant amounts of water vapor [1]. The water vapor present in these flue gasses can condense on the walls of the stack and, together with the trace amounts of acidic impurities still present in the flue gas after treatment, causes corrosion and irreversible damages on the chimney [1]. Furthermore, large amounts of valuable water are emitted to the atmosphere. Water vapor removal of the flue gasses before emission to the atmosphere thus safes large amounts of water and reduces the energy costs, because it eliminates reheating of the flue gas stream to prevent condensation of water vapor in the stack [1].

Commercial dehydration processes such as the use of a condenser or a desiccant system have several disadvantages. The water produced in the condenser is relatively dirty and corrosive, while a desiccant system requires regeneration of the desiccant, which is an energy intensive process and generates low quality water.

Membrane technology is an attractive, energy efficient alternative for dehydration processes: it has a small footprint, it is easy to scale up, to implement and to operate, it is reliable (no moving parts) and it reduces the energy costs.

Transport through dense membranes occurs via the so-called solution-diffusion mechanism [2]. The gas molecules first dissolve in the dense polymer membrane and subsequently diffuse through the membrane. The product of solubility and diffusivity is the permeability.

The simplest description of gas diffusion through a dense membrane is Fick's Law [3]:

$$J = -D \cdot \frac{dc}{dx}$$

(1)

with J the flux through the membrane at standard temperature and pressure (cm³ (STP) /(cm²·s)), D is the diffusion coefficient (cm²/s) and dc/dx is the driving force for gas transport (e.g. the concentration gradient over the membrane).

Equation 2 can be integrated, assuming steady state conditions resulting in:

$$J_i = \frac{D_i \cdot (c_{i,0} - c_{i,l})}{l}$$

(2)

with $c_{i,0}$ and $c_{i,l}$ the concentrations of component i at the feed and the permeate side of the membrane [mol/cm³], respectively, l the thickness of the membrane [cm] and $D_i$ the diffusion coefficient of component i [cm²/s].
At low pressures, Henry's law directly relates the concentration of component i $c_i$ to its partial pressure $p_i$ [3].

$$c_i = S_i \cdot p_i$$

(3)

Where $S_i$ is the solubility coefficient of component i [cm³ (STP)/cm³·cmHg] and $p_i$ is the partial pressure of component i [cmHg]. Substitution of this Equation in Equation 2 and taking into account that te permeability P is the product of solubility and diffusivity, this generates the following equation for the flux of species i through a dense membrane:

$$J_i = \frac{P_i}{l} \cdot (p_{i,feed} - p_{i,permeate})$$

(4)

With $J_i$ the flux of component i through the membrane [$cm^3/(cm^2 \cdot s)$], $P_i$ the permeability of component i [$cm^3 \cdot cm/cm^2 \cdot s \cdot cmHg$], l is the thickness of the membrane [cm], and $p_{i,feed}$ and $p_{i,permeate}$ are the partial pressures of component i at the feed and permeate side of the membrane [cmHg] respectively.

This equation shows that the flux of component i through a dense membrane is proportional to the permeability of that component through the membrane and the partial pressure difference of component i over the membrane. It is inversely proportional to the thickness of the membrane [3]. (Due to swelling of the polymer material as a response to the dissolution of the water or gas molecules, the permeability coefficient can be a complex function of the feed gas characteristics (pressure, composition, relative humidity and temperature), which will be addressed later on in this thesis.)

Figure 1 and Table 1 show the molecular separation properties of several polymers available as potential membrane material for the dehydration of gas streams. The selectivity for water over nitrogen is shown as a function of water permeability at infinite diluted water activity.
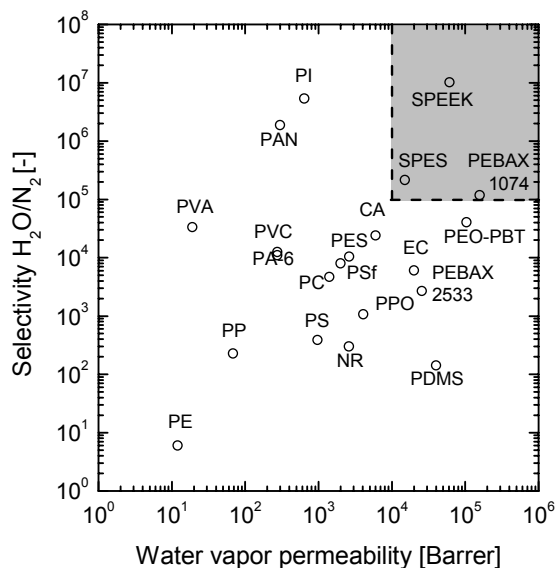


**Figure 1:** Water vapor permeability versus water vapor/$N_2$ selectivity of various polymeric membrane materials at 30°C. (Data obtained from Metz *et al.* [4], Nunes *et al.* [5] and Sijbesma *et al.* [1]).

**Table 1:** Water vapor permeability and water vapor over nitrogen selectivity for various polymers at 30°C.

| Polymer | Abbreviation | $H_2O$ permeability [Barrer] | $H_2O/N_2$ selectivity [-] | Reference |
|---|---|---|---|---|
| Poly ethylene | PE | 12 | 6 | [3, 6] |
| Poly amide 6 (Nylon 6) | PA-6 | 275 | 11000 | [3, 7] |
| Poly styrene | PS | 970 | 388 | [3, 6] |
| Sulfonated poly ether sulfone | S-PES | 15000 | 20000 | [8] |
| Poly ethylene oxide – poly amide | PEBAX® 1074 | 30000 | 100000 | [1] |
| Sulfonated poly ether ether ketone | S-PEEK | 61000 | 10000000 | [9] |
| Poly ethylene oxide – poly butylene terephtalate | PEO-PBT | 85500 | 40500 | [10] |

These data clearly show that especially sulfonated polymers (e.g. S-PEEK, S-PES) or commercially available hydrophilic PEO-based block copolymers (e.g. PEBAX® 1074) are attractive as potential membrane material for the dehydration of gas streams, because of their extremely high water vapor over nitrogen selectivities, combined with extremely high water vapor permeabilities. These three polymers are mentioned in the right upper corner of Figure 1. The molecular structure of S-PEEK and PEBAX® are presented in Figure 2.

a) PEBAX® 1074 (X = 0.55)
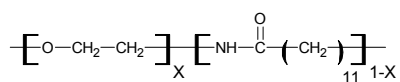
b) SPEEK (X = 0.59)
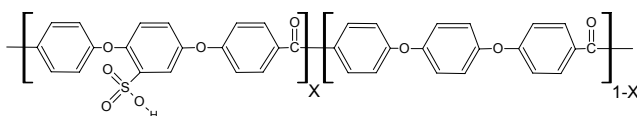
**Figure 2:** Chemical structure of a) PEBAX® and b) S-PEEK.

PEBAX® 1074 is a block copolymer consisting of 45% hard phase (1-X = poly amide 12, PA12) and 55% of soft phase (X = poly ethylene oxide, PEO) [11]. Permeation of gas

and water vapor preferentially occurs through the soft, hydrophilic PEO phase, whereas the hard PA12 phase provides the mechanical stability of the membrane material [11-18]. Sulfonated poly ether ether ketone (S-PEEK) can be obtained by sulfonation of poly ether ether ketone [19]. The degree of sulfonation is a measure for the amount of sulfonic acid groups per repeat unit and offers a method to tune especially the hydrophilicity of the polymers. Sulfonated polymers are extensively studied in especially fuel cell applications [20-22], but only a few papers report the use of S-PEEK as material for dehydration purposes. Liu *et al.* [9] and Wang *et al.* [23] publish their research on the sulfonation of PEEK and report some gas/water permeability data which proof that the sulfonation of polymers is an effective method to increase both the permeability of water vapor and the selectivity of water vapor over nitrogen.

## Scope of this thesis

The work presented in this thesis focuses on the characterization molecular transport properties of two of the polymeric materials shown in Figure 1: the segmented block-copolymer PEBAX 1074 and the sulfonated PEEK. The fundamental understanding of water vapor and gas transport phenomena through these materials is particularly interesting since both materials are different in their chemistry and physical state:

- PEBAX shows molecular transport through a soft rubbery phase based on polyethylene oxide
- S-PEEK shows transport through an amorphous glassy phase with ionic groups present which will preferentially hydrate over the apolar matrix.

The two polymeric systems may vary strongly in relation to polymer/vapor interactions, relaxation phenomena, and separation performance of the membranes.

**Chapter 2** investigates the sorption of water vapor in sulfonated poly ether ether ketones with different degrees of sulfonation. The kinetic sorption isotherms of water vapor in these polymers at 20°C are determined and analyzed and the relative contribution of Fickian diffusion and relaxational phenomena is determined using the Hopfenberg Berens model, which allows to analyze non-fickian diffusion behavior of gasses and vapors in glassy polymers.

**Chapter 3** presents a thermodynamic analysis of water vapor sorption in two hydrophilic polymers: sulfonated poly ether ether ketone (S-PEEK) and a commercially available block copolymer composed of poly ethylene oxide and polyamide (PEBAX® 1074). Sorption isotherms at four different temperatures are determined and the Gibbs free energy, the enthalpy and the entropy of water vapor sorption in these polymers are calculated. The results provide a more fundamental understanding of the water vapor sorption behavior in these hydrophilic polymers.

**Chapter 4** investigates the simultaneous permeation of water vapor and nitrogen through a PEBAX® 1074 membrane as a potential candidate for flue gas dehydration. The influence of water vapor activity and temperature on the water vapor and gas transport is investigated and the water vapor over nitrogen selectivity is calculated. Kinetic water vapor sorption measurements are performed and analyzed to determine the Fickian diffusion coefficient of water in the polymer.

**Chapter 5** describes the controlled humidification of gas streams using membrane assisted gas absorption. Composite hollow fiber membranes with a dense top layer of sulfonated poly (ether ether ketone) are characterized with respect to the obtained relative humidity of the gas stream and the water vapor flux through the membrane as a function of temperature and gas flow rate. Membrane assisted gas humidification generates humidified gas streams with extremely high purities, making it especially interesting for applications where high purities are required (e.g. fuel cells, the semiconductor industry and in medical systems).

**Chapter 6** presents the development of porous, hydrophilic S-PEEK structures via the phase inversion process and investigates the effect of different types of non-solvent on the formation of macro void free porous structures.

**Chapter 7** summarizes the main conclusions of the work described in this thesis and gives an outlook for future work, especially focusing on the removal of water vapor and the capture of $CO_2$ from gas streams.

# References

1.  H. Sijbesma, K. Nymeijer, R. van Marwijk, R. Heijboer, J. Potreck, M. Wessling, Flue gas dehydration using polymer membranes, Journal of Membrane Science 313 (2008) 263-276.

2.  J.G. Wijmans, R.W. Baker, The solution-diffusion model - a review, Journal of Membrane Science 107 (1995) 1-21.

3.  M.H.V. Mulder, Basic principles of membrane technology, Kluwer Academic Publisher Dordrecht, 1996.

4.  S.J. Metz, W.J.C. van de Ven, J. Potreck, M.H.V. Mulder, M. Wessling, Transport of water vapor and inert gas mixtures through highly selective and highly permeable polymer membranes, Journal of Membrane Science 251 (2005) 29-41.

5.  S.P. Nunes, K.V. Peinemann, Membrane technology in the chemical industry, Wiley-VCH Weinheim, 2001.

6.  J.A. Barrie, G.S. Crank, Diffusion in polymers, Academic Press 1968.

7.  M.S. Allen, M. Fujji, V. Stannet, H.B. Hopfenberg, J.L. Williams, The barrier properties of polyacrylonitrile, Journal of Membrane Science 2 (1977) 153-164.

8.  L. Jia, X. Xu, H. Zhang, J. Xu, Permeation of nitrogen and water vapor through sulfonated polyetherethersulfone membrane, Journal of Polymer Science Part B-Polymer Physics 35 (1997) 2133-2140.

9.  S. Liu, F. Wang, T. Chen, Synthesis of poly(ether ether ketone)s with high content of sodium sulfonate groups as gas dehumidification membrane materials, Macromolecular Rapid Communications 22 (2001) 579-582.

10. S. Metz, M. Mulder, M. Wessling, Gas-permeation properties of poly(ethylene oxide) poly(butylene terephthalate) block copolymers, Macromolecules 37 (2004) 4590-4597.

11. V.I. Bondar, B.D. Freeman, I. Pinnau, Gas transport properties of poly(ether-b-amide) segmented block copolymers, Journal of Polymer Science: Part B-Polymer Physics 38 (2000) 2051-2062.

12. V. Barbi, S.S. Funari, R. Gehrke, N. Scharnagl, N. Stribeck, SAXS and the gas transport in polyether-block-polyamide copolymer membranes, Macromolecules 36 (2003) 749-758.

13. V.I. Bondar, B.D. Freeman, I. Pinnau, Gas sorption and characterization of poly(ether-b-amide) segmented block copolymers, Journal of Polymer Science Part B-Polymer Physics 37 (1999) 2463-2475.

14. Y. Cen, C. Staudt-Bickel, R.N. Lichtenthaler, Soprtion properties of organic solvents in PEBA membranes, Journal of Membrane Science 206 (2002) 341-349.

15. J.H. Kim, S.Y. Ha, Y.M. Lee, Gas permeation of poly(amide-6-b-ethylene oxide) copolymer, Journal of Membrane Science 190 (2001) 179-193.

16. J.H. Kim, Y.M. Lee, Gas permeation properties of poly(amide-6-b-ethylene oxide)-silica hybrid membranes, Journal of Membrane Science 193 (2001) 209-225.

17. L. Liu, A. Chakma, X. Feng, Preparation of hollow fiber poly(ether block amide)/polysulfone composite membranes for separation of carbon dioxide from nitrogen, Chemical Engineering Journal 105 (2004) 43-51.

18. M.E. Rezac, T. John, P.H. Pfromm, Effect of copolymer composition on the solubility and diffusivity of water and methanol in a series of polyether amides, Journal of Applied Polymer Sience 65 (1997) 1983-1993.

19. E.N. Komkova, M. Wessling, J. Krol, H. Strathmann, N.P. Berezina, Influence of the nature off polymer matrix and the degree of sulfonation on the properties of membranes, Polymer Science Series A 43 (2001) 300-307.

20. M. Gil, X.L. Ji, X.F. Li, H. Na, J.E. Hampsey, Y.F. Lu, Direct synthesis of sulfonated aromatic poly(ether ether ketone) proton exchange membranes for fuel cell applications, Journal of Membrane Science 234 (2004) 75-81.

21. S. Vetter, B. Ruffmann, I. Buder, S.R. Nunes, Proton conductive membranes of sulfonated poly(ether ketone ketone), Journal of Membrane Science 260 (2005) 181-186.

22. P.X. Xing, G.P. Robertson, M.D. Guiver, S.D. Mikhailenko, K.P. Wang, S. Kaliaguine, Synthesis and characterization of sulfonated poly(ether ether ketone)

for proton exchange membranes, Journal of Membrane Science 229 (2004) 95-106.

23.     F. Wang, T.L. Chen, J.P. Xu, Synthesis of poly(ether ether ketone) containing sodium sulfonate groups as gas dehumidification membrane material, Macromolecular Rapid Communications 19 (1998) 135-137.

# Chapter 2

# Sorption induced relaxations during water diffusion in S-PEEK

## Abstract

This paper presents an analysis of the sorption kinetics of water vapor and liquid water in the glassy polymer sulfonated poly ether ether ketone (S-PEEK). Sorption isotherms are determined experimentally using a gravimetric sorption balance, and the relative contributions of Fickian diffusion and relaxational phenomena are quantified as a function of the water concentration in the polymer using the model of Hopfenberg and Berens.

Analysis of the sorption isotherms and determination of the sorption kinetics proof the occurrence of both Fickian sorption behavior and relaxational phenomena already at very low water concentrations in the polymer. With increasing water concentration, the relative importance of relaxation phenomena increases, whereas the relative contribution of Fickian diffusion decreases.

Based on the water vapor sorption kinetics only, the Fickian diffusion coefficient increases over two orders of magnitude with increasing water vapor concentration. Taking also the diffusion kinetics from liquid water sorption experiments into account reveals a change of even three orders of magnitude of the Fickian diffusion coefficient when the water concentration in the polymer increases.

# Introduction

The removal of water vapor from gas streams is an important industrial operation and many applications can be found in e.g. the dehydration of flue gases [1], the drying of compressed air [2] and the storage of fruits and vegetables under protective atmosphere [3]. Membrane technology using polymeric membranes is a promising and attractive method for dehydration purposes: it has a small footprint, it is energy efficient and it is easy to implement and operate. In general, polymeric membranes used for such processes have a dense separating layer and water transport occurs through dissolution and diffusion [4]. Often, hydrophobic membranes are used for air humidification control [5, 6], but membranes based hydrophilic polymers gain increasing interest as gas humidification membrane [1, 7-9]. Hydrophilic polymers absorb high amounts of water and therefore enhance the transport of water which is governed by diffusivity and solubility [10, 11]. However, sorption of water renders the physical properties of the polymer (e.g. the glass transition temperature and the degree of swelling, which results in changes in solubility and diffusivity of the penetrant [12]) and makes transport highly concentration dependent. Sorption phenomena and transport properties of water in polymeric materials are complex and their understanding is of major importance.

We recently demonstrated that a membrane based on sulfonated poly (ether ether ketone) (S-PEEK) shows excellent transport properties in terms of both permeability of water vapor and selectivity of water vapor over nitrogen [1]. However, very little is known about the fundamental properties and kinetics of diffusion and solubility of water (vapor) in this polymer. In the present work, we analyze the kinetic sorption behavior of water vapor in polymeric films of the glassy polymer S-PEEK. It is known that the sorption of penetrant molecules in a glassy polymer can induce strong plasticization effects [13-16] . Next to Fickian diffusion on a short time scale, long time scale relaxations can be observed [16]. Equilibrium is not reached due to the glassy state of the polymer. Penetrant sorption induces a depression of the glass transition temperature of the polymer [12, 17]. Such observations are extensively described for the sorption of carbon dioxide in glassy polymers, however very little systematic experiments are performed for water transport in such ionomeric materials.

# Theoretical background

*Water vapor sorption kinetics*

Transport of gases and vapors in dense, glassy polymer membranes is determined by the solubility and diffusivity of these components in the polymer. According to this so called solution-diffusion mechanism, the solute first dissolves in the polymer and subsequently diffuses through the polymer along a concentration gradient [4].

The sorption kinetics of highly sorbing gases and vapors (e.g. water vapor) into glassy polymers can be complex. During sorption, not only Fickian sorption behavior can occur, but next to that, additional mass uptake due to complex non Fickian relaxation phenomena may be observed [16, 18-21]. Fickian transport behavior is a rapid, elastic and reversible process, whereas non Fickian transport involves relaxational motions on a much longer time scale. Hopfenberg and Berens [22] proposed that the overall non-Fickian sorption behavior of a penetrant in a polymer matrix $(M(t)_{total})$ can be considered as the sum of two different sorption regimes: A Fickian sorption regime $(M(t)_F)$ and a relaxational regime $(M(t)_R)$:

$$M(t)_{total} = M(t)_F + M(t)_R \tag{1}$$

Crank [23] showed that the mass uptake in time due to ideal Fickian sorption of a penetrant in a polymer matrix $(M(t)_F)$ can be described as a function of the square root of time, assuming a constant diffusion coefficient:

$$\frac{M(t)}{M_\infty} = 1 - \frac{8}{\pi^2} \sum_{m=0}^{\infty} \frac{1}{(2m+1)^2} \exp\left\{ -\frac{D(2m+1)^2 \cdot \pi^2 \cdot t}{L^2} \right\} \tag{2}$$

Where $M(t)$ [g] is the total amount of vapor absorbed by the polymer at time t [s], $M_\infty$ [g] is the equilibrium sorption mass, D is the diffusion coefficient [$cm^2$/s] and L is the

polymer film thickness [cm]. The Fickian diffusion coefficient can thus be easily determined from a fit of this equation through the experimentally determined sorption data.

The relaxational contribution to non-Fickian sorption can be described as a series of relaxational regimes, of which each can be characterized by its specific relaxation time constant $\tau_R$. Because according to the Hopfenberg-Berens model, non Fickian diffusion can be considered as the sum of the occurrence of a Fickian sorption regime and relaxational regimes, Equation 3 can be derived to describe the overall sorption process:

$$\frac{M(t)}{M_\infty} = M_{F,\infty}\left[1 - \frac{8}{\pi^2}\sum_{m=0}^{\infty}\frac{1}{(2m+1)^2}\right]\exp\left\{-\frac{D(2m+1)^2\cdot\pi^2\cdot t}{L^2}\right\}$$
$$+ \sum_{i=1}^{\infty}M_{R_i}\left[1 - \exp\left\{-\frac{t}{\tau_{R_i}}\right\}\right] \tag{3}$$

Where $M_{F,\infty}$ [g] and $M_{Ri}$ [g] represent the infinite sorbed mass of the Fickian part and the relaxation part of sorption respectively, and $\tau_{Ri}$ [s] is the characteristic time constant for relaxation.

The diffusion-relaxation model can only be used to determine the contribution of Fickian diffusion and that of relaxational diffusion, when the diffusion contribution and the relaxation contribution are very well separated, e.g. it requires the diffusion rate to be much higher than the rate of relaxation phenomena.

Relaxational contributions in glassy polymers can be considered to be independent of the dimensions of the polymer film. Diffusion phenomena on the other hand, depend on the square of the length of the diffusion path way and thus the film thickness. The film thickness therefore determines to a large extend if a well defined diffusion and relaxation profile can be distinguished or if both phenomena overlap. To have a well-separated diffusion and relaxation regime, one desires the use of thinner films. Thinner films,

however, have much lower the time scales for diffusion, thus limiting an accurate determination of the diffusion coefficient because the rapid weight uptake can not be measured accurately. Proper choice of the film thickness is thus extremely important when analyzing diffusion and relaxation data [16].

The Deborah number for diffusion $(DEB)_D$ quantifies the ratio of the relative magnitude of the rates of diffusion and relaxation [24]:

$$(DEB)_D = \frac{\tau_R \cdot D}{L_0^2} \tag{4}$$

In this Equation, $\tau_R$ (s) is the characteristic relaxation time and $L_0^2/D$ is the characteristic diffusion time ($L_0$ is the sample thickness (cm) and D is the diffusion coefficient ($cm^2$/s)). If the Deborah number is >> 1, the rate of diffusion is much faster than the rate of the relaxations, while for DEB = 1, the rates of diffusion and relaxation are equal, resulting in a superposition of the two processes. When the Deborah number is smaller than unity, the rate of relaxation is faster than that of diffusion.

Wessling *et al.* [25] used the proposed model to analyze the experimentally determined sorption-induced dilation kinetics of $CO_2$ in a polymer film and related the fast dilation kinetics to reversible Fickian relaxation, whereas the slower dilation kinetics could be related to irreversible relaxational phenomena. They proved that it is often sufficient to fit the data with the sum of the Fickian diffusion contribution and two additional relaxation contributions. Visser *et al.* [16] used this diffusion–relaxation model to quantify the separate contributions of diffusion and relaxation phenomena for different gasses in a glassy polyimide Matrimid film. The work demonstrated that any gas shows a Fickian and a relaxational contribution, and may thus induce relaxational changes into the polymer matrix upon reaching a critical amount of volume dilation.

During gas or vapor sorption, the molecular structure of the polymer film can change due to relaxational changes, and this may have an influence on the material properties as well [26]. An important material property in relation to vapor sorption and relaxational effects

is the glass transition temperature ($T_g$), which characterizes the transition of a polymer from its glassy state to its rubbery state. The Fox equation can be used to calculate the theoretical effect of the presence of water vapor inside the polymer on its glass transition temperature [27]:

$$\frac{1}{T_g} = \frac{W_w}{T_{g,w}} + \frac{W_p}{T_{g,p}} \qquad (5)$$

Where $T_g$ [K] is the glass transition temperature of the water/polymer mixture, $T_{g,w}$ [K] and $T_{g,p}$ [K] are the glass transition temperatures of the water and the polymer respectively and $W_w$ [-] and $W_p$ [-] are the weight fractions of the water and the polymer, respectively. Francis *et al.* [27] showed that the theoretical values of the glass transition temperature calculated from the Fox equation are maximum 5% higher than the experimental values, making the Fox equation a valuable tool to estimate the glass transition temperature of a water swollen polymer.

# Experimental part

## *Membrane preparation*

S-PEEK (Figure 1) was prepared by sulfonation of 60 g of PEEK, supplied by Victrex (USA), according to the procedure earlier described by Komkova *et al.* [28]. The reaction was performed in 1 l sulfuric acid (concentration 95-97 %) at ambient temperature (25°C) under continuous stirring. When the desired sulfonation degree was reached, the polymer was precipitated in ice water and washed until pH 6-7. After that, the polymer was dried under nitrogen atmosphere at 60°C for three days. To remove residual water, the sulfonated polymer was further dried in a 30°C vacuum oven until its mass was constant.
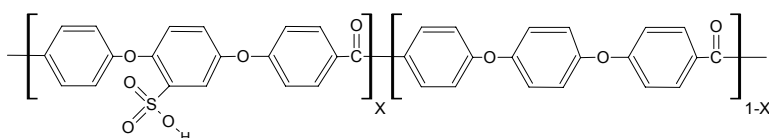


**Figure 1:** Chemical structure of sulfonated poly ether ether ketone (S-PEEK).

Membranes were cast on a glass plate from a 15 wt.% solution of S-PEEK in N-methyl-2-pyrrolidon (NMP) supplied by Acros Organics, with a 0.47 mm casting knife. After evaporation of the NMP in nitrogen atmosphere, the film was removed from the glass plate by immersion in demineralized water. The film was washed in ultra pure water for 3 days and the washing water was refreshed twice a day. Subsequently the film was dried under nitrogen atmosphere at 60°C for four days. Further drying was performed in a 30°C vacuum oven until the mass of the film was constant (~10 days). The final thickness of the obtained films was measured with a digital screw micrometer. For the sorption measurements, sulfonated PEEK with a sulfonation degree of 59 and 75% was used.

After this treatment, the films are considered to be dry. Nevertheless, this does not imply all water molecules are removed from the 'dry' sample. Complete removal of water would require treatment of the film under harsh conditions at temperatures at which degradation and cross linking occur. For this reason, the measured water vapor sorption data are the values obtained relative to the amount of water molecules still present in the

'dry' polymer. However, the amount of water molecules still present after drying is much smaller than the additional amount of water molecules due to water sorption. This, combined with the fact that the films are all treated in exactly the same way, allows us to draw conclusions from these sorption measurements without taking into account the presence of water molecules in the 'dry' film.

*Sorption experiments*

Water vapor sorption experiments were carried out using a gravimetric sorption balance (SGA-CX Symmetrical gravimetric analyzer from VTI (USA) supplied by Ankersmid (The Netherlands)). The membrane sample (weight ~3mg, thickness ~ 40 μm) was placed in the apparatus and flushed for 24 hours with dry nitrogen to remove any residues. The final dry weight of the sample was measured. Subsequently a wet nitrogen stream (saturated with Milli-Q water ((18.2 MΩ·cm at 25°C)) was mixed with a dry nitrogen stream to obtain the desired water vapor activity. The water vapor activity in the gas stream is defined as the ratio of the water vapor pressure at a certain temperature and the maximum water vapor pressure at that temperature. It can be instantaneously changed by varying the mixing ratio of the dry and the wet nitrogen flow. The activity of the gas stream was varied from 0 to 0.99.

The humidified gas stream was fed into the thermo stated measuring chamber and the actual activity in the sample chamber was measured and controlled with a dew point mirror. The total gas flow velocity was kept constant to avoid any upward drag force on the sample. The weight of the sample in time was monitored continuously. Sorption and desorption experiments were carried out at 20°C and the sorption and desorption isotherms were constructed from a stepwise or interval increase or decrease of the water vapor activity [29]. The concentration of water vapor inside the polymer film [cm$^3$ STP/cm$^3$ polymer] was calculated from the equilibrium mass uptake of the sample at a certain water vapor activity using Equation 6:

$$c = \frac{\left(M_\infty - M_{polymer,dry}\right) \cdot V_{H_2O}}{V_{polymer,dry} \cdot M_{w,H_2O}} \tag{6}$$

where $M_\infty$ [g] is the equilibrium mass of the polymer sample and the absorbed water at a certain water vapor activity, $M_{polymer,dry}$ [g] is the dry weight of the polymer, $V_{H2O}$ [22414 cm$^3$] is the volume of 1 mol $H_2O$ at standard temperature [273.15 K] and standard

pressure [1.013 bar], $V_{polymer,dry}$ [cm³] is the volume of the dry polymer and $V_{H2O}$ [18 g/mol] is the molecular weight of water.

The sorption data were analyzed using the Hopfenberg-Berens model as described earlier, to distinguish between Fickian sorption and non-ideal relaxation phenomena. Calculations and fitting of the experimental data to the theoretical model were performed using graphing and data analysis software from Originlabs (Origin Pro 7.5).

Not only the sorption of water vapor was investigated, but also the swelling of the polymer sample in liquid water (a = 1) was taken into account. Polymer samples (5 x 5 cm) with a thickness of approximately 200 μm were cut from pre-washed membrane films (films were washed for 3 days in ultra pure water by changing the washing water twice a day), and subsequently dried till equilibrium weight was reached. The size and weight of the sample was chosen this high, to be able to perform accurate swelling measurements. The amount of liquid water absorbed in the polymer sample was determined in time by immersing the membrane sample in Milli-Q water (18.2 MΩ·cm at 25°C) and measuring its weight in time. During each measurement, the sample was removed from the water, carefully dried between tissue paper and the mass of the swollen sample was determined. All experiments were repeated 3 times. The swelling degree (SwD [%]) of the polymer film in liquid water at each time was determined according to Equation 7:

$$SwD = \left( \frac{M_\infty - M_{polymer,dry}}{M_{polymer,dry}} \right) \cdot 100\% \tag{7}$$

Where $M_\infty$ [g] is the equilibrium mass of the polymer sample and the absorbed water at a certain water vapor activity and $M_{polymer,dry}$ [g] is the dry weight of the polymer.

# Results and Discussion

## *Sorption isotherms*

Form the equilibrium mass uptake of water vapor at different water vapor activities, the sorption isotherms of water vapor in S-PEEK can be constructed. Analysis of these sorption isotherms using the Hopfenberg-Berens model allows quantifying the separate contributions of Fickian diffusion and relaxation phenomena. In addition, these isotherms can be used to calculate the tendency of water vapor molecules to form clusters in the polymer matrix and to calculate the theoretical glass transition temperature of the water vapor/polymer mixture.

The sorption isotherm at 20°C for water vapor and liquid water (a = 1.0) in S-PEEK films with two different sulfonation degrees (59 and 75%) is shown in Figure 2. The X-axis reports the water vapor activity (a = 1.0 - liquid water), whereas the Y-axis represents the corresponding water concentration in $cm^3$ absorbed water (vapor) at standard temperature and pressure per $cm^3$ of dry polymer ($cm^3$ STP/$cm^3$ polymer).
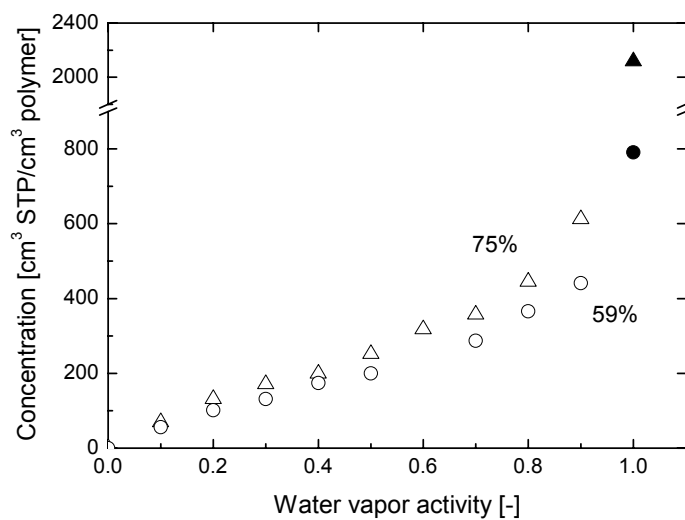


**Figure 2:** Water (vapor) sorption isotherms for S-PEEK with a sulfonation degree of 59 and 75% at 20°C [open symbols represent sorption from water vapor, filled symbols represent swelling in liquid water].

The water vapor concentration in the polymer films increases with increasing water vapor activity as shown in Figure 2. The sorption isotherms show a concave increase for water vapor activities a < 0.5 (often described by the simple Dual Mode sorption model [30, 31] or the more extended energy site distribution model [32, 33]). For activities a > 0.5, the sorption isotherm has an inflection point turning to convex with an exponential increase, which is often described by the Flory-Huggins model. The amount of liquid water absorbed in the polymer follows the exponential increase as predicted by the Flory-Huggins description. Especially at higher water vapor activities the degree of sulfonation has an effect on the solubility of water in the polymer, with the higher sulfonation degree leading to higher water vapor concentrations. The reason for this is the higher concentration of hydrophilic sulfon groups attached to the polymer backbone at higher sulfonation degrees. Nevertheless, the number of water molecules per sulfonic acid group is nearly comparable for both sulfonation degrees and increases with increasing water vapor activity (Figure 3).
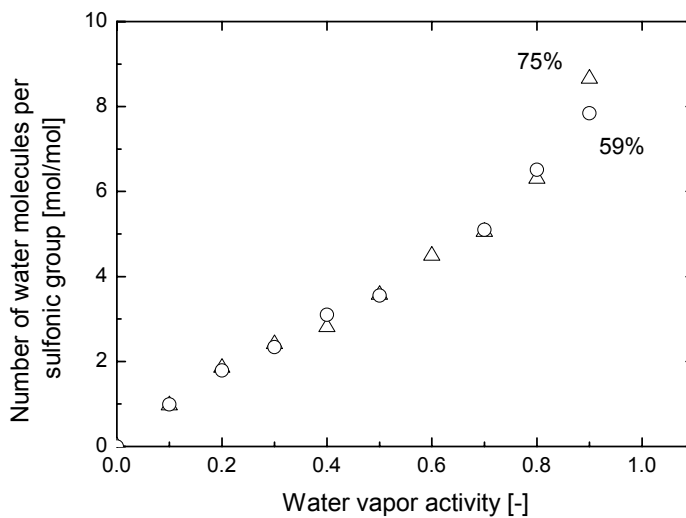


**Figure 3:** Number of water molecules per sulfonic acid group for S-PEEK with a sulfonation degree of 59 and 75% at 20°C.

Figure 4 compares the sorption and the desorption isotherms for both sulfonation degrees (59 and 75%). The open symbols represent the sorption run and the filled symbols represent the desorption run respectively.
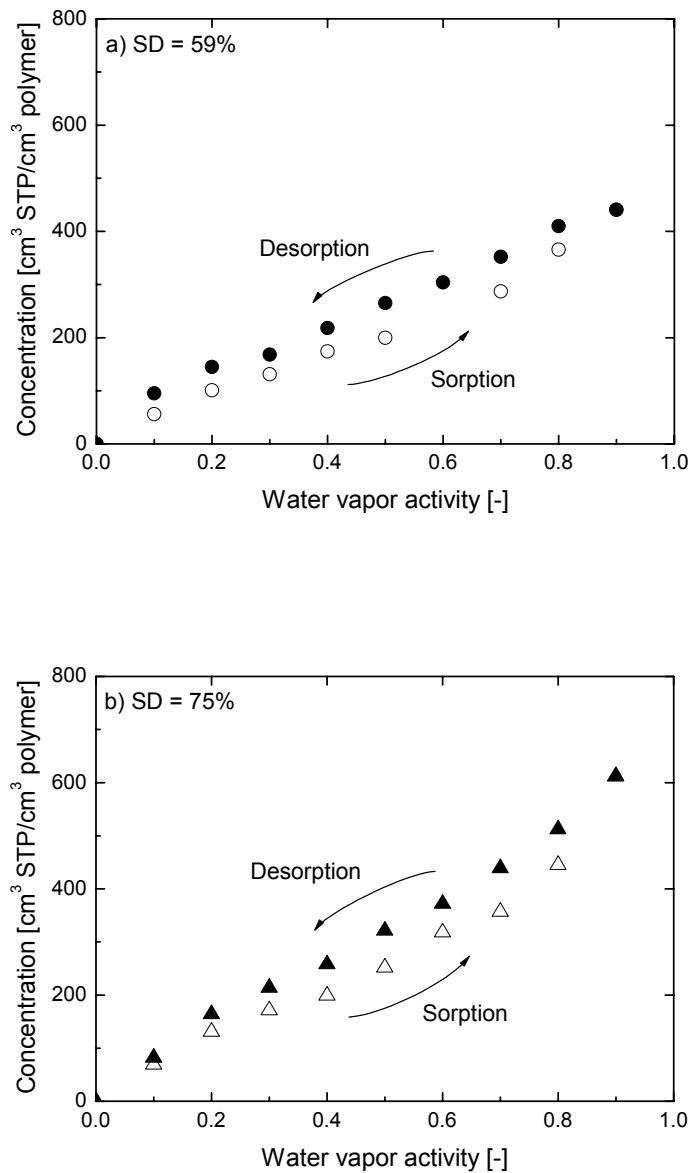


**Figure 4:** Sorption-desorption isotherms for S-PEEK with a sulfonation degree of a) 59% and b) 75% at 20°C. Open symbols represent sorption runs and filled symbols represent desorption runs.

Desorption values are higher for both sulfonation degrees. Berens *et al.* [34] and Wessling *et al.* [35] interpret this hysteresis as the induction of new free volume sites and subsequent filling of the extra free volume during the sorption cycle. Desorption of the penetrant however, occurs more rapidly than the collapse of the free volume, thus a higher amount of free volume is available in the desorption runs, resulting in higher water vapor concentration during desorption [26, 34, 35].

### *Kinetic sorption behavior*

Figure 5 shows typical plots of the normalized water vapor uptake [$M_t/M_\infty$] versus the logarithm of time for a sorption and desorption run of water vapor in S-PEEK with a sulfonation degree of 75% for water vapor activities of a) 0-0.1 b) 0.1-0.2 c) 0.5-0.6, and d) 0.7-0.8.
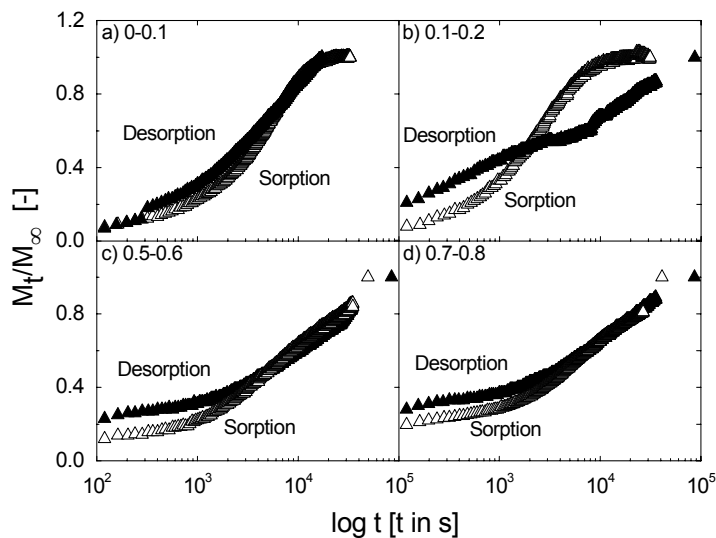


**Figure 5:** Typical water vapor sorption/desorption runs in S-PEEK with a sulfonation degree of 75% for water vapor activities of a) 0-0.1, b) 0.1-0.2, c) 0.5-0.6, and d) 0.7-0.8. The actual mass uptake is normalized for the final equilibrium mass gain of the sample.

Figure 5 proofs the presence of the different contributions of Fickian sorption and relaxational phenomena at different water vapor activities. Water vapor sorption at low activities (Figure 5a) shows typical Fickian sorption behavior of water vapor in the polymer. Fickian diffusion is usually accompanied by an increase in relative mass uptake in time, followed by a leveling off of this mass uptake to a constant value at longer time scales (in this case at approximately $\log(t) = 2 \cdot 10^4$). This is clearly visible in Figure 5a, both for sorption and desorption. Figure 5b indicates the onset of the relaxational sorption kinetics. While for sorption Fickian behavior still prevails, desorption shows already non-Fickian contributions to the overall sorption value as a result of relaxational phenomena. The difference between the behavior of the polymer film during sorption and desorption is due to hysteresis, which results in higher water vapor concentrations in the polymer during desorption at the same activity. In the case of relaxational phenomena, the leveling off of the relative mass up take to a constant value is overlapped and followed by an additional, continuous increase of the relative mass uptake, without leveling off at longer time scales. This additional mass uptake after the initial mass uptake is due to relaxation phenomena. Water vapor sorption/desorption at higher water vapor activities (Figure 5c and d) thus shows a significant contribution of both Fickian sorption and relaxational phenomena, both for sorption and desorption.

The Hopfenberg-Berens model described earlier can be used to fit the sorption and desorption data presented in Figure 5 and allows the extraction of the Fickian diffusion coefficient from the experimental results. Figure 6 presents this Fickian diffusion coefficient of water vapor in S-PEEK with a sulfonation degree of 59 and 75% for a) sorption and b) desorption.
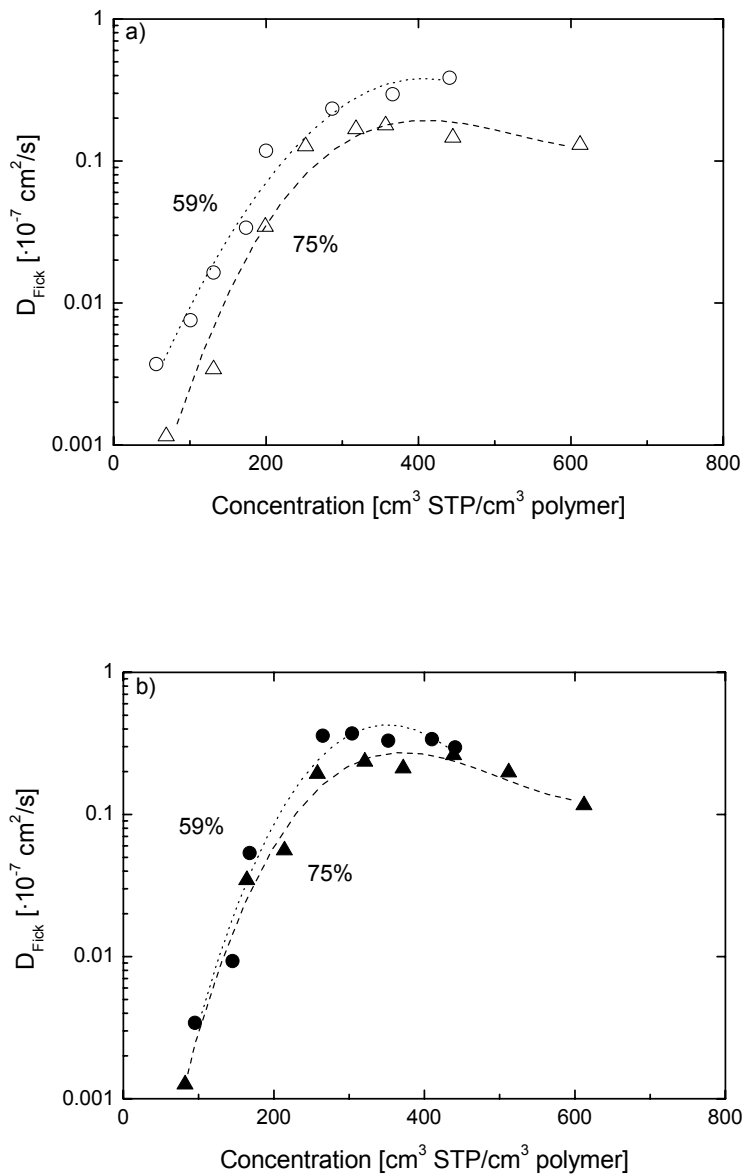
**Figure 6:** Calculated Fickian diffusion coefficient of water vapor in S-PEEK with a sulfonation degree of 59 and 75% at 20°C for a) sorption and b) desorption.

The Fickian diffusion coefficient increases for both sulfonation degrees with increasing water vapor concentration, but levels off to a plateau value at a certain concentration. The plateau is clearly visible for the high degree of sulfonation, and starts to occur for the lower sulfonation degree. The diffusion coefficients from desorption runs almost coincide

for different sulfonation degrees, whereas the Fickian diffusion coefficient for sorption runs differs slightly with increasing sulfonation degree. This is in good agreement with the work of Piroux *et al.* who report diffusion coefficients for water vapor in sulfonated copolyimides [11]. As discussed earlier, the sorption isotherms show two different sorption mechanisms, Dual Mode sorption for lower water vapor activities (a < 0.5) and Flory Huggins sorption for higher water vapor activities (a > 0.5). According to Yampolskii *et al.* [36], an increase in diffusion coefficient with increasing water vapor concentration can be expected for both Dual Mode and Flory Huggins sorption behavior. This increase in diffusion coefficient can indeed be observed at lower water vapor concentrations (c approximately < ~200 cm$^3$ STP/cm$^3$ polymer). Flory Huggins sorption behavior is usually also accompanied by an increase in diffusion coefficient with an increase in penetrant concentration, but clustering phenomena can lead to reduced diffusion coefficients at higher water vapor activities [36]. The appendix shows that clustering phenomena do not occur in this system.

The thickness of the polymer films used for water vapor sorption analysis is a critical parameter and proper choice of the films thickness is crucial to allow accurate determination of both contributions. To be able to discriminate well between Fickian diffusion and relaxational phenomena, one would desire thinner films. A measure for the ability to discriminate between these two phenomena is the Deborah number (DEB)$_D$. In all our experiments and with the film thickness chosen, this Deborah number was greater than unity (we will come back later to the absolute values of the Deborah number). This shows that Fickian diffusion and relaxtion are well separated and in principle allows the extraction of the Fickian diffusion coefficient from the data. Nevertheless we observe an unexpected leveling off in the Fickian diffusion coefficient at high concentrations (Figure 6). We think this stems from an inaccuracy in the measurements at high water concentrations. In thinner films the time scale for diffusion is relatively low, limiting the accurate determination of the value of the Fickian diffusion coefficient, because the extremely rapid weight uptake cannot be measured accurately. We think this explains the leveling off in Fickian diffusion coefficient at high water concentrations. This idea is supported by our results from liquid water swelling measurements with thicker films, as will be shown later.

Figure 7 shows the relative contribution of Fickian equilibrium sorption ($m_F$) and relaxation equilibrium sorption ($m_{R1} + m_{R2}$) as calculated with the Hopfenberg-Berens model as a function of the water vapor concentration inside the polymer for the sorption run in S-PEEK with a sulfonation degree of 59 and 75%. The total fraction of Fickian diffusion and relaxational sorption at equilibrium is set to 1. The Hopfenberg-Berens model only allows the quantification of Fickian diffusion and relaxation phenomena when the diffusion contribution and the relaxation contribution are very well separated, e.g. it requires the diffusion rate to be much higher than the rate of relaxation phenomena [16]. The same accounts for the difference between fast relaxational sorption ($m_{R1}$) and slow relaxational sorption ($m_{R2}$): differences can only be observed when both relaxations are very well separated. In the present work fast and slower relaxations overlap and a clear distinction between both is not visible. Figure 7 therefore shows the relative contribution of Fickian diffusion and the combined fractional contribution of both fast and slow relaxations.
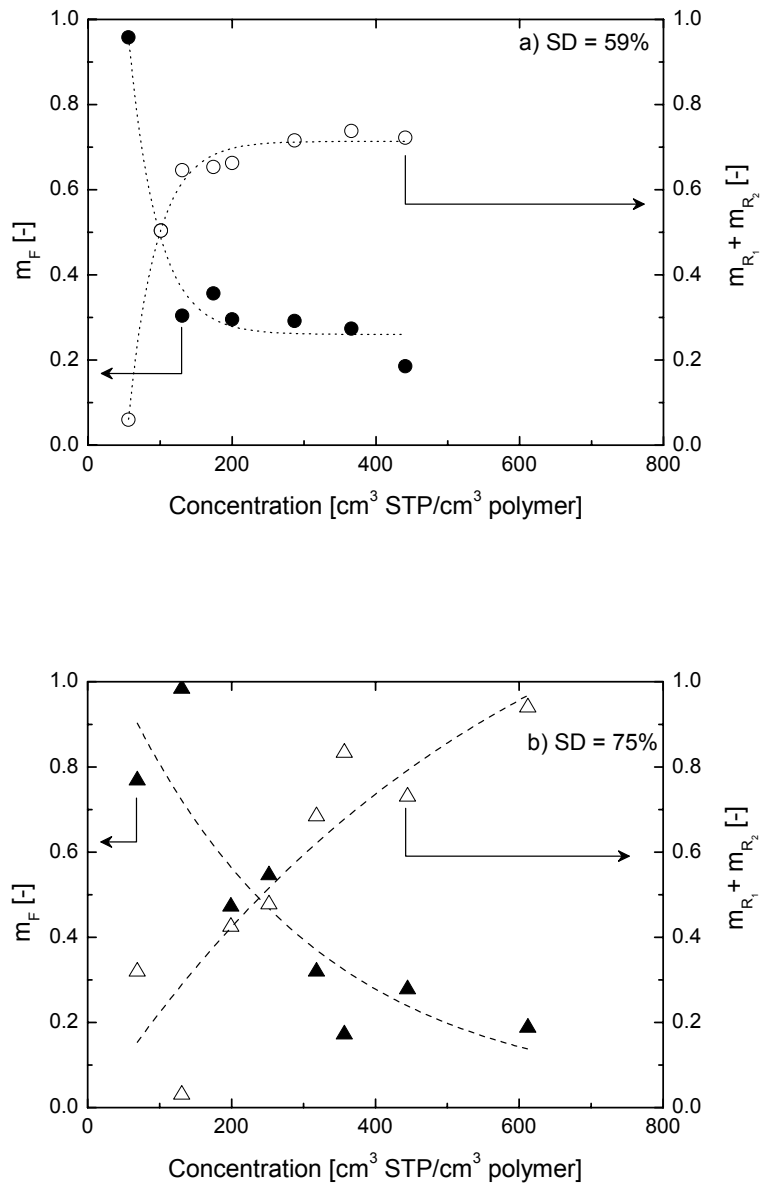
**Figure 7:** Relative contribution of Fickian equilibrium sorption ($m_{F,\infty}$) and relaxation phenomena ($m_{R1}$ + $m_{R2}$) calculated from sorption isotherms for S-PEEK with a sulfonation degree of a) 59% and b) 75%. All measurements performed at 20°C.

For water vapor sorption in S-PEEK with a sulfonation degree of 59 and 75%, the occurrence of solely Fickian sorption can only be observed at low water vapor concentrations (c < ~ 100 $cm^3$ STP/$cm^3$ polymer). The relative contribution of Fickian equilibrium sorption is close to one below this concentration. Above ~ 100 $cm^3$ STP/$cm^3$ polymer, the kinetic sorption behavior becomes non-Fickian due to the onset of relaxations, as indicated by an increase in the fractional contribution of relaxations ($m_{R1}$ + $m_{R2}$) and a decrease in the contribution of Fickian diffusion ($m_F$) with increasing water vapor activity. The Hopfenberg-Berens model allows to quantify the relative contribution of Fickian equilibrium sorption and relaxational equilibrium sorption, and the results show that already very early in the sorption process (~ above 100 $cm^3$ STP/$cm^3$ polymer for both sulfonation degrees) relaxational changes appear.

Frequently, data analysis is performed without taking the relaxational contribution into account [10]. This has significant consequences for the interpretation of the dynamic sorption data. The initial concentration dependent increase of the Fickian diffusion coefficient would still be visible; however the slower relaxation weight uptake occurring during sorption runs at higher activities would fall together with faster Fickian weight uptake. This fusion of two distinctly different mechanisms would be falsely interpreted as a slowing down of the Fickian diffusion. Such an apparent leveling off is then in turn interpreted to be related to a clustering of the water penetrant molecules. The appendix shows that clustering does not occur in this system.

Figure 8 shows the contribution of Fickian equilibrium sorption ($m_F$) and relaxation equilibrium sorption ($m_{R1}$ + $m_{R2}$) depending on the water vapor concentration inside the polymer as calculated from desorption data in S-PEEK with a sulfonation degree of 59 and 75%.
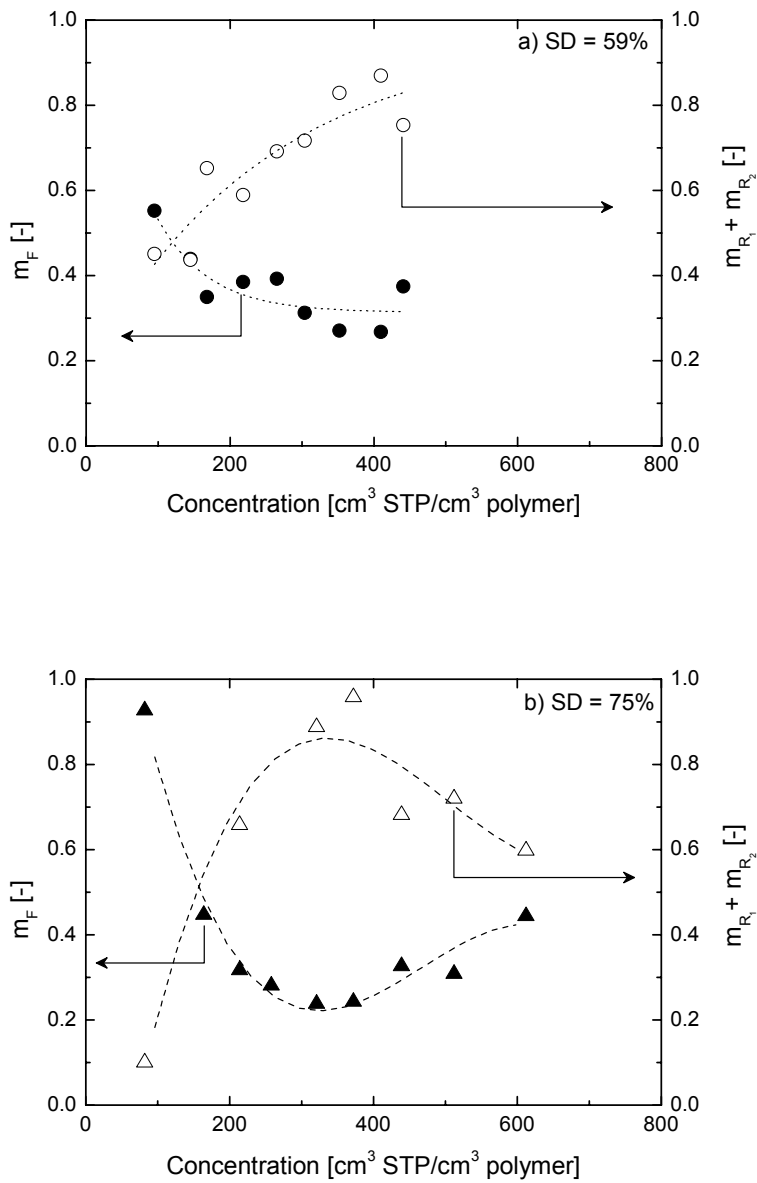
**Figure 8:** Contribution of Fickian equilibrium sorption ($m_F$) and relaxation equilibrium sorption ($m_{R1} + m_{R2}$) at desorption runs for S-PEEK with a sulfonation degree of a) 59% and b) 75%. All measurements performed at 20°C.

Figure 8 shows the same trends for desorption, as observed for sorption runs. The occurrence of solely Fickian sorption can only be observed at low water vapor concentrations (c < ~ 100 cm$^3$ STP/cm$^3$ polymer) where the relative contribution of Fickian diffusion is close to unity. With increasing water concentration, the relative contribution of Fickian diffusion decreases, whereas that of relaxational contributions increases. For water vapor concentrations above ~ 400 cm$^3$ STP/cm$^3$ polymer, the contribution of Fickian sorption equilibrium ($m_F$) increases again, whereas the relative contribution of relaxation sorption equilibrium ($m_{R1}$ + $m_{R2}$) decreases again. This minimum for the Fickian contribution and the maximum for the relaxational contribution are unexpected. This effect might be related to a change in glass transition temperature with increasing water concentration in the polymer and the subsequent transition of the polymer from the glassy state to the rubbery, fully relaxed state at high water vapor concentrations during desorption (during sorption, the polymer mixture does not reach the rubbery, fully relaxed state, as will be shown below). Furthermore, at these high water vapor activities, the build up of the diffusion profile is too fast to allow accurate determination of the Fickian diffusion coefficient.

### *Glass transition temperature*

The behavior of the polymers during sorption and desorption runs already indicated a change in polymer network structure during water vapor uptake due to slow relaxations. The glass transition temperature is another measure to describe the state of a polymer. The glass transition temperature characterizes the transition of the polymer from the glassy state where both Fickian diffusion and relaxational changes may occur during sorption, to the rubbery state where only Fickian sorption kinetics play a role and the relaxation contribution is considered to be zero because the polymer is in its fully relaxed state. Penetrant sorption reduces the glass transition temperature and the Fox equation is a useful tool to calculate the theoretical glass transition temperature of a polymer at different water concentrations inside that polymer [27]. Figure 9 shows this theoretical glass transition temperature ($T_g$) as a function of the water concentration inside the polymer.
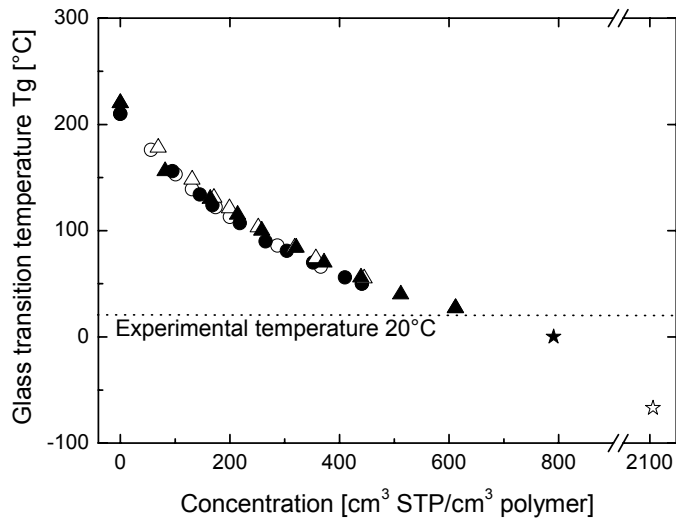
32

**Figure 9:** Calculated glass transition temperature as a function of the water concentration in S-PEEK with a sulfonation degree of 59% (circles) and 75% (triangles) for sorption (open symbols) and desorption (filled symbols) at 20°C. Values for sorption in liquid water for S-PEEK with a sulfonation degree of 59% (filled stars) and 75% (open stars) are also presented.

The calculated values for the glass transition temperature of the polymer at different concentrations of water inside the polymer for different degrees of sulfonation perfectly coincide. A decrease in glass transition temperature with increasing water concentration is clearly visible. The calculated glass transition temperature of the water vapor swollen material almost reaches the experimental temperature of 20 °C, indicating a region close to the transition from a glassy state to a rubbery state. The glass transition temperature calculated from the swelling experiments in liquid water drops even below the measurement temperature, predicting rubbery behavior in this case.

Figure 10 shows the relative contribution of relaxational phenomena ($m_{R1}$ + $m_{R2}$) as a function of the measurement temperature (20°C) minus the calculated glass transition temperature of the polymer at each water vapor concentration during sorption and desorption for both sulfonation degrees.
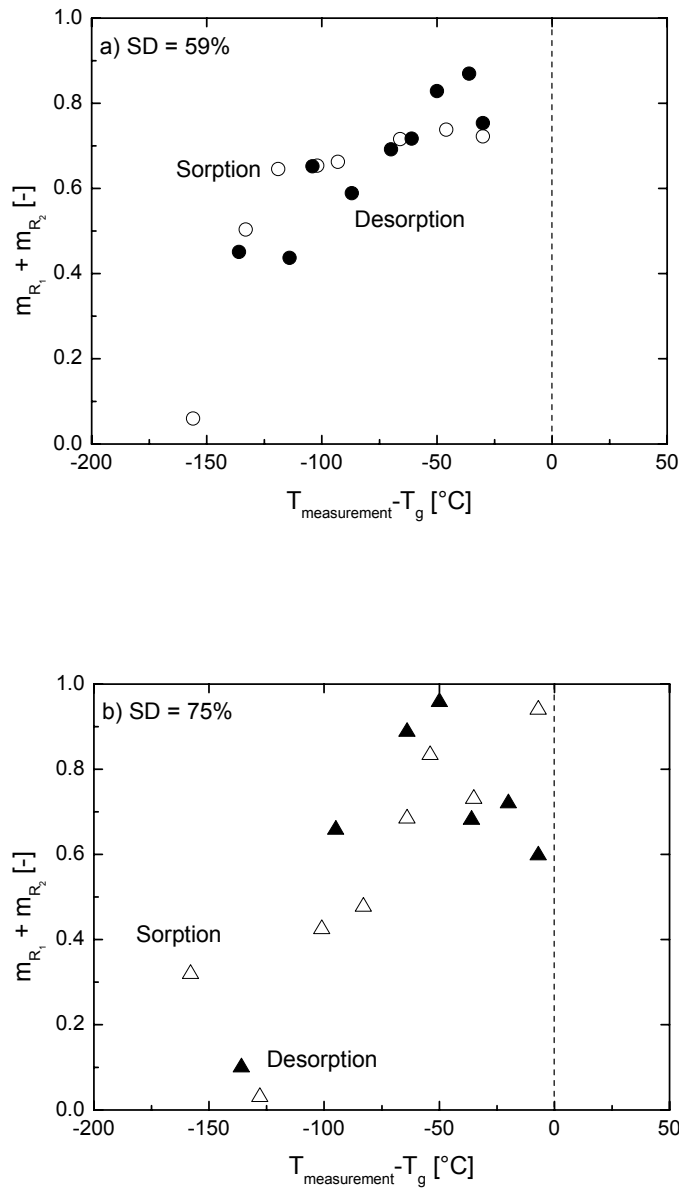
33

**Figure 10:** Relative contribution of relaxation phenomena $(m_{R1} + m_{R2})$ for S-PEEK with a sulfonation degree of a) 59% and b) 75% as a function of the difference between the measurement temperature and the calculated glass transition temperature for sorption (open symbols) and desorption (closed symbols).

The contribution of relaxation phenomena ($m_{R1}$ + $m_{R2}$) during sorption and desorption increases when the calculated glass transition temperature of the swollen polymer approaches the experimental measurement temperature (20°C) for both sulfonation degrees. The contribution of relaxation shows an increasing trend with decreasing difference between the calculated glass transition temperature and the experimental temperature in both polymers. Based on the work of Kamiya *et al.* [26], Wessling *et al.* [25] and Visser and Wessling [16], we hypothesize the occurrence of solely Fickian behavior when the glass transition temperature of the polymer/water sample drops below the actual experimental temperature and the system reaches its rubbery and fully relaxed state. To prove this hypothesis, one would need to perform kinetic sorption measurements at higher experimental temperatures or more sorption experiments above a > 0.9 with very small step-wise increases in activity. However, such measurements are experimentally intricate and a challenge for future research.

*Swelling in liquid water*

Figure 11 shows the increase in water concentration inside the polymer during swelling experiments in liquid water.
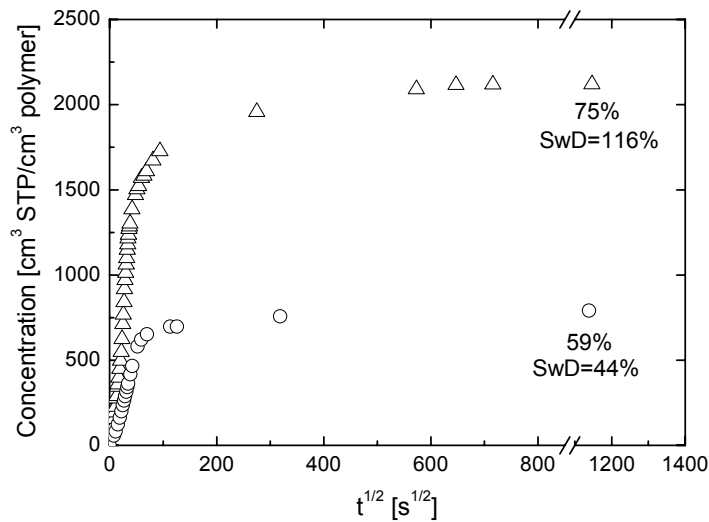


**Figure 11:** Concentration of water inside S-PEEK with a sulfonation degree of 59 and 75% in liquid water as a function of the square root of time (T = 20°C).

The concentration of water in the polymer initially increases rapidly in time and finally levels off to its equilibrium value. The equilibrium swelling degree (SwD) of S-PEEK with a sulfonation degree of 59% is 44% and a value of 116% is obtained for S-PEEK with a sulfonation degree of 75%. This difference in swelling degree for the two materials is due to the higher concentration of hydrophilic sulfon groups present in the highly sulfonated material.

As mentioned earlier, the film thickness plays a crucial role in the determination of the Fickian diffusion coefficient and the relaxation phenomena. The Deborah number quantifies the ratio of the rate of Fickian diffusion and that of relaxation. Values larger than unity indicate that diffusion and relaxation are well separated, thus allowing the

application of the Hopfenberg-Berens model and the extraction of the Fickian diffusion coefficient from the sorption data, as presented in the present work. Table 1 shows the calculated Deborah numbers for all our experiments.

**Table 1:** Deborah number to quantify the relative contribution of the rate of Fickian diffusion and relaxational phenomena for water sorption in S-PEEK with a sulfonation degree of 59 and 75 % at 20°C (all values are calculated from water vapor sorption data, except the last row which is marked with * and calculated from the sorption data in liquid water).

| Sulfonation degree 59% | | Sulfonation degree 75% | |
|---|---|---|---|
| Water vapor concentration $[cm^3 (STP)/cm^3$ polymer] | $(DEB)_D$ [-] | Water vapor concentration $[cm^3 (STP)/cm^3$ polymer] | $(DEB)_D$ [-] |
| 101 | 1.64 | 199 | 4.7 |
| 174 | 1.83 | 252 | 21.9 |
| 200 | 10.38 | 318 | 16.0 |
| 287 | 29.65 | 357 | 52.8 |
| 366 | 42.50 | 445 | 15.1 |
| 441 | 15.26 | 612 | 30.9 |
| 791* | 6.22* | 2113* | 8.3* |

Table 1 shows that in all cases, also for swelling in liquid water, the Deborah number was indeed (significantly) larger than unity. Nevertheless, we observed an unexpected leveling off in the Fickian diffusion coefficient at high concentrations, and attributed this to the very fast build-up of the diffusion profile at high concentrations for these thin film thicknesses. The determination of the sorption kinetics in liquid water, however, requires the use of much thicker films, to allow an accurate determination of the weight uptake and corresponding diffusion coefficient. By doing so, we were able to accurately determine the Fickian diffusion coefficient in liquid water at sufficiently high Deborah numbers. Because of the increased film thickness, the Deborah number of course decreased relative to the measurements with thinner films. The use of thicker films over

the whole activity range investigated would not be possible, because in that case the Deborah number would drop below unity at lower activities.

Figure 12 compares the Fickian diffusion coefficient extracted from water vapor sorption experiments at different water concentrations in the polymer (Figure 6) and these obtained form liquid water sorption kinetics (Figure 11), both calculated with the Hopfenberg-Berens model [22] for the two sulfonation degrees investigated.
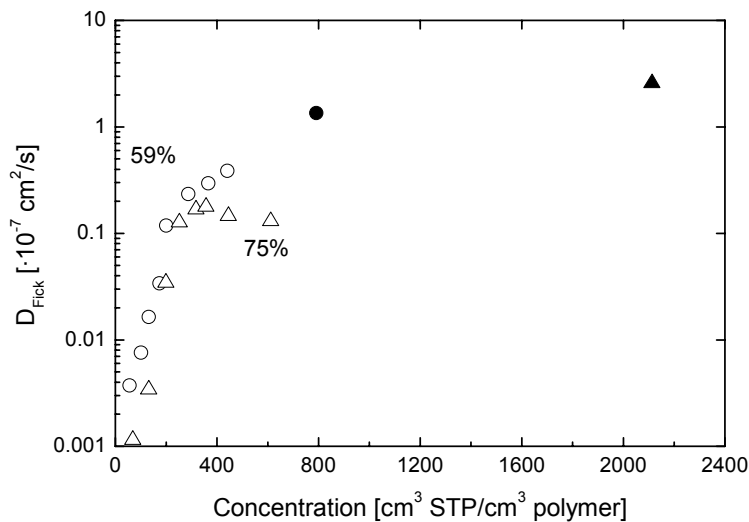


**Figure 12:** Fickian diffusion coefficient as determined from either water vapor or liquid water sorption experiments in S-PEEK with a sulfonation degree of 59 (○) and 75% (△) at 20°C (open symbols: water vapor sorption; filled symbols: liquid water sorption).

Below a water vapor concentration of ~300 cm$^3$ STP/cm$^3$ polymer the Fickian diffusion coefficient increases with increasing water vapor concentration. Above a water vapor concentration of ~300 cm$^3$ STP/cm$^3$ polymer a plateau can be distinguished in which the Fickian diffusion coefficient as determined form water vapor measurements, seems to be more or less independent of the water vapor concentration in the polymer. Due to the use of relatively thick films for the liquid water swelling experiments (filled symbols in

Figure 12), distinct separation of diffusion and relaxation phenomena and an accurate determination of the Fickian diffusion coefficient is possible again from liquid water swelling kinetics [16]. Based on the water vapor sorption kinetics only, the Fickian diffusion coefficient increases over two orders of magnitude with increasing water vapor concentration. Taking also the diffusion kinetics from liquid water sorption experiments into account, reveals a change of even three orders of magnitude of the Fickian diffusion coefficient when the water concentration in the polymer increases.

## Conclusions

This paper presents an analysis of the sorption kinetics of water vapor and liquid water in the glassy polymer sulfonated poly ether ether ketone (S-PEEK). Sorption isotherms are determined experimentally using a gravimetric sorption balance and the relative contributions of Fickian diffusion and relaxational phenomena are quantified as a function of the water concentration in the polymer using the model of Hopfenberg and Berens.

The sorption isotherms show Dual Mode sorption behavior for lower water vapor activities (a < 0.5) and Flory Huggins type of sorption for higher water vapor activities (a > 0.5). Hysteresis between sorption and desorption runs is observed. The hydrophilic nature of the material, especially for higher degrees of sulfonation, results in high water vapor sorption values and high liquid water swelling degrees.

Analysis of the sorption isotherms and determination of the sorption kinetics proof the occurrence of both Fickian sorption behavior and relaxational phenomena already at very low water concentrations in the polymer. With increasing water concentration, the relative importance of relaxation phenomena increases, whereas the relative contribution of Fickian diffusion decreases.

Based on the water vapor sorption kinetics only, the Fickian diffusion coefficient increases over two orders of magnitude with increasing water vapor concentration. Taking also the diffusion kinetics from liquid water sorption experiments into account,

reveals a change of even three orders of magnitude of the Fickian diffusion coefficient when the water concentration in the polymer increases.

## Appendix: Clustering analysis of sorption isotherms

In addition to relaxation, other phenomena e.g. clustering of water molecules in the polymer matrix may occur, which can influence the sorption behavior and diffusion kinetics of water vapor in polymers. Solvent molecules like water potentially tend to cluster when absorbed in a polymer. This effect has been attributed to self-hydrogen bonding of water molecules [37]. Water clusters can influence the diffusion of water vapor through the polymer by hindering the diffusion of other water molecules, and thus elongating the diffusion pathway of water vapor molecules.

To provide a measure for clustering, Zimm and Lundberg defined the clustering function [37]:

$$\frac{G_{ww}}{V_w} = -\Phi_p \left[ \partial(a / \Phi_w) / \partial a \right] - 1 \tag{8}$$

With a being the vapor activity ($p_{H2O}/p_{H2O, \text{saturated}}$ [-]) and $\Phi_p$ and $\Phi_w$ the polymer and water volume fractions [-] determined from the equilibrium mass at sorption runs. $V_w$ is the molar volume of the water vapor penetrant [$cm^3$/mol] and $G_{ww}$ is the cluster integral. The quantity $G_{ww}/V_w$ is a measure for the tendency of solvent molecules to cluster inside the polymer. When $G_{ww}/V_w = -1$, the solution is ideal: water vapor molecules do not experience any effect of the other water molecules present and have no effect on their distribution. When $G_{ww}/V_w = 0$, the excluding effect of the central water molecule is just sufficient, whereas when $G_{ww}/V_w > 0$, the water molecules touch each other and form a cluster. When $G_{ww}/V_w < -1$, the water molecules prefer to remain isolated.

Water vapor clustering phenomena inside polymer matrices are reported in literature [10, 11, 38-41]. Detallante *et al.* [10] report the water vapor sorption in naphtalenic sulfonated polyimide. The diffusion coefficient calculated via Ficks law of diffusion seems to pass a maximum with increasing water vapor concentration. The authors attribute this to water clusters formed in the polymer during water vapor sorption. Nonetheless, the authors did not perform a cluster analysis.

From the sorption isotherms as presented in this work and Equation 8, the cluster integral (or the tendency of water molecules to form clusters in the polymer) can be calculated (Figure A1).
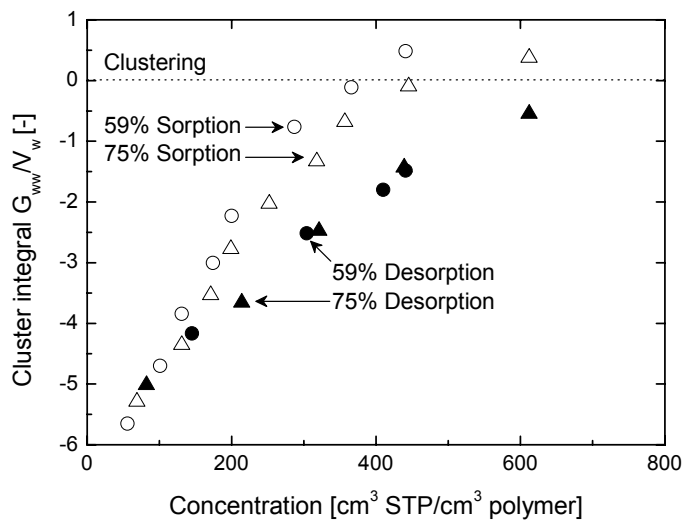


**Figure A1:** Cluster integral as a function of the water vapor concentration in the polymer during sorption (open symbols) and desorption (filled symbols) at 20°C for S-PEEK with a sulfonation degree of 59 and 75%.

When the cluster integral $G_{ww}/V_w > 0$, the water molecules tend to form clusters in the polymer. Figure A1 clearly shows that water molecules do not tend to cluster in the S-PEEK films investigated. The results show that the water molecules in the sulfonated PEEK films investigated remain isolated at almost all water vapor concentrations, and

that cluster formation does not influence the sorption kinetics of water vapor molecules in the S-PEEK films investigated in this work.

The cluster integral increases with increasing water vapor concentration and the values for sorption and desorption at low water vapor concentrations (c approximately < 200 cm$^3$ STP/cm$^3$ polymer) are comparable. At higher water vapor concentrations, the values obtained from desorption runs are lower than the ones from sorption runs. This is most probably due to the higher amount of free volume accessible in desorption runs [34].

# References

1.  H. Sijbesma, K. Nymeijer, R. van Marwijk, R. Heijboer, J. Potreck, M. Wessling, Flue gas dehydration using polymer membranes, Journal of Membrane Science 313 (2008) 263-276.

2.  C.M. Balik, On the extraction of diffusion coefficients from gravimetric data for sorption of small molecules by polymer thin films, Macromolecules 29 (1996) 3025-3029.

3.  B.H. Dijkink, M.M. Tomassen, J.H.A. Willemsen, W.G. van Doorn, Humidity control during bell pepper storage, using a hollow fiber membrane contactor system, Postharvest Biology and Technology 32 (2004) 311-320.

4.  J.G. Wijmans, R.W. Baker, The solution-diffusion model - a review, Journal of Membrane Science 107 (1995) 1-21.

5.  K. Kneifel, S. Nowak, W. Albrecht, R. Hilke, R. Just, K.V. Peinemann, Hollow fiber membrane contactor for air humidity control: Modules and membranes, Journal of Membrane Science 276 (2006) 241-251.

6.  L.Z. Zhang, Mass diffusion in a hydrophobic membrane humidification/dehumidification process: The effects of membrane characteristics, Separation Science and Technology 41 (2006) 1565-1582.

7.  H.Y. Fu, L. Jia, J.P. Xu, Studies on the sulfonation of poly phenylene oxide (PPO) and permeation behavior of gases and water vapor through sulfonated PPO membranes, Journal of Applied Polymer Science 51 (1994) 1405-1409.

8.  S. Liu, F. Wang, T. Chen, Synthesis of poly(ether ether ketone)s with high content of sodium sulfonate groups as gas dehumidification membrane materials, Macromolecular Rapid Communications 22 (2001) 579-582.

9.  L. Jia, X. Xu, H. Zhang, J. Xu, Permeation of nitrogen and water vapor through sulfonated polyetherethersulfone membrane, Journal of Polymer Science Part B-Polymer Physics 35 (1997) 2133-2140.

10. V. Detallante, D. Langevin, C. Chappey, M. Metayer, R. Mercier, M. Pineri, Kinetics of water vapor sorption in sulfonated polyimide membranes, Desalination 148 (2002) 333-339.

11. F. Piroux, E. Espuche, R. Mercier, M. Pineri, Water vapour transport mechanism in naphthalenic sulfonated polyimides, Journal of Membrane Science 223 (2003) 127-139.

12. T.S. Chow, Molecular interpretation of the glass-transition temperature of polymer-diluent systems, Macromolecules 13 (1980) 362-364.

13. Y. Kamiya, K. Mizoguchi, Y. Naito, Plasticization of poly(ethyl methacrylate) by dissolved argon, Journal of Polymer Science Part B-Polymer Physics 30 (1992) 1177-1181.

14. P. Pissis, L. Apekis, C. Christodoulides, M. Niaounakis, A. Kyritsis, J. Nedbal, Water effects in polyurethane block copolymers, Journal of Polymer Science Part B-Polymer Physics 34 (1996) 1529-1539.

15. S.I. Semenova, H. Ohya, S.I. Smirnov, Physical transitions in polymers plasticized by interacting penetrant, Journal of Membrane Science 136 (1997) 1-11.

16. T. Visser, M. Wessling, When do sorption-induced relaxations in glassy polymers set in? Macromolecules 40 (2007) 4992-5000.

17. B. Krause, R. Mettinkhof, N.F.A. van der Vegt, M. Wessling, Microcellular foaming of amorphous high-Tg polymers using carbon dioxide, Macromolecules 34 (2001) 874-884.

18. M.A. Delnobile, G. Mensitieri, P.A. Netti, L. Nicolais, Anomalous diffusion in poly-ether-ether-ketone, Chemical Engineering Science 49 (1994) 633-644.

19. Z.J. Grzywna, J. Stolarczyk, Diffusion in glassy polymer membranes submitted to induced stresses, Polimery 46 (2001) 351-358.

20. S. Joshi, G. Astarita, Diffusion-relaxation coupling in polymers which show 2-stage sorption phenomena, Polymer 20 (1979) 455-458.

21. Y.M. Sun, Sorption/desorption properties of water vapour in poly(2-hydroxyethyl methacrylate).2. Two-stage sorption models, Polymer 37 (1996) 3921-3928.

22. A.R. Berens, H.B. Hopfenberg, Diffusion and relaxation in glassy polymer powders: 2. Separation of diffusion and relaxation parameters, Polymer 19 (1978) 489-496.

23. J. Crank, The mathematics of diffusion, Oxford University Press London, 1975.

24.     J.S. Vrentas, C.M. Jarzebski, J.L. Duda, A deborah number for diffusion in polymer-solvent systems, AICHE Journal 21 (1975) 894-901.

25.     M. Wessling, I. Huisman, T. Vanderboomgaard, C.A. Smolders, Dilation kinetics of glassy, aromatic polyimides induced by carbon-dioxide sorption, Journal of Polymer Science Part B-Polymer Physics 33 (1995) 1371-1384.

26.     Y. Kamiya, T. Hirose, Y. Naito, K. Mizoguchi, Sorptive dilation of polysulfone and poly(ethylene-terephthalate) films by high-pressure carbon-dioxide, Journal of Polymer Science Part B-Polymer Physics 26 (1988) 159-177.

27.     B. Francis, S. Thomas, J. Jose, R. Ramaswamy, V.L. Rao, Hydroxyl terminated poly(ether ether ketone) with pendent methyl group toughened epoxy resin: miscibility, morphology and mechanical properties, Polymer 46 (2005) 12372-12385.

28.     E.N. Komkova, M. Wessling, J. Krol, H. Strathmann, N.P. Berezina, Influence of the nature off polymer matrix and the degree of sulfonation on the properties of membranes, Polymer Science Series A 43 (2001) 300-307.

29.     J. Boom, I. Punt, H. Zwijnenberg, R. de Boer, D. Bargeman, C. Smolders, H. Strathmann, Transport through zeolite filled polymeric membranes, Journal of Membrane Science 138 (1998) 237-258.

30.     R.M. Barrer, Diffusivities in glassy-polymers for the dual mode sorption model, Journal of Membrane Science 18 (1984) 25-35.

31.     J.A. Horas, F. Nieto, A generalization of dual-mode transport-theory for glassy polymers, Journal of Polymer Science Part B-Polymer Physics 32 (1994) 1889-1898.

32.     R. Kirchheim, Sorption and partial molar volume of small molecules in glassy-polymers, Macromolecules 25 (1992) 6952-6960.

33.     R. Kirchheim, Partial molar volume of small molecules in glassy-polymers, Journal of Polymer Science Part B-Polymer Physics 31 (1993) 1373-1382.

34.     A.R. Berens, Effects of sample history, time, and temperature on the sorption of monomer vapor by PVC, Journal of Macromolecular Science: Physical Edition 14 (1977) 483-498.

35. M. Wessling, M.L. Lopez, H. Strathmann, Accelerated plasticization of thin-film composite membranes used in gas separation, Separation and Purification Technology 24 (2001) 223-233.

36. Y. Yampolskii, I. Pinnau, B.D. Freeman, Materials science of membranes for gas and vapor separation, Wiley Chichester, 2006.

37. B.H. Zimm, J.L. Lundberg, Sorption of vapors by high polymers, Journal of Physical Chemistry 60 (1956) 425-428.

38. M.S. Vicente, J.C. Gottifredi, J.G. de la Campa, A.E. Lozano, J. Abajo, Water vapor sorption and diffusion in sulfonated aromatic polyamides, Journal of Polymer Science Part B-Polymer Physics 45 (2007) 2007-2014.

39. H. Takata, N. Mizuno, M. Nishikawa, S. Fukada, M. Yoshitake, Adsorption properties of water vapor on sulfonated perfluoropolymer membranes, International Journal of Hydrogen Energy 32 (2007) 371-379.

40. F. Toribio, J.P. Bellat, P.H. Nguyen, M. Dupont, Adsorption of water vapor by poly(styrenesulfonic acid), sodium salt: isothermal and isobaric adsorption equilibria, Journal of Colloid and Interface Science 280 (2004) 315-321.

41. T. Watari, H.Y. Wang, K. Kuwahara, K. Tanaka, H. Kita, K. Okamoto, Water vapor sorption and diffusion properties of sulfonated polyimide membranes, Journal of Membrane Science 219 (2003) 137-147.

# Chapter 3

# Thermodynamics of water vapor sorption in hydrophilic polymers

## Abstract

In this work we study the sorption thermodynamics of water vapor in two hydrophilic polymers (sulfonated poly ether ether ketone (S-PEEK) and a poly ethylene oxide-poly amide block copolymer (PEBAX® 1074)). The thermodynamic approach presented offers a strong method to distinguish between enthalpic and entropic contributions of water vapor sorption. It allows to explain the nature of water sorption in both polymers and to address the state of water in the polymer. The results are discussed in relation to water clustering phenomena and the thermodynamics of water vapor sorption in liquid water (self-solvation of water).

Analysis of water vapor sorption in the two polymers shows that the Gibbs energy of sorption has a negative value. In all cases, the enthalpy of water sorption is negative, i.e. the sorption process is exothermic. The results suggest that in PEBAX® additional sorbed water molecules experience a water-like environment, whereas in S-PEEK the polymer-water interactions prevail. This is supported by data obtained from cluster analysis. The entropy of water sorption for both polymers is negative over the full range of water vapor activities (sorption is entropically unfavorable).

The thermodynamic analysis shows that for both polymers water sorption is driven by a favorable water sorption enthalpy. For S-PEEK, water sorption is governed by enthalpy-entropy compensation. In the case of PEBAX® enthalpy-entropy compensation is observed only at lower activities. At higher water vapor activities, the more favorable Gibbs energy of water sorption in PEBAX® is driven by the entropy.

# Introduction

Transport of gases and vapors in polymeric membranes is often described by the so called solution-diffusion mechanism [1] in which the solubility and diffusivity of a penetrant in the polymeric membrane determine its separation performance. The solubility is defined as the concentration of dissolved gas or vapor in the polymer, normalized for the applied equilibrium vapor pressure. For ideal systems, e.g. the sorption of light gases (e.g. He, $H_2$, $N_2$, $O_2$, $CH_4$) and vapors in rubbers, the solubility is independent of the concentration [2]. The sorption isotherm follows Henry's law and the concentration inside the polymer is proportional to the applied pressure. In many other (non ideal) cases, sorption isotherms are far from linear and the solubility coefficient is dependent on the solute concentration. Sorption isotherms observed for such systems are either concave or convex towards the pressure axis, especially at high gas or vapor concentrations [3]. Sorption isotherms which show a concave increase towards the pressure axis are typically observed in glassy polymers [2], and can be described by the dual mode sorption model [4-6] or the more extended energy site distribution model [7, 8]. Convex isotherms are typically observed for the sorption of strongly interacting gases and vapors in polymers [2]. Such isotherms can be described by the Flory-Huggins model [9-12]. The Flory-Huggins model is used often to fit sorption isotherms and to describe the interaction between the solute and the polymer through the Flory-Huggins interaction $\chi$ parameter [13]. This interaction parameter is an 'overall' parameter that is often concentration-dependent, while it was originally introduced as a concentration-independent parameter. This concentration dependence of the Flory-Huggins interaction parameter complicates the physical-chemical interpretation of the sorption behavior [3].

Dissolution of a solute in a polymer includes both an enthalpic and an entropic effect, which can be obtained from temperature dependent solubility measurements. Recently Metz *et al.* [3] performed such measurements and analyzed the sorption behavior of water vapor in block copolymers of poly ethylene oxide-poly butylene terephtalate.

In this work we study the sorption thermodynamics of water vapor in two hydrophilic polymers (sulfonated poly ether ether ketone (S-PEEK) and a poly ethylene oxide-poly amide block copolymer (PEBAX® 1074)). The Gibbs energy of water vapor sorption in both polymers is determined. The thermodynamic approach presented offers a strong method to distinguish between enthalpic and entropic contributions of water vapor sorption. It allows to explain the nature of water sorption in both polymers and to address the state of water in the polymer. The results are discussed in relation to water clustering phenomena [14] and the thermodynamics of water vapor sorption in liquid water (self-solvation of water) [15]. Calculations based on both the dry or the wet volume are done, but the interpretation of the data is based on the wet swollen volume of the polymer, because this is more realistic and better resembles the environment a water molecule experiences upon sorption in the (partially) swollen polymer and provides a more realistic way to interpret the thermodynamic data.

# Theoretical background

## *Water vapor sorption isotherms*

The concentration of water vapor inside a polymer [$cm^3$ STP/$cm^3$ polymer] can be calculated from the equilibrium mass uptake of the sample at each water vapor activity based on either the dry volume of the polymer i.e. not taking into account the swelling of the film due to water vapor sorption (Equation 1a), or the wet, swollen volume of the film (Equation 1b):

$$c_{dry} = \frac{\dfrac{\left(M_\infty - M_{polymer,dry}\right)}{M_{w,H_2O}} \cdot V_{H_2O,gas}}{V_{polymer,dry}} \qquad (1a)$$

$$c_{wet} = \frac{\dfrac{\left(M_\infty - M_{polymer,dry}\right)}{M_{w,H_2O}} \cdot V_{H_2O,gas}}{V_{polymer,dry} + \left(\dfrac{\left(M_\infty - M_{polymer,dry}\right)}{M_{w,H_2O}} \cdot V_{H_2O,liquid}\right)} \qquad (1b)$$

where $M_\infty$ [g] is the equilibrium mass of the polymer sample and the absorbed water at a certain water vapor activity, $M_{polymer,dry}$ [g] is the dry weight of the polymer, $V_{H2O,gas}$ is the molar volume of water vapor at standard temperature and pressure [22414 $cm^3$/mol], $V_{polymer,dry}$ [$cm^3$] is the volume of the dry polymer, $M_{w,H2O}$ [g/mol] is the molecular weight of water and $V_{H2O,liquid}$ is the assumed (ideal) molar volume of liquid water in the polymer at standard temperature and pressure [18 $cm^3$/mol]. It is assumed that this molar volume of liquid water in the polymer is equal to the molar volume of water in liquid water and that this molar volume is not influenced by the presence of the polymer matrix. One may argue if this assumption is fully correct because the value can slightly change upon sorption in a polymer matrix instead of sorption in liquid water. Nevertheless it allows us to calculate the concentration of water in the water swollen polymer reasonably accurate.

## Solvation Thermodynamics

The free energy (Gibbs energy) of water sorption, $\Delta G$ [kJ/mol], is defined as the free energy required to transfer a single water molecule from a fixed position in the vapor phase to a fixed position in the polymer phase at constant pressure P, temperature T and composition [3, 16]. This quantity can be directly extracted from experimental sorption data [3, 16] according to:

$$\Delta G = - R \cdot T \cdot \ln\left(\frac{\rho_S}{\rho_S^{ig}}\right)_{eq} \tag{2}$$

where $\rho_S$ and $\rho_S^{ig}$ are the solute molar densities [mol/m$^3$] in the polymer and vapor phase, respectively. The vapor phase is assumed to follow ideal gas behavior (superscript ig). R is the universal gas constant [8.314 J/mol·K] and T is the experimental temperature [K]. The Ostwald solubility L, defined as $L \equiv (\rho_s/\rho_s^{ig})_{eq}$ is related to the solubility coefficient S [cm$^3$ (STP)/cm$^3$ cmHg] according to [17]:

$$L = S \cdot 75.187 \cdot R \cdot T \cdot \frac{P_0}{R \cdot T_0} \tag{3}$$

where $T_0$ is the standard temperature (273.15 K) and $P_0$ is the standard pressure (1.013 bar). The solubility coefficient can be determined directly from the amount of water [cm$^3$ (STP)] sorbed by the polymer during sorption experiments. The volume of the sample is calculated as the sum of the dry polymer volume and the increase in volume due to water vapor sorption. The latter is obtained from the weight of absorbed water and the molar volume of water, which is assumed to be 18 cm$^3$/mol at standard temperature and pressure (ideal volume).

The free energy consists of an enthalpic ($\Delta H$ [kJ/mol]) and an entropic ($\Delta S$ [kJ/mol·K]) contribution. The sorption enthalpy can be derived from the temperature dependency of the free energy through determination of the isosteric heat of sorption from the

51

experimental data. The sorption entropy can be deduced from the relationship $\Delta G = \Delta H - T \cdot \Delta S$.

The isosteric heat of water sorption $\Delta H_c$ [kJ/mol] can be obtained from Equation 4 [18]:

$$\left( \frac{\partial \ln(a)}{\partial \left( \frac{1}{T} \right)} \right)_{P,c} = \frac{\Delta H_c}{R} \tag{4}$$

A plot of the experimental data of ln (a) versus the reciprocal value of the temperature allows extracting the value of this isosteric heat of sorption from the slope at different fixed values of the water concentration.

Metz *et al.* [3] derived the relation between $\Delta H_c$ and $\Delta H$. When ideal gas behavior is assumed, the relationship between the activity and the Ostwald solubility can be deduced from the definition of the Ostwald solubility L (Equation 2):

$$a = \frac{p_{H_2O}}{p_{H_2O,sat.}} = \frac{R \cdot T \cdot \rho_S}{p_{H_2O,sat.} \cdot L} \tag{5}$$

Substitution of this Equation in Equation 4 results in the following relationship between the activity, the temperature and the Ostwald solubility:

$$\left( \frac{\partial \ln(a)}{\partial(1/T)} \right)_{P,c} = \left( \frac{\partial \ln(R \cdot T \cdot \rho_s / p_{H_2O,sat.})}{\partial(1/T)} \right) - \left( \frac{\partial \ln(L)}{\partial(1/T)} \right)_{P,c} \tag{6}$$

Using the Clausius-Clapeyron relation to the temperature dependence of the saturated water vapor pressure, allows rearrangement of the first term of the right hand side of Equation 6 to $(\Delta H_{vap} - R \cdot T)/R$. As stated in Equation 2, $\ln(L) = -\Delta G/R \cdot T$, so when the Gibbs-Helmholtz relation is used, the second term on the right hand side of Equation 6 can be written as $\Delta H/R$. Equation 6 thus simplifies to:

$$\left( \frac{\partial \ln(a)}{\partial \left( \frac{1}{T} \right)} \right)_{P,c} = \frac{\Delta H_{vap} + \Delta H - R \cdot T}{R} \tag{7}$$

The right hand side of this Equation $((\Delta H_{vap} + \Delta H - RT)/R)$ equals the right hand side of Equation 4 $(\Delta H_c/R)$ and consequently, the heat of water sorption can directly be determined from a plot of the experimental data of ln a versus the reciprocal value of the temperature.

The water sorption entropy $\Delta S$ is subsequently obtained from the relationship between the free energy, the enthalpy and the entropy of water sorption:

$$\Delta G = \Delta H - T \cdot \Delta S \tag{8}$$

**Clustering analysis**

Solvent molecules, such as water, have a tendency to cluster when absorbed in a polymer. This effect has been attributed to hydrogen bonding between water molecules [19]. To provide a measure for clustering, Zimm and Lundberg defined the clustering function [19]:

$$\frac{G_{ww}}{V_w} = -\Phi_p \left[ \partial(a/\Phi_w)/\partial a \right] - 1 \tag{9}$$

where a is the vapor activity ($p_{H2O}/p_{H2O, saturated}$ [-]) and $\Phi p$ and $\Phi w$ are the polymer and water volume fractions [-] as determined from the equilibrium mass at sorption runs. $V_w$ is the molar volume of the water vapor penetrant [$cm^3$/mol] and $G_{ww}$ is the cluster integral. If $G_{ww}/V_w = -1$, the solution is ideal: water molecules are statistically distributed in the matrix; excess coordination of water molecules by surrounding water does not occur. If $G_{ww}/V_w = 0$, the excluding effect of the central water molecule is still sufficient to prevent clustering, whereas when $G_{ww}/V_w > 0$, water molecules tend to accumulate

with other water molecules thereby forming regions with excess water concentration relative to the average value based on $\Phi_w$.

# Experimental

## *Materials*

Two different polymers were used. The glassy polymer sulfonated poly (ether ether ketone) (S-PEEK) and a commercially available rubbery block copolymer, PEBAX® 1074 (supplied by Arkema Inc. The Netherlands). Figure 1 presents the molecular structure of both polymers.
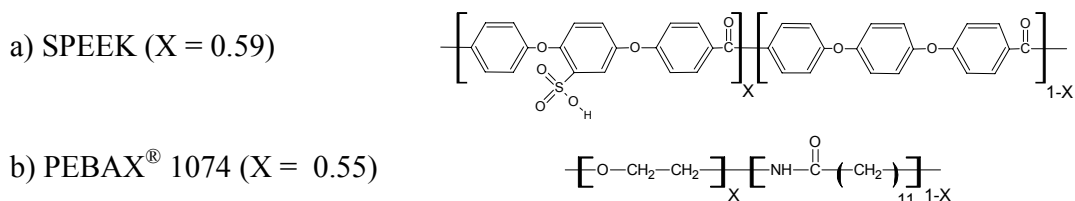
a) SPEEK (X = 0.59)

b) PEBAX® 1074 (X = 0.55)

**Figure 1:** Chemical structure of a) S-PEEK and b) PEBAX®.

Sulfonated poly ether ether ketone was prepared by sulfonation of poly ether ether ketone (supplied by Victrex, USA), according to the procedure described elsewhere [20]. The sulfonation degree, a measure for the amount of sulfonic acid groups per repeating unit, was 59% (X = 0.59).

PEBAX® 1074 is a block copolymer consisting of 45% of a hard phase (1-X = poly amide 12, PA12) and 55% of a soft phase (X = poly ethylene oxide, PEO) [21]. Permeation of water vapor preferentially occurs through the soft, hydrophilic PEO phase, whereas the hard PA12 phase provides the mechanical stability of the membrane material.

Both polymers were dissolved in N-methyl-2-pyrrolidon (10 wt.% solution). NMP was supplied by Acros Organics, Belgium. PEBAX® was dissolved at 100°C and the hot solution was cast on a warm glass plate (80°C) using a 0.47 mm casting knife. S-PEEK was dissolved and cast at room temperature. After casting the solvent was evaporated under nitrogen atmosphere (4 days at room temperature and 14 days at 60°C). After removal of the solvent, the films were washed in demineralised water to remove the films from the glass plate. Subsequently the films were washed for another three days in ultra pure water (Milli-Q water, 18.2 MΩ·cm) at 25°C and the wash water was replaced three

times to remove residual solvent from the films. After washing, the films were dried in a 30°C vacuum oven until the mass of the film was constant. The final thickness of the PEBAX® 1074 films was 34 μm, whereas the S-PEEK films had a final dry thickness of 36 μm.

### *Sorption measurements*

Sorption measurements were performed using a gravimetric sorption balance (SGA-100 (Ankersmid, The Netherlands). The membrane sample (weight ~ 3 mg) was positioned in the measurement chamber and dried for 24h to remove absorbed water and residuals. Interval sorption runs were performed by a stepwise increase (decrease) of the relative humidity in the measurement chamber and subsequent recording of the weight increase (or decrease) of the membrane sample. The detailed procedure is described in our previous work [22]. The free energy of water sorption in the polymer and the clustering analysis were determined directly from the sorption isotherms (based on both dry and wet, water swollen polymer volume). The sorption enthalpy was calculated from the temperature dependence of the free energy and the sorption entropy was determined from the relationship between the free energy and the sorption enthalpy.

# Results and discussion

## *Water vapor sorption isotherms*

The water vapor sorption isotherms for the glassy polymer sulfonated poly (ether ether ketone) with a sulfonation degree of 59% (S-PEEK) and the rubbery block copolymer poly ethylene oxide poly amide (PEBAX$^{®}$) at 20, 30, 50 and 70°C are presented in Figure 2. Figure 2a shows the isotherms in the case the calculations are based on the dry polymer volume, while Figure 2b shows the isotherms for the calculations based on the wet, swollen volume of the polymer. The sorption isotherms show the behavior typical for either a glassy (S-PEEK) or a rubbery (PEBAX$^{®}$) polymer.
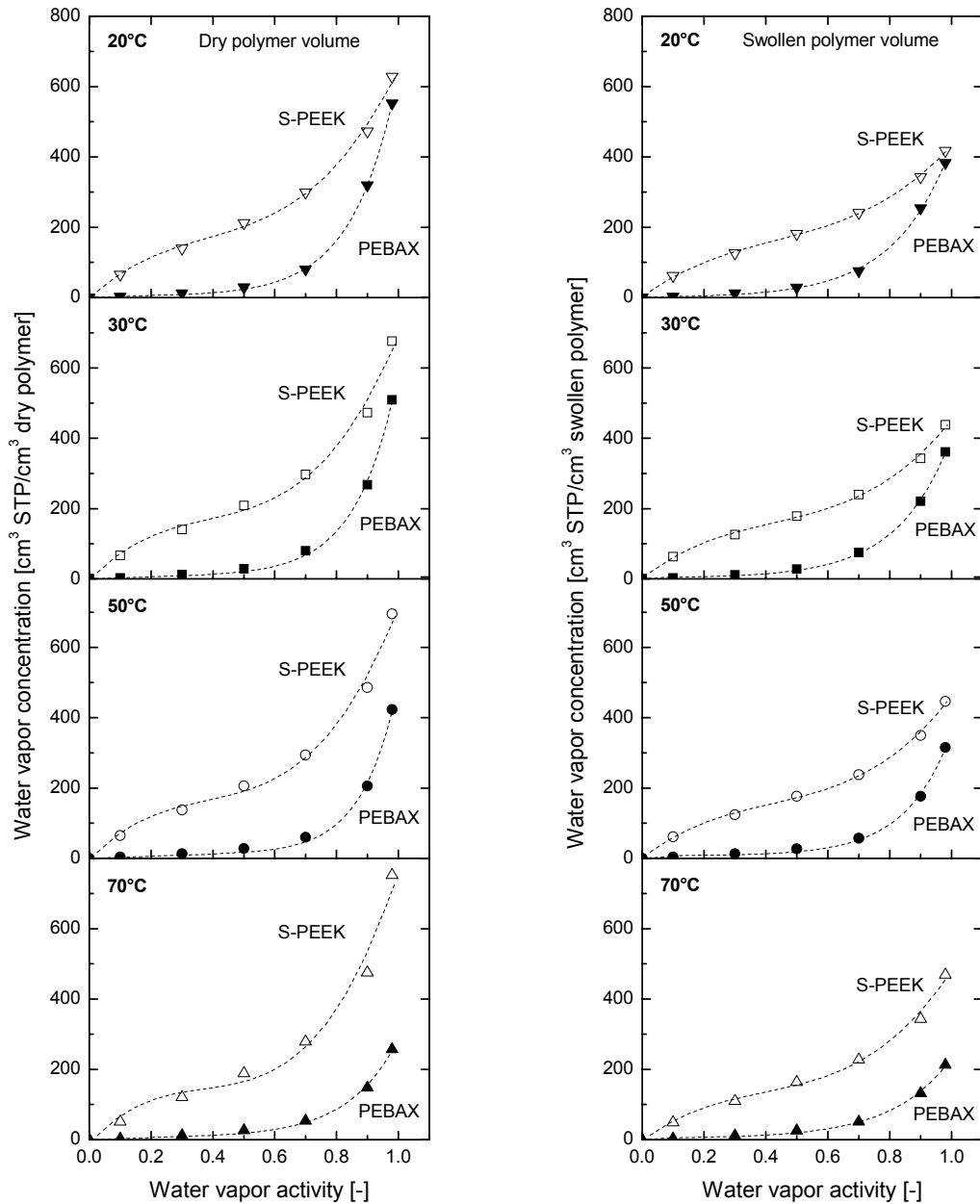
**Figure 2:** Water vapor concentration as a function of the water vapor activity for S-PEEK with a sulfonation degree of 59% and PEBAX® 1074 at 20, 30, 50 and 70°C. Left graphs: calculations based on the dry polymer volume; Right graphs: calculations based on the wet, swollen volume of the polymer.

For the glassy polymer S-PEEK, the sorption isotherms at low water vapor activities (a < 0.5) show a concave increase towards the x-axis and can be described with a dual mode sorption model. At higher water vapor activities (a > 0.5) the isotherms show a convex increase towards the x-axis and the Flory-Huggins sorption model can be used to describe the isotherms. The sorption isotherms of the rubbery polymer PEBAX$^®$ exhibit Flory-Huggins type of sorption, which is reflected in the convex increase of the water vapor concentration over the full range of water vapor activities [2]. The water vapor concentration increases for both polymers with increasing water vapor activity and the values for S-PEEK are higher than the values for PEBAX$^®$ over the complete water vapor activity range. The isotherms based on the wet, swollen polymer volume lay below the isotherms based on the dry polymer volume, which is of course because these isotherms are based on a larger polymer volume.

### *Thermodynamics of water sorption*

Figure 3 presents the free energy of water sorption of water vapor in S-PEEK and PEBAX$^®$ for 20, 30, 50 and 70°C. For comparison, also the free energy of water vapor sorption into liquid water, at activity 1, is presented as a black star (∗). The calculation of the free energy of water sorption from the isotherms offers a way to express the sorption isotherms in terms of a very well defined thermodynamic system.

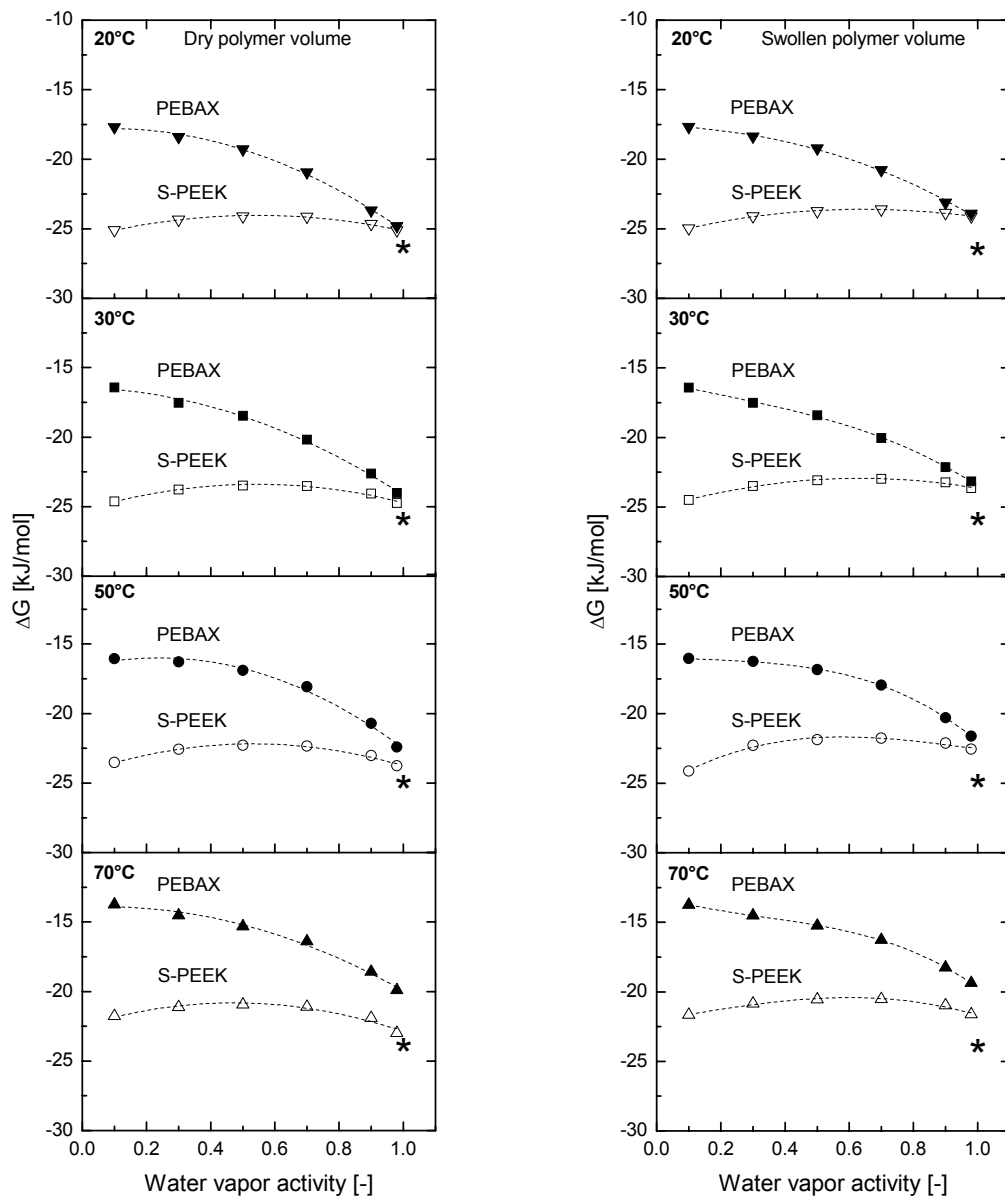**Figure 3:** Free energy of water sorption as a function of the water vapor activity for S-PEEK with a sulfonation degree of 59% and PEBAX[®] 1074 at 20, 30, 50 and 70°C. Left graphs: calculations based on the dry polymer volume; Right graphs: calculations based on the wet, swollen volume of the polymer. The star at water vapor activity 1 represents the free energy of water sorption in liquid water at water/vapor coexistence [15].

For both polymers the free energy of water vapor sorption is negative over the full activity range and becomes less negative with increasing temperature. The free energy of water sorption in S-PEEK is however stronger negative than in PEBAX®, indicating that water molecules interact more favorable with the S-PEEK backbone.

For PEBAX® the free energy becomes more negative with increasing water vapor activity as expected based on the convex shape of the sorption isotherm. It reflects that water vapor sorption is thermodynamically more favorable at higher water vapor activities. The free energy for S-PEEK shows a maximum. This maximum coincides with that water vapor activity where the sorption isotherm (Figure 2) changes from a concave to a convex shape. It indicates that water vapor sorption in S-PEEK is thermodynamically favored at especially low and high water vapor activities.

Although the free energy of water sorption approaches the free energy of water self-solvation (indicated by the black star at water vapor activity 1 in Figure 3), the free energy of water self solvation remains more negative than the free energy of water sorption in S-PEEK and PEBAX® over the full range of water vapor activities (including a = 1), at all investigated temperatures. In the case the free energy of water sorption in the polymer at a = 1 would fall below the free energy of water self-solvation, the polymer would become water soluble.

Differences between the free energy calculated based on the dry polymer volume or the wet, swollen volume are not very significant, except at very high water vapor activities (a > 0.8), where the calculations based on the swollen polymer volume show somewhat higher (less negative) values, due to the excessive swelling at especially high water vapor activities.

The free energy consists of an enthalpic and an entropic contribution. The approach presented in this work allows us to distinguish between both contributions. It thus offers a method to discriminate between the effect of the enthalpy and the entropy of water vapor sorption on the free energy and to address the nature of water sorption and the state of water in both polymers. Figure 4 and 5 present the enthalpic ($\Delta H$) and entropic ($T \cdot \Delta S$)

contribution of water vapor sorption as a function of the water vapor activity at 20, 30, 50 and 70°C calculated based on the dry or the swollen polymer volume using Equations 7 and 8. For comparison, also the free energy of water vapor sorption into liquid water, at activity 1 is presented as a black star (∗) [15].

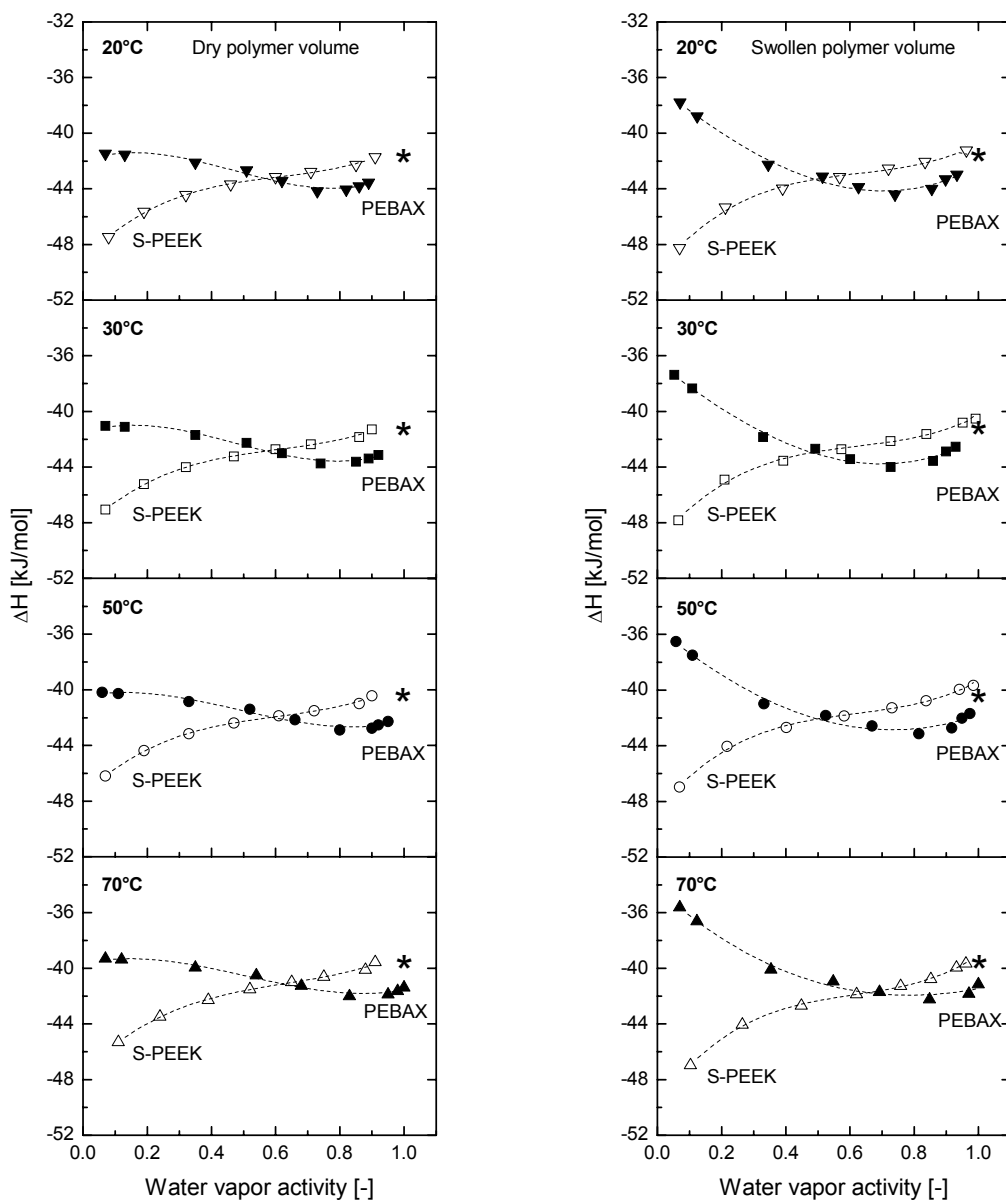**Figure 4:** Heat of water sorption as a function of the water vapor activity for S-PEEK with a sulfonation degree of 59% and PEBAX® 1074 at 20, 30, 50 and 70°C. Left graphs: calculations based on the dry polymer volume; Right graphs: calculations based on the wet, swollen volume of the polymer. The star at water vapor activity 1 represents the free energy of water sorption in liquid water at water/vapor coexistence [15].

In general the differences between the values calculated based on the dry or the swollen polymer volume are small, except for the enthalpy at very low water activities. Because the values based on the swollen state are most close to the environment a water molecule experiences upon sorption in the (partially) swollen polymer, further consideration are based on the calculations based on the swollen polymer.

In all cases, the enthalpy of water sorption in both polymers is negative, i.e. the sorption process is exothermic and heat is released. This is also reflected in the response of the system towards temperature changes: the enthalpy of water sorption becomes less negative with increasing temperature.

Especially at water vapor activities above 0.2, the heat of water sorption in PEBAX$^®$ approximately equals the heat required to solvate a water molecule from the equilibrium vapor phase into pure liquid water (star at water vapor activity 1). This suggests that the interactions an additional water molecule experiences upon sorption in the water swollen polymer PEBAX$^®$ are of equal strength as the interactions it experiences during sorption in liquid water. This leads us to speculate that additional sorbed water molecules experience a water-like environment. This is supported by data obtained from cluster analysis as we will show later. At very low water vapor activities, water molecules absorb in the almost dry polymer and the interactions between the penetrant and the polymer backbone, which are apparently less favorable than the interactions of water self solvation, prevail.

In the sulfonated polymer S-PEEK and especially at lower water vapor activities, the sorption enthalpy has a higher value (more negative) than the amount of heat released when solvating a water molecule into pure liquid water (the heat of vaporization). This indicates that polymer-water interactions prevail over water-water interactions. We hypothesize the more fovarable polymer-water interactions stem from the hydration of the ionogenic sulfon groups present in the sulfonated polymer ($H_3O^+$ formation is energetically favorable), which again is supported by the analysis of the state of water in the polymer (cluster analysis) as we present later. With increasing activity the enthalpy of water sorption moves towards the value of the heat of water sorption in liquid water and

finally levels off, most probably due to the saturation of the ionogenic groups in S-PEEK. Paddison *et al.* [23] showed that the uniform hydration of sulfonated side chains in perfluorosulfonic acid membranes especially at low water vapor concentrations is energetically very favorable. With increasing degree of hydration this favorable state of the system decreases, and finally even disappears. These observations are consistent with our observations.

Figure 5 shows the entropic (T·ΔS) contribution of the sorption of water vapor in the polymers as a function of the water vapor activity and temperature. For comparison, also the free energy of water vapor sorption into liquid water, at activity 1 is presented as a black star (∗) [15].
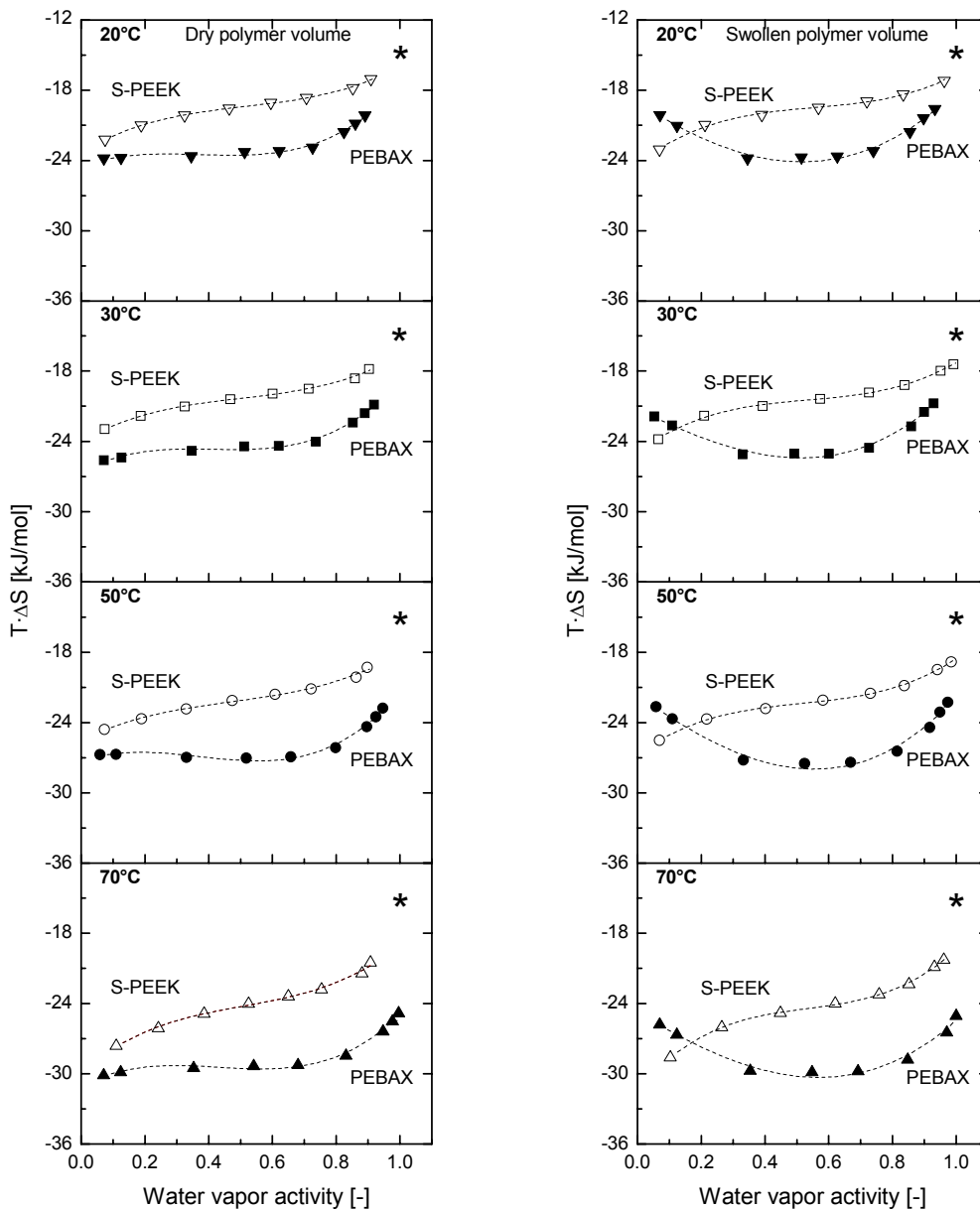
**Figure 5:** Entropy of water sorption as a function of the water vapor activity for S-PEEK with a sulfonation degree of 59% and PEBAX[®] 1074 at 20, 30, 50 and 70°C Left graphs: calculations based on the dry polymer volume; Right graphs: calculations based on the wet, swollen volume of the polymer. The star at water vapor activity 1 represents the free energy of water sorption in liquid water at water/vapor coexistence [15].

The entropy of water sorption for both polymers is negative over the full range of water vapor activities, showing that the dissolution of water molecules in the polymers is

entropically unfavorable. An increase in temperature results in a stronger negative entropic contribution, reflecting the opposing effect of the temperature against water vapor sorption in the polymer.

For PEBAX$^{®}$ the entropy increases (becomes more negative) with increasing water vapor activity and only at very high water vapor activities it increases again (becomes less negative). As we will show later, the reason for more negative entropic contribution with increasing water vapor activity most probably comes from the formation of water clusters in the polymer. Water cluster formation introduces a certain level of organization and reduces the degree of freedom of the molecules in the polymer, resulting in a more negative entropic contribution. At high water vapor activities, were the polymer becomes extremely swollen, this effect of the increased level of organization is, at least partly, compensated by an increased degree of freedom due to the extremely large swelling degree of the polymer.

For SPEEK, the entropic contribution decreases (less negative value) with increasing water vapor activity, suggesting an entropy gain upon water sorption. Water vapor sorption hydrates the ionogenic sulfon groups present in the sulfonated polymer, and this leads to an increased degree of freedom of the protons attached to the negatively charged sulfon groups (the sulfonic acid groups split into negatively charged -$SO_3^-$ and protons). In addition to that also the increase in swelling degree with increasing water vapor sorption contributes to an increase in entropy. Overall, the sorption of water vapor increases the degree of freedom, resulting in an entropically more favorable state.

At higher water vapor activities, the entropic contribution of water vapor sorption in the two polymers converges towards the value found for the entropic contribution of water self solvation, reflecting the large amounts of water absorbed in both hydrophilic polymers, especially at higher water vapor activities.

Together the enthalpic and entropic contributions determine the Gibbs energy of water vapor sorption in the polymers and water vapor sorption can thus be an enthalpy and/or

an entropy driven process. For both polymers, the relation between these two thermodynamic quantities at each specific water vapor activity is presented in Figure 6 for the different temperatures investigated. To avoid confusion, only the values calculated based on the wet, swollen volume of the polymer are shown.
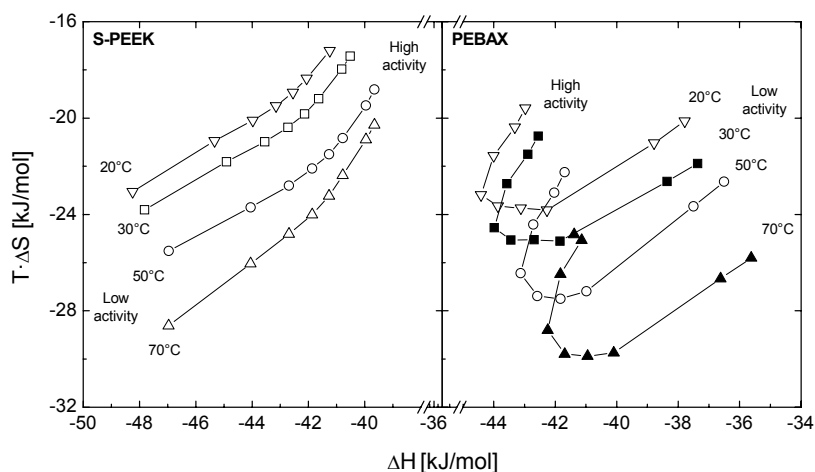


**Figure 6:** Relation between enthalpic and entropic contribution of water vapor sorption at each specific water vapor activity for S-PEEK with a sulfonation degree of 59% and PEBAX[®] 1074 at 20, 30, 50 and 70°C. Calculations based on the wet, swollen volume of the polymer.

Water sorption in both S-PEEK and PEBAX[®] is driven by a favorable water sorption enthalpy. The sorption entropy is unfavorable in both polymers.

In S-PEEK, the change of the water sorption enthalpy and entropy is positive with increasing water vapor activity. The enthalpic contribution becomes less favorable (decreases, shifts to less negative values), whereas the entropic contribution moves in the direction of a more favorable state (lower negative values) with increasing water vapor activity, as shown in Figure 6. This so-called enthalpy-entropy compensation is a well known, but not yet fully understood phenomenon [24] and has been reported earlier in literature for water sorption in polymers [25, 26]. While the water sorption enthalpy (interactions between water and polymer) becomes less favorable (less negative) with increasing water vapor activity, the entropic effects (degree of freedom) become more favorable (less negative). Yampolskii *et al.* [27] showed similar behavior especially for glassy polymers.

PEBAX® shows different behavior. At low activities (< 0.7), enthalpy-entropy compensation is observed as well, although in the case of PEBAX® the enthalpic contribution becomes more negative (favors water sorption) with increasing water vapor activity, whereas at the same time the entropic contribution also becomes more negative and opposes water sorption. At higher water vapor activities, the enthalpy hardly changes with increasing activity (remains negative and favors water sorption), whereas the entropic contribution becomes less negative, thus explaining the more favorable Gibbs energy of water sorption in PEBAX® at higher water vapor activities.

### *Clustering analysis of sorption isotherms*

Figure 7 shows the tendency of water molecules to cluster in the polymer upon sorption of water vapor in S-PEEK and PEBAX® at 20, 30, 50 and 70°C as calculated from the Zimm-Lundberg clustering theory and the experimentally determined sorption isotherms.

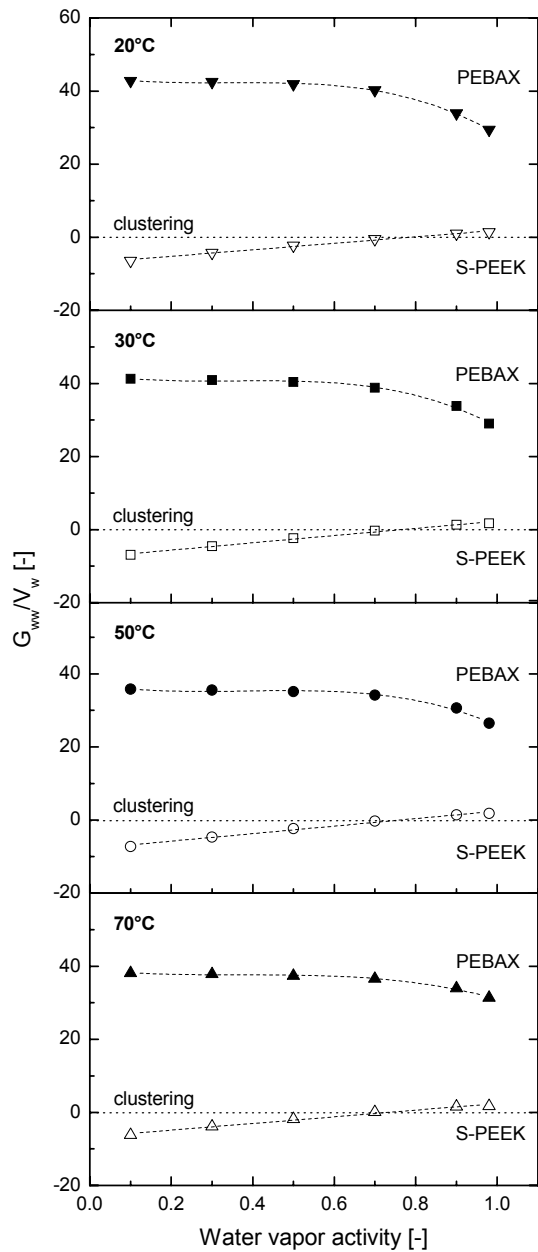**Figure 7:** Cluster integral as a function of the water vapor activity for S-PEEK with a sulfonation degree of 59% and PEBAX® 1074 at 20, 30, 50 and 70°C.

Figure 7 clearly shows that water molecules hardly tend to form clusters in the sulfonated polymer S-PEEK, independent of the water vapor activity and the temperature. Water molecules remain isolated. This supports the observations from the sorption enthalpies

(Figure 4), which are, especially at low water vapor activities, more favorable than the enthalpy of water self solvation (sorption of water in liquid water). Apparently, water molecules that sorb in the polymer matrix form polymer-water interactions instead of water-water interactions. This most probably stems from the ionogenic character of the polymer. The absence of cluster formation also supports the entropic data (Figure 5), which indicate that the sorption of water molecules in S-PEEK does not result in an extra level of organization (water cluster formation) in the polymer-solvent system.

In PEBAX[®] sorbed water molecules have a significant tendency to form water cluster in the polymer at each water vapor activity and temperature (clustering occurs when $G_{ww}/V_w > 0$). Water clustering in polymers is attributed to self-hydrogen bonding of water molecules [19]. One may expect cluster formation when penetrant-penetrant interactions are stronger than penetrant-polymer interactions [28]. This is supported by the thermodynamic analysis presented in this work. The relation between the enthalpy and the water vapor activity (Figure 4) shows that enthalpically penetrant-penetrant interactions are more favorable than polymer-penetrant interactions in PEBAX[®] as shown in Figure 5, and especially at higher water vapor activities, the thermodynamic data show that the newly sorbed water vapor molecule experiences a water-like environment in the polymer PEBAX[®]. The results of the cluster analysis indeed confirm this observation.

# Conclusions

In this work we study the sorption thermodynamics of water vapor in two hydrophilic polymers (sulfonated poly ether ether ketone (S-PEEK) and a poly ethylene oxide-poly amide block copolymer (PEBAX® 1074)). The thermodynamic approach presented offers a strong method to distinguish between enthalpic and entropic contributions of water vapor sorption. It allows to explain the nature of water sorption in both polymers and to address the state of water in the polymer. Calculations based on both the dry or the wet volume are done, but the interpretation of the data is based on the wet swollen volume of the polymer, because this is more realistic and better resembles the environment a water molecule experiences upon sorption in the (partially) swollen polymer and provides a more realistic way to interpret the thermodynamic data.

Analysis of water vapor sorption in S-PEEK and PEBAX® shows that the Gibbs energy of sorption has a negative value in both polymers. For PEBAX® water vapor sorption becomes thermodynamically more favorable at higher water vapor activities, whereas for S-PEEK the free energy shows a maximum. In all cases, the enthalpy of water sorption is negative, i.e. the sorption process is exothermic and heat is released. Especially at higher water vapor activities, the heat of water sorption in PEBAX® equals the heat required to solvate a water molecule from the equilibrium vapor phase into pure liquid water, suggesting that additional sorbed water molecules experience a water-like environment. This is supported by data obtained from cluster analysis which confirm the formation of water clusters in the polymer matrix over the full activity range. In S-PEEK the polymer-water interactions prevail, especially at lower water vapor activities, most probably stemming from the hydration of the ionogenic sulfon groups present in the sulfonated polymer.

The entropy of water sorption for both polymers is negative over the full range of water vapor activities (sorption is entropically unfavorable). For PEBAX® the entropy decreases with increasing water vapor activity over almost the full activity range due to the formation of water clusters which introduces an additional level of organization. For SPEEK the entropy increases (less negative) with increasing sorption due to the increased degree of freedom and the increase in swelling degree.

The thermodynamic analysis shows that for both polymers water sorption is driven by a favorable water sorption enthalpy, whereas the sorption entropy is intrinsically unfavorable. For S-PEEK, water sorption is governed by enthalpy-entropy compensation (with increasing activity the enthalpy and the entropy become less negative). In the case of PEBAX® enthalpy-entropy compensation is observed only at lower activities (with increasing activity, the enthalpy and the entropy become more negative). At higher water vapor activities, the more favorable Gibbs energy of water sorption in PEBAX® is driven by the entropy.

# References

1.  J.G. Wijmans, R.W. Baker, The solution-diffusion model - a review, Journal of Membrane Science 107 (1995) 1-21.

2.  Y. Yampolskii, I. Pinnau, B.D. Freeman, Materials science of membranes for gas and vapor separation, Wiley Chichester, West Sussex, 2006.

3.  S.J. Metz, N.F.A. van der Vegt, M.H.V. Mulder, M. Wessling, Thermodynamics of water vapor sorption in poly(ethylene oxide) poly(butylene terephthalate) block copolymers, Journal of Physical Chemistry B 107 (2003) 13629-13635.

4.  R.M. Barrer, Diffusivities in glassy-polymers for the dual mode sorption model, Journal of Membrane Science 18 (1984) 25-35.

5.  J.A. Horas, F. Nieto, A generalization of dual-mode transport-theory for glassy-polymers, Journal of Polymer Science Part B-Polymer Physics 32 (1994) 1889-1898.

6.  D.R. Paul, Gas sorption and transport in glassy-polymers, Berichte Der Bunsen-Gesellschaft-Physical Chemistry Chemical Physics 83 (1979) 294-302.

7.  R. Kirchheim, Sorption and partial molar volume of small molecules in glassy-polymers, Macromolecules 25 (1992) 6952-6960.

8.  R. Kirchheim, Partial molar volume of small molecules in glassy-polymers, Journal of Polymer Science Part B-Polymer Physics 31 (1993) 1373-1382.

9.  D.K. Lee, Y.W. Kim, K.J. Lee, B.R. Min, J.H. Kim, Thermodynamic model of gas permeability in polymer membranes, Journal of Polymer Science Part B-Polymer Physics 45 (2007) 661-665.

10. J. Ubbink, M.I. Giardiello, H.J. Limbach, Sorption of water by bidisperse mixtures of carbohydrates in glassy and rubbery states, Biomacromolecules 8 (2007) 2862-2873.

11. G.E. Serad, B.D. Freeman, M.E. Stewart, A.J. Hill, Gas and vapor sorption and diffusion in poly(ethylene terephthalate), Polymer 42 (2001) 6929-6943.

12. P.J. Flory, Principles of polymer chemistry, Cornell University Press London, 1953.

13. G.J. Price, D.A. Haddon, A. Bainbridge, J.M. Buley, Vapour sorption studies of polymer-solution thermodynamics using a piezoelectric quartz crystal microbalance, Polymer International 55 (2006) 816-824.

14. B.H. Zimm, J.L. Lundberg, Sorption of vapors by high polymers, Journal of Physical Chemistry B 60(4) (1956) 425-428.

15. A. Ben-Naim, Solvation thermodynamics, Plenum Press (1987).

16. N.F.A. van der Vegt, A molecular dynamics simulation study of solvation thermodynamical quantities of gases in polymeric solvents, Journal of Membrane Science 205 (2002) 125-139.

17. N.F.A. van der Vegt, W.J. Briels, M. Wessling, H. Strathmann, Free energy calculations of small molecules in dense amorphous polymers. Effect of the initial guess configuration in molecular dynamics studies, Journal of Chemical Physics 105 (1996) 8849-8857.

18. G. Skirrow, K.R. Young, Sorption, diffusion and conduction in polyamide-penetrant Systems.1. Sorption phenomena, Polymer 15 (1974) 771-776.

19. B.H. Zimm and J.L. Lundberg, Sorption of vapors by high polymers, Journal of Physical Chemistry B 60(4) (1956) 425-428.

20. E.N. Komkova, M. Wessling, J. Krol, H. Strathmann, N.P. Berezina, Influence of the nature off polymer matrix and the degree of sulfonation on the properties of membranes, Polymer Science Series A 43 (2001) 300-307.

21. V.I. Bondar, B.D. Freeman, I. Pinnau, Gas transport properties of poly(ether-b-amide) segmented block copolymers, Journal of Polymer Science: Part B-Polymer Physics 38 (2000) 2051-2062.

22. J. Potreck, F. Uyar, H. Sijbesma, K. Nijmeijer, D. Stamatialis, M. Wessling, Sorption induced relaxations during water diffusion in SPEEK, Physical Chemistry Chemical Physics DOI: 10.10391/B810638J (2008).

23. S.J. Paddison, J.A. Elliott, Selective hydration of the 'short-side-chain' perfluorosulfonic acid membrane. An ONIOM study, Solid State Ionics 178 (2007) 561-567.

24. E.B. Starikov, B. Norden, Enthalpy-entropy compensation: A phantom or something useful? Journal of Physical Chemistry B 111 (2007) 14431-14435.

25.    R. Moreira, F. Chenlo, M.D. Torres, N. Vallejo, Thermodynamic analysis of experimental sorption isotherms of loquat and quince fruits, Journal of Food Engineering 88 (2008) 514-521.

26.    R.N. Zuniga, P.C. Moyano, F. Pedreschi, Enthalpy-entropy compensation for water loss of potato slices during deep-fat frying, Journal of Food Engineering 88 (2008) 1-8.

27.    Y.P. Yampolskii, N.E. Kaliuzhnyi, S.G. Durgarjan, Thermodynamics of sorption in glassy poly(vinyltrimethylsilane), Macromolecules 19 (1986) 846-850.

28.    J.A. Barrie, B. Platt, The diffusion and clustering of water vapour in polymers, Polymer 4 (1963) 303-313.

# Chapter 4

# Mixed water vapor/gas transport through the rubbery polymer PEBAX® 1074

## Abstract

This work investigates the transport behavior of a hydrophilic, highly permeable type of PEO based block copolymer (PEBAX® 1074) as membrane material for the removal of water vapor from light gasses. Water vapor sorption isotherms in PEBAX® 1074 represent Flory-Huggins type of sorption and the highly hydrophilic nature of the block copolymer results in high amounts of absorbed water (up to 0.4 g of water per gram of dry polymer at 20°C). When taking into account the swelling of the polymer due to water vapor sorption, the Fickian diffusion coefficient increases over the full activity range and changes over two orders of magnitude. As determined from measurements with binary gas mixtures, the water vapor permeability increases exponentially with increasing water vapor activity whereas the nitrogen permeability slightly decreases with increasing water vapor activity. Consequently, the water over nitrogen selectivity increases with increasing water vapor activity.

The results not only show the high potential of hydrophilic PEO-based block copolymers for dehydration purposes (e.g. the dehydration of flue gasses, natural gas dew pointing or the humidification of air). Because of the high interaction of $CO_2$ with the polar ether linkages in PEO based block copolymers, these polymers also offer attractive routes to the integration of dehydration and $CO_2$ capture using membrane technology.

# Introduction

The removal of water vapor from gas streams is an important industrial operation and many applications can be found in e.g. the dehydration of flue gas [1], natural gas dew pointing [2, 3], the drying of compressed air [4] and the storage of fruits and vegetables under protective atmosphere [5]. Membrane technology using polymeric membranes is a promising and attractive technology for dehydration purposes: it has a small footprint, it is easy to operate and it reduces energy costs [1].

In the present work we investigate the potential of membranes for the removal of water vapor from flue gasses. Nowadays, about 85% of our energy is produced by fossil fuel fired power plants which generate tremendous amounts of flue gasses. These gasses consist mostly of nitrogen (~72 vol.%), but also contain ~11 vol.% of water vapor and ~14 vol.% carbon dioxide [1].

Water vapor may condense, which, in combination with traces of sour gasses, causes corrosion in the chimney. Current technologies to avoid condensation include reheating of the gas before emission to the atmosphere, and the use of condensing systems [6] or desiccant methods [7-9]. Membrane technology is a potentially attractive technology for the dehydration of flue gas streams, because of its easy implementation in power plants and its cost effectiveness. Furthermore, the product water can be reused in the steam cycle, as the use of highly selective membrane materials results in extremely high water purities.

This work investigates the behavior of a hydrophilic, highly permeable type of PEO based block copolymer (PEBAX® 1074) as membrane material for the removal of water vapor from flue gasses. Water vapor sorption measurements and mixed water vapor/gas separation measurements are conducted and analyzed to provide insight into the mass transport phenomena of water vapor and nitrogen in the rubbery polymer film. The literature contains several studies on the sorption of vapors into rubbery and glassy polymers [7-12] and more recently these data were used to explain vapor permeation data [11-14]. Nevertheless, only few papers report the simultaneous permeation of gasses and vapors, especially for the combination of water vapor and light gasses, although permeation of one component of a gas mixture through a membrane can significantly

influence the transport behavior of the other components in this mixture [15-17]. The challenge in these experiments lays especially in the determination of the permeability of rapidly and strongly permeating components (i.e. water vapor in PEBAX® 1074) and the simultaneous determination of the permeability of relatively low permeating gasses (i.e. $N_2$ in PEBAX® 1074).

The results of this work are not only of importance for the dehydration of flue gasses to prevent condensation, but it is also of major interest for e.g. natural gas dew pointing or for the drying or humidification of air.


# Theoretical background

## *Water vapor sorption*

Transport of gasses and vapors through dense polymeric films can be described according to the solution-diffusion model [18]. Under the influence of a driving force (e.g. a pressure or concentration gradient), gas molecules first dissolve in the polymer and subsequently diffuse through it. Separation is obtained due to differences in solubility and/or diffusivity of the permeating species. According to the solution-diffusion model, the permeability of component i through a dense polymer membrane ($P_i$ [(cm$^3$·cm)/(cm$^2$·s·cmHg)]) is defined as the product of the diffusivity $D_i$ [cm$^2$/s] and the solubility coefficient $S_i$ [cm$^3$ (STP)/(cm$^3$·cmHg)] of the penetrant in the polymer membrane.

The solubility of a vapor in a polymer can be determined from the weight increase of that polymer due to a change in concentration in the vapor phase it is exposed to. The concentration c of gas or vapor inside a polymer film [g/g] at every water vapor activity can thus be calculated from:

$$c = \frac{M_\infty - M_{dry}}{M_{dry}} \tag{1}$$

where $M_\infty$ [g] is the equilibrium mass of the polymer sample and the absorbed water at a certain water vapor activity, and $M_{dry}$ [g] is the dry weight of the polymer.

*Fickian diffusion model*

Diffusion coefficients of penetrants in polymers can be determined from kinetic sorption data. The mathematical theory of diffusion in isotropic substances is based on the assumption that the rate of transfer of the diffusing substance i per unit area is proportional to the concentration gradient measured perpendicular to that area [18]. For thin film geometries in which diffusion from the edges of the film is neglected, only a concentration gradient along the x-axis exists. Based on Fick's first and second law, Crank [19] deduced that in these cases the diffusion coefficient at short time scales can be described by:

$$\frac{M_t}{M_\infty} = \frac{4}{l_p} \sqrt{\frac{D \cdot t}{\pi}}$$

(2)

where $M_t$ [g] is the mass of sorbed water vapor at time t [s], $M_\infty$ [g] is the mass sorbed at $t = \infty$, $l_p$ [m] is the polymer film thickness and D [m²/s] is the Fickian diffusion coefficient.

The Fickian diffusion coefficient for water in the polymer matrix can thus be determined from the initial slope of a plot of $M_t/M_\infty$ versus $t^{1/2}$ (as can be extracted from kinetic sorption experiments).

At longer time scales the Fickian diffusion coefficient can be calculated from:

$$\ln\left(1 - \frac{M_t}{M_\infty}\right) = \ln\frac{8}{\pi^2} - \frac{\pi^2 D \cdot t}{l_p^2}$$

(3)

where $M_t$ [g] is the mass of sorbed water at time t [s], $M_\infty$ [g] is the mass penetrated at $t = \infty$, $l_p$ [m] is the polymer film thickness and D [m²/s] is the Fickian diffusion coefficient. In this case the Fickian diffusion coefficient can be deduced from the slope of a plot of $\ln(1-M_t/M_\infty)$ versus t.

Equation 2 and 3 cross at $D \cdot t/l^2 = 0.05326$ ($M_t/M_\infty \approx 0.52$) and the combination of these two first-term approximations provides an excellent approximation to extract the diffusion coefficient over the entire sorption-time domain [4].

# Experimental part

## *Membrane preparation*

PEBAX[®] 1074 was used as membrane material. It is a hydrophilic, commercially available block copolymer consisting of 45 wt.-% hard poly amide blocks (PA12 or Nylon 12) and 55 wt-% soft poly ethylene oxide (PEO) blocks [20]. Dissolution of gas and water vapor and subsequent diffusion primarily occurs through the (soft) amorphous PEO phase in the polymer. The hard crystalline PA blocks provide mechanical stability to the membrane. Figure 1 shows the chemical structure of PEBAX[®].
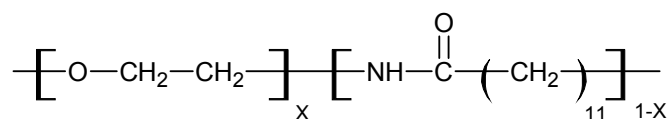


**Figure 1:** Chemical structure of PEBAX[®].

To prepare the membranes, 7 wt.-% of PEBAX[®] 1074 was dissolved at 100°C in N-methyl-2-pyrrolidone (NMP, purchased from Acros Organics). The hot solution was cast on a preheated glass plate (80°C) with a 0.47-mm casting knife. The solvent was evaporated under nitrogen atmosphere and subsequently the membranes were placed in a nitrogen oven at 80°C for one week to remove any residual solvent. After that the membranes were removed from the glass plate with water and subsequently washed with water for another three days. Finally, the membranes were stored in a vacuum oven at 30°C. Membranes were used when no further mass decrease in time was observed (~14 days).

## *Water vapor sorption experiments*

Water vapor sorption experiments were carried out using a gravimetric sorption balance (SGA-100 symmetrical gravimetric analyzer from VTI (USA) supplied by Ankersmid (The Netherlands)). The membrane sample (weight ~ 3mg) was placed in the device and flushed with dry nitrogen for 24 hours to remove any residues. The final dry weight of the sample was measured. Subsequently, a humidified nitrogen stream was mixed with a dry

nitrogen stream to obtain the desired water vapor activity, which is defined as the ratio of the water vapor pressure at a certain temperature and the maximum water vapor pressure at that temperature. It can be changed instantaneously by varying the mixing ratio of the dry and wet nitrogen flow. The humidified gas stream was fed into the thermostated measuring chamber and the actual activity in the sample chamber was controlled with a dew point mirror. The total gas flow velocity was kept constant to avoid any upward drag force on the sample. The weight of the sample was monitored continuously. Sorption and desorption experiments were carried out at 20, 30, 50 and 70°C and the corresponding isotherms were obtained through a stepwise increase or decrease of the water vapor activity.

### *Mixed water vapor/gas permeation*

The mixed water vapor/nitrogen permeabilities of PEBAX® 1074 were measured in the setup earlier described by Sijbesma *et al.* [1] and Metz *et al.* [16]. It allows the simultaneous permeation of water vapor and nitrogen at different water vapor activities ($p_{H2O}/p_{H2O, \text{ saturated}}$) and temperatures (30, 50 and 70°C). The original setup [16] was modified such that the temperature of the system was controlled by an oven (Binder, Tuttlingen-Germany) to achieve a homogeneous heat distribution in the system [1]. Both the water vapor flux and the nitrogen flux were measured simultaneously in time, and the respective permeabilities were calculated according to the method earlier described [1, 16].

# Results

## *Water vapor sorption*

Water vapor sorption experiments in PEBAX® 1074 were performed to analyze the uptake of water vapor at 20, 30, 50 and 70°C. Figure 2 shows the concentration of water vapor inside the polymer as a function of the water vapor activity at different temperatures. Data obtained from both sorption (open symbols) and desorption (closed symbols) runs are presented (both sorption and desorption are measured at each water vapor activity, but the symbols overlap).
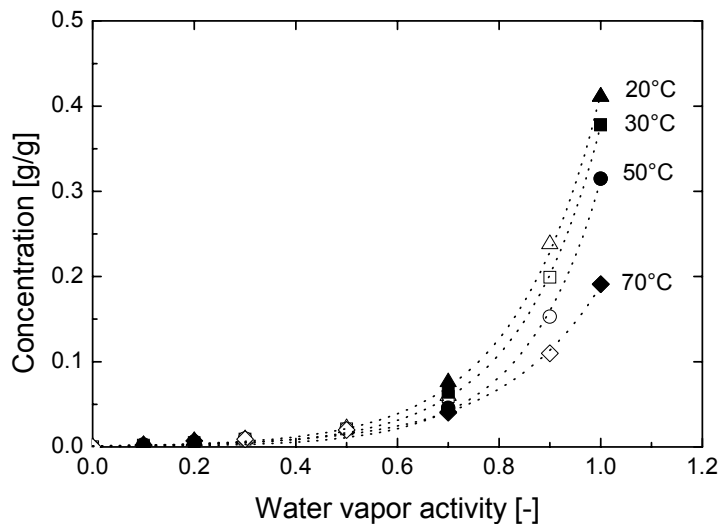


**Figure 2:** Water concentration in PEBAX® 1074 as a function of the water vapor activity for sorption (open symbols) and desorption (closed symbols) runs at 20, 30, 50 and 70°C

The concentration of water vapor inside PEBAX® 1074 increases exponentially with increasing water vapor activity. The sorption isotherms represent Flory-Huggins type sorption (convex increase towards the x-axis). This behavior is typical for rubbery polymers like PEBAX® 1074 [21].

Especially at higher water vapor activities (a > 0.6), temperature has a significant effect on the amount of water vapor absorbed into the polymer: the concentration of water vapor inside the polymer decreases with increasing temperature.

As expected for rubbery polymers, hysteresis is not observed and the isotherms for sorption and desorption coincide. Berens [22] and Wessling [23] interpret hysteresis as the induction of new free volume sites due to relaxation phenomena in the polymer during sorption and subsequent filling of the extra free volume. In rubbery polymers such as PEBAX® 1074, relaxation phenomena do not occur and hysteresis is not observed. As the sorption and desorption isotherms show similar behavior, only sorption runs are used for further analysis.

### Fickian Diffusion

The experimentally obtained kinetic sorption data were analysed and the diffusion coefficient of water vapor in PEBAX® 1074 as a function of the water vapor activity and the temperature was determined. Fickian diffusion is expected because PEBAX® 1074 is in its rubbery state at all measurement temperatures, and relaxation effects do not occur (no hysteresis is observed). Figure 3 shows the Fickian diffusion coefficient of water vapor in PEBAX® 1074 versus the water vapor activity at 20, 30, 50 and 70°C, as calculated from Equations 2 and 3.
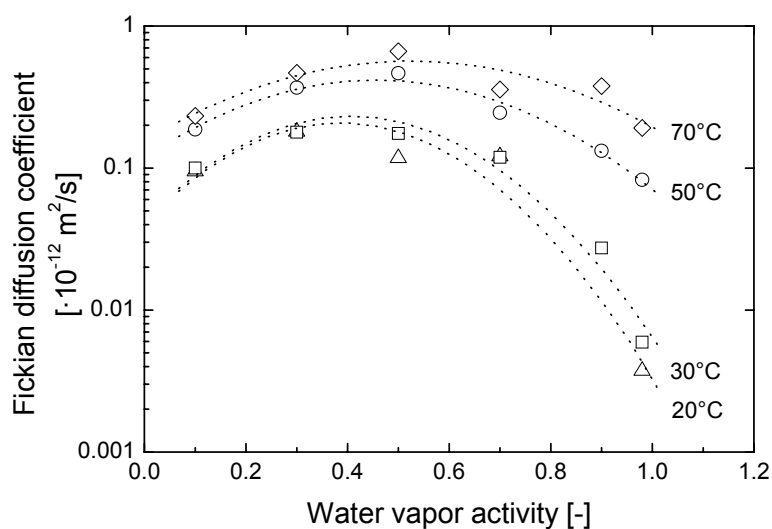


**Figure 3:** Fickian diffusion coefficient of water vapor as a function of the water vapor activity for PEBAX® 1074 at 20, 30, 50 and 70°C

The diffusion coefficient increases with increasing temperature and increasing water vapor activity at low water vapor activities (a < 0.5). For higher water vapor activities (a > 0.5), the diffusion coefficient decreases again with increasing water vapor activity. This maximum in Fickian diffusion coefficient is often explained from clustering phenomena. According to Yampolskii et al. [21], Flory-Huggins sorption behavior is usually accompanied by an increase in diffusion coefficient at higher activities, but clustering phenomena can lead to a decrease in diffusion coefficients at higher water vapor activities. One may argue if this water clustering due to hydrogen bonding, which is a dynamic process and typically occurs in the order of (tenth of) pico seconds [24], indeed hinders the diffusion of water molecules, which typically occurs over much larger time scales, as presented here. We hypothesize that the maximum is at least also partly due to the high degree of swelling of the polymer, especially at higher water vapor activities, which is not taken into account when calculating the Fickian diffusion coefficient presented in Figure 3 [25]. Due to the high degree of swelling of the polymer, especially at high water vapor concentrations, the assumed frame of constant polymer dimensions is no longer true. We can take this swelling effect into account and correct the Fickian diffusion coefficient for this using Equation 4, in which the swelling effect is expressed in the volume fraction of water vapor in the swollen polymer [25]:

$$D_{Fick,c} = \frac{D_{Fick}}{(1-\Phi_s)^{\frac{5}{3}} \frac{\partial \ln a}{\partial \ln \Phi_s}} \tag{4}$$

Where $D_{Fick,c}$ is the Fickian diffusion coefficient corrected for the swelling of the polymer during water vapor sorption ($m^2$/s), a is the water vapor activity of the vapor phase (-) and $\Phi_s$ is the volume fraction of the penetrant (-) obtained from the weight uptake due to water sorption and the partial molar volume of the penetrant at each specific water vapor activity and measurement temperature.
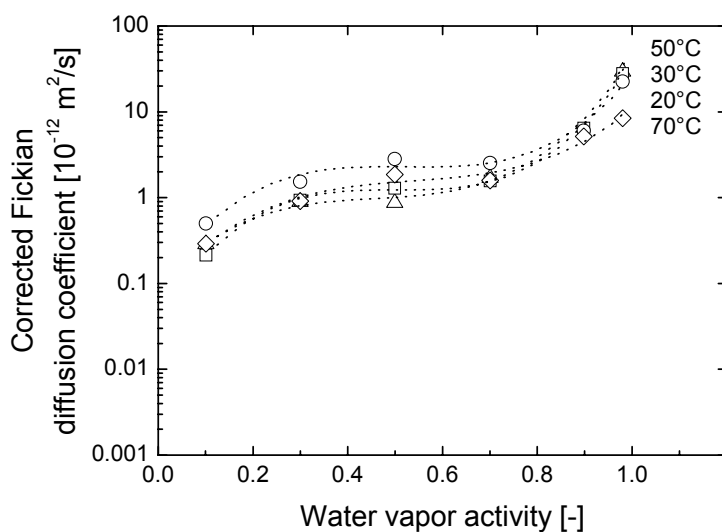
**Figure 4:** Fickian diffusion coefficient of water vapor corrected for the swelling of the polymer as a function of the water vapor activity for PEBAX® 1074 at 20, 30, 50 and 70°C

After correction for the swelling of the polymer due to water vapor sorption, the Fickian diffusion coefficient indeed increases over the full range of activities (Figure 4). Counter intuitively, in the high activity range, the diffusion coefficient at 70°C is slightly lower that the values found for the other temperatures, but this is due to the lower degree of swelling of the polymer at that temperature, resulting in a denser structure for the water molecules to diffuse through. Apparently this effect dominates the effect of an increase in diffusion coefficient with increasing temperature. The strong increase in Fickian diffusion coefficient at especially higher water vapor activities is due to the exponential increase in water vapor uptake with increasing activity.

## *Water vapor and gas transport*

The occurrence of sorption and diffusion and thus permeation of one component of a gas or vapor mixture through a membrane can influence the transport behavior of the other components in this mixture as well [15, 26]. To the best of our knowledge, only very few papers report the simultaneous permeation of water vapor/light gas mixtures through dense polymer membranes [16]. The challenge in these experiments lays especially in the

determination of the permeability of rapidly and strongly permeating components (i.e. water vapor in PEBAX® 1074) and the simultaneous determination of the permeability of relatively low permeating gasses (i.e. $N_2$ in PEBAX® 1074). In the present work we performed such measurements for the separation of the binary mixture water vapor/nitrogen using PEBAX® 1074 as membrane material.

Figure 5 shows the mixed water vapor permeability of PEBAX® 1074 versus the water vapor activity at 30, 50 and 70°C, as measured using a binary water vapor/nitrogen mixture.
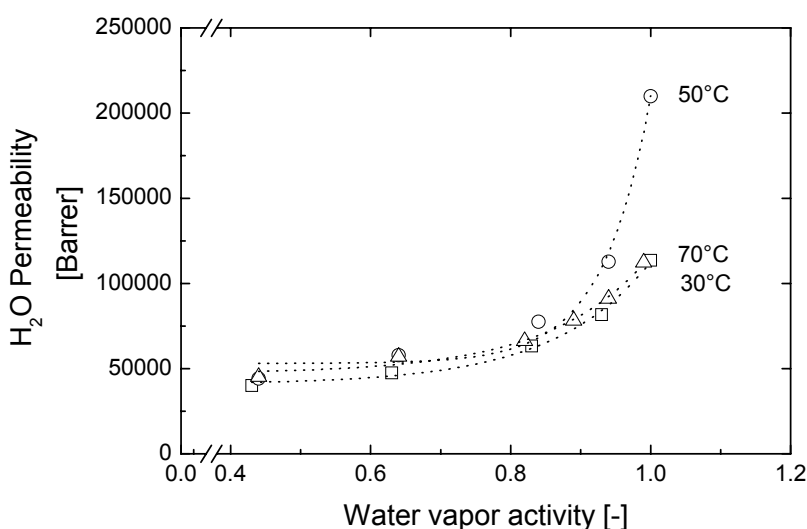


**Figure 5:** Water vapor permeability of PEBAX® 1074 as a function of the water vapor activity at 30, 50 and 70°C measured from a mixed water vapor/nitrogen feed.

The water vapor permeability increases exponentially with increasing water vapor activity. This effect is especially pronounced at 50°C while the values for 30 and 70°C are lower and almost overlap. This can be explained from the relative contribution of solubility and diffusivity to the overall permeability of the vapor in the polymer. The diffusivity increases with increasing temperature and the solubility decreases with increasing temperature. At 50°C the relative increase in diffusivity is more pronounced than the relative decrease in solubility of water vapor in the polymer, resulting in a net increase in permeability at 50°C compared to the other two temperatures. At 30°C, the

lower permeability at higher activities compared to 50°C is due to the low diffusivity at that temperature, whereas at 70°C the lower permeability at higher activities is the result of the relatively larger decrease in solubility at higher temperatures.

Figure 6 shows the nitrogen permeability as a function of the water vapor activity of PEBAX® 1074 as determined from a mixed water vapor/nitrogen feed at 30, 50 and 70°C.
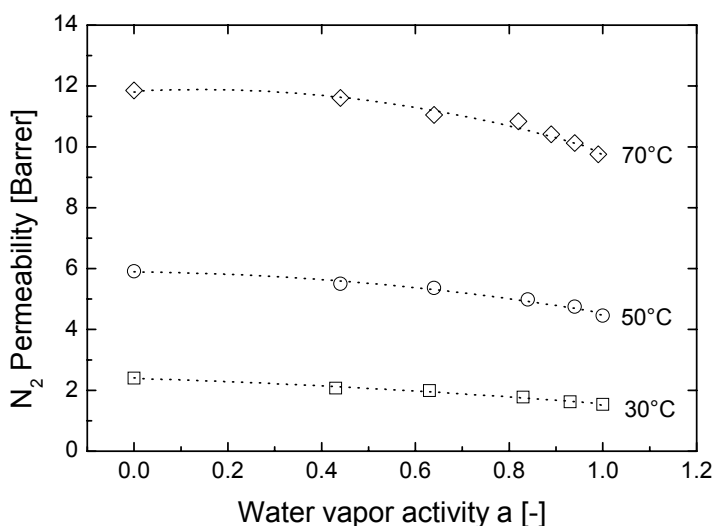


**Figure 6:** Nitrogen permeability as a function of the water vapor activity for PEBAX® 1074 as determined from mixed water vapor/nitrogen permeation experiments at 30, 50 and 70°C.

Figure 6 shows that the 'dry' nitrogen permeability in PEBAX® (at zero activity) is 2.2 Barrer at 30°C. This is comparable to the dry nitrogen permeability in PEBAX® as reported by Bondar *et al.* [10]. The nitrogen permeability slightly decreases with increasing water vapor activity. We hypothesize that an explanation for that could be that the presence of water in the polymer effects the solubility of the gas in the water swollen polymer film. With increasing activity, the amount of water sorbed in the polymer increases, and as a result nitrogen molecules that dissolve in and diffuse through the film experience a more water-like environment, in contrast to the polymer environment at low water vapor activities. The same effect was observed by Freeman *et al.* [27] who show

that with increasing $n-C_4H_{10}$ concentration in the rubbery polymer PDMS, the polymer environment changes to an environment more similar to that of $n-C_4H_{10}$ in which $CH_4$ is more soluble, resulting in higher $CH_4$ solubility with increasing $n-C_4H_{10}$ activity.

The nitrogen permeability increases with increasing temperature. This is the result of the more significant increase in diffusion coefficient of the gas than the decrease in solubility with increasing temperature.

The selectivity of a membrane for a certain set of gasses or vapors is a measure of its separating performance: it shows the ability of the material to discriminate between the components. Often, selectivities calculated from single gas permeation experiments are reported although permeation of one component of a gas mixture through a membrane can significantly influence the transport behavior of the other components in this mixture [15-17]. Figure 7 reports the water vapor over nitrogen selectivity as determined from the binary feed mixture (water vapor/nitrogen) for PEBAX® 1074 as a function of the water vapor activity and the three experimental temperatures investigated.
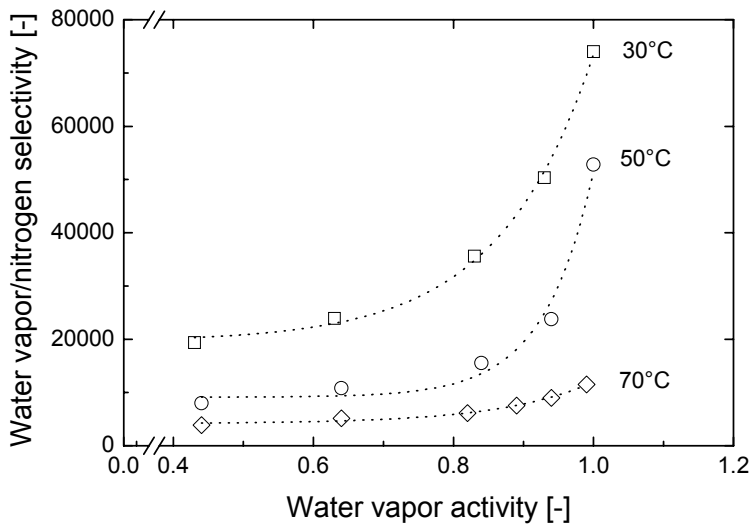


**Figure 7:** Water vapor over nitrogen selectivity as a function of the water vapor activity for PEBAX® 1074 at 30, 50 and 70°C

The water over nitrogen selectivity as determined from permeation experiments with binary mixtures increases with increasing water vapor activity. This is mainly due to the increase in water vapor permeability with increasing water vapor activity and in addition to that to the decrease in nitrogen permeability with increasing water vapor activity. Single gas water vapor and nitrogen permeation experiments would underestimate the separating performance of PEBAX$^{®}$ 1074 because the presence of water vapor influences the permeance of nitrogen.

The decrease in selectivity with increasing temperature is mainly due to the higher nitrogen permeabilities at higher temperatures. The water vapor over nitrogen selectivity obtained for PEBAX$^{®}$ at 50°C (~50.000) is higher than the corresponding water vapor over nitrogen selectivities reported in literature for PEO-PBT block copolymers (~10.000) [28], which is mainly due to the higher water vapor permeability of PEBAX$^{®}$ compared to PEO-PBT at 50°C.


The combination of the very high water vapor permeabilities with the high water vapor over nitrogen selectivities not only shows the high potential of such hydrophilic PEO-based block copolymers for dehydration purposes (e.g. the dehydration of flue gasses, natural gas dew pointing or the humidification of air). Because of the high interaction of $CO_2$ with the polar ether linkages in PEO based block copolymers, it also offers attractive routes to the integration of dehydration and $CO_2$ capture using membrane technology.

# Conclusions

The present work investigated the behavior of a hydrophilic, highly permeable type of PEO based block copolymer (PEBAX$^{®}$ 1074) as membrane material for the removal of water vapor from nitrogen using a multiple component feed mixture (water vapor and nitrogen). The sorption isotherms represent Flory-Huggins type sorption and the highly hydrophilic nature of the block copolymer results in high amounts of absorbed water, especially at low temperatures. Hysteresis phenomena are not observed.

When taking into account the swelling of the polymer due to water vapor sorption, the Fickian diffusion coefficient increases with increasing activity and temperature and changes over two orders of magnitude.

As determined from measurements with binary gas mixtures, the water vapor permeability increases exponentially with increasing water vapor activity whereas the nitrogen permeability slightly decreases with increasing water vapor activity. Consequently, the water over nitrogen selectivity increases with increasing water vapor activity.

The combination of the very high water vapor permeabilities with the high water vapor over light gas selectivities, not only shows the high potential of such hydrophilic PEO-based block copolymers for dehydration purposes (e.g. the dehydration of flue gasses, natural gas dew pointing or the humidification of air). Because of the interaction of $CO_2$ with the polar ether linkages in PEO based block copolymers, it also provides attractive opportunities for the integration of dehydration and $CO_2$ capture using membrane technology.

# References

1. H. Sijbesma, K. Nymeijer, R. van Marwijk, R. Heijboer, J. Potreck, M. Wessling, Flue gas dehydration using polymer membranes, Journal of Membrane Science 313 (2008) 263-276.

2. K. Ohlrogge, T. Brinkmann, Natural gas cleanup by means of membranes, Advanced Membrane Technology 984 (2003) 306-317.

3. K. Ohlrogge, B. Keil, J. Wind, Dehydration and hydrocarbon dewpointing of natural gas by membrane technology., Abstracts of Papers of the American Chemical Society 221 (2001) U225-U225.

4. C.M. Balik, On the extraction of diffusion coefficients from gravimetric data for sorption of small molecules by polymer thin films, Macromolecules 29 (1996) 3025-3029.

5. B.H. Dijkink, M.M. Tomassen, J.H.A. Willemsen, W.G. van Doorn, Humidity control during bell pepper storage, using a hollow fiber membrane contactor system, Postharvest Biology and Technology 32 (2004) 311-320.

6. M. Strand, J. Pagels, A. Szpila, A. Gudmundsson, E. Swietlicki, M. Bohgard, M. Sanati, Fly ash penetration through electrostatic precipitator and flue gas condenser in a 6 MW biomass fired boiler, Energy & Fuels 16 (2002) 1499-1506.

7. X.H. Liu, Y. Zhang, K.Y. Qu, Y. Jiang, Experimental study on mass transfer performances of cross flow dehumidifier using liquid desiccant, Energy Conversion and Management 47 (2006) 2682-2692.

8. S.A. Abdul-Wahab, Y.H. Zurigat, M.K. Abu-Arabi, Predictions of moisture removal rate and dehumidification effectiveness for structured liquid desiccant air dehumidifier, Energy 29 (2004) 19-34.

9. Y.H. Zurigat, M.K. Abu-Arabi, S.A. Abdul-Wahab, Air dehumidification by triethylene glycol desiccant in a packed column, Energy Conversion and Management 45 (2004) 141-155.

10. V.I. Bondar, B.D. Freeman, I. Pinnau, Gas transport properties of poly(ether-b-amide) segmented block copolymers, Journal of Polymer Science: Part B-Polymer Physics 38 (2000) 2051-2062.

11.    R.S. Prabhakar, B.D. Freeman, I. Roman, Gas and vapor sorption and permeation in poly(2,2,4-trifluoro-5-trifluoromethoxy-1,3-dioxole-co-tetrafluoroethylene), Macromolecules 37 (2004) 7688-7697.

12.    Y.M. Sun, C.H. Wu, A. Lin, Permeation and sorption properties of benzene, cyclohexane, and n-hexane vapors in poly [bis(2,2,2-trifluoroethoxy)phosphazene] (PTFEP) membranes, Polymer 47 (2006) 602-610.

13.    A.Y. Alentiev, V.P. Shantarovich, T.C. Merkel, V.I. Bondar, B.D. Freeman, Y.P. Yampolskii, Gas and vapor sorption, permeation, and diffusion in glassy amorphous teflon AF1600, Macromolecules 35 (2002) 9513-9522.

14.    K.A. Lokhandwala, S.M. Nadakatti, S.A. Stern, Solubility and transport of water-vapor in some 6FDA-based polyimides, Journal of Polymer Science: Part B-Polymer Physics 33 (1995) 965-975.

15.    P. Kumar, S. Kim, J. Ida, V.V. Guliants, Polyethyleneimine-modified MCM-48 membranes: Effect of water vapor and feed concentration on $N_2/CO_2$ selectivity, Industrial & Engineering Chemistry Research 47 (2008) 201-208.

16.    S. Metz, W. van de Ven, J. Potreck, M. Mulder, M. Wessling, Transport of water vapor and inert gas mixtures through highly selective and highly permeable polymer membranes, Journal of Membrane Science 251 (2005) 29-41.

17.    F. Piroux, E. Espuche, R. Mercier, The effects of humidity on gas transport properties of sulfonated copolyimides, Journal of Membrane Science 232 (2004) 115-122.

18.    J.G. Wijmans, R.W. Baker, The solution-diffusion model - a review, Journal of Membrane Science 107 (1995) 1-21.

19.    J. Crank, The mathematics of diffusion, Oxford University Press London, 1975.

20.    Bondar V.I., Freeman B.D., Pinnau I., Gas sorption and characterization of poly(ether-b-amide) segmented block copolymers, Journal of Polymer Science, Part B: Polymer Physics 37 (1999) 2463-2475.

21.    Y. Yampolskii, I. Pinnau, B.D. Freeman, Materials science of membranes for gas and vapor separation, Wiley 2006.

22.     A.R. Berens, Effects of sample history, time, and temperature on the sorption of monomer vapor by PVC, Journal of Macromolecular Science: Physical Edition 14 (1977) 483-498.

23.     M. Wessling, M.L. Lopez, H. Strathmann, Accelerated plasticization of thin-film composite membranes used in gas separation, Separation and Purification Technology 24 (2001) 223-233.

24.     S. Yeremenko, M.S. Pshenichnikov, D.A. Wiersma, Hydrogen-bond dynamics in water explored by heterodyne-detected photon echo, Chemical Physics Letters 369 (2003) 107-113.

25.     I. Blume, P.J.F. Schwering, M.H.V. Mulder, C.A. Smolders, Vapour sorption and permeation of poly(dimethylsiloxane) films, Journal of Membrane Science 61 (1991) 85-97.

26.     S.S. Dhingra, E. Marand, Mixed gas transport study through polymeric membranes, Journal of Membrane Science 141 (1998) 45-63.

27.     R.D. Raharjo, B.D. Freeman, E.S. Sanders, Pure and mixed gas $CH_4$ and n-$C_4H_{10}$ sorption and dilation in poly(dimethylsiloxane), Journal of Membrane Science 292 (2007) 45-61.

28.     S.J. Metz, W.J.C. van de Ven, M.H.V. Mulder, M. Wessling, Mixed gas water vapor/$N_2$ transport in poly(ethylene oxide) poly(butylene terephthalate) block copolymers, Journal of Membrane Science 266 (2005) 51-61.

# Chapter 5

## Membranes for controlled humidification of gas streams

## Abstract

The present work investigates the potential of hydrophilic membranes based on sulfonated poly (ether ether ketone) for the controlled humidification of gas streams and the temperature and gas flow rate are used as tools to tune and control the relative humidity. The proposed membrane material allows the passage of water only, while most of the contaminations are retained. As such, membrane assisted gas humidification integrates purification and humidification in one single step.

Water vapor fluxes up to 11 kg/m$^2$·h could be obtained and relative humidities ranging from 40 up to 100% could be realized with a single hollow fiber membrane coated with a dense layer of S-PEEK. The water vapor flux increases with increasing nitrogen flow rate and increasing temperature of the liquid water. The overall membrane resistance is five orders of magnitude higher than the resistance at the permeate side and mainly governs the humidification process. The results prove that membrane assisted gas humidification is a promising alternative for conventional humidification methods.

# Introduction

We recently demonstrated that a membrane based on sulfonated poly ether ether ketone (S-PEEK) has excellent transport properties for water vapor and extremely high selectivities for water vapor over nitrogen [1]. These membranes were successfully tested for the dehydration of flue gas [1], but are also suitable candidates for the controlled humidification of gas streams. The present work investigates the potential and operating window of these membranes for the controlled humidification of gas streams.

Traditional humidification processes use bubblers [2], unheated humidifiers [2], sprayers [3] or rotating discs [4] to humidify gas streams. One of the biggest disadvantages of these conventional methods is the required pretreatment of water to create ultra pure water vapor. Extremely pure water vapor is required in a wide range of industrial applications, but especially important in fuel cells [5, 6], the semiconductor industry [7, 8] and in medical systems [9].

Membrane assisted gas humidification integrates purification and humidification in one single step. The proposed membrane material allows the passage of water only, while most of the contaminations are retained. Variation of a single parameter to tune the relative humidity for the specific application is preferred to keep the system simple. On the other hand, control over a wide range of relative humidities is needed to create flexibility in the process. In the present work we apply membrane assisted gas humidification to humidify a nitrogen stream and we use the temperature and/or the gas flow rate as tools to tune and control this relative humidity.

# Experimental

### *Composite hollow fiber membrane preparation*

Composite hollow fiber membranes were used for humidification experiments. A thin layer of sulfonated poly ether ether ketone (S-PEEK) as highly water vapor permeable separating layer was applied on top of a porous poly ether sulfone (PES) microfiltration membrane (Norit/X-Flow, The Netherlands) using dipcoating. S-PEEK (Figure 1) was prepared by sulfonation of 60 g of PEEK (Victrex, USA), according to the procedure earlier described by Komkova *et al.* [10]. In this work S-PEEK with a sulfonation degree

of 73% was used. The degree of sulfonation reflects the fraction of sulfonic acid groups present in the polymer chain, which in this particular case means that 73% of the repeating unit of the polymer chain is sulfonated (X=0.73).
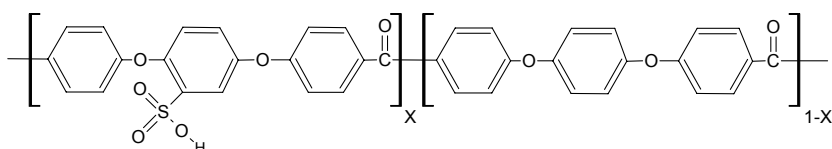


**Figure 1:** Chemical structure of sulfonated poly ether ether ketone (S-PEEK).

The coating solution was prepared by dissolving 3 wt.-% of S-PEEK in methanol (Aldrich). After filtration of the coating solution over a 15 μm metal filter, the porous PES fibers were dip coated 3 to 5 times in the S-PEEK-methanol solution to achieve a dense, defect free separating layer. The applied coating layer had a thickness of approximately 20 μm, homogeneously applied over the whole length of the fiber. Figure 2 shows a scanning electron microscopy (SEM) picture of this coated fiber.
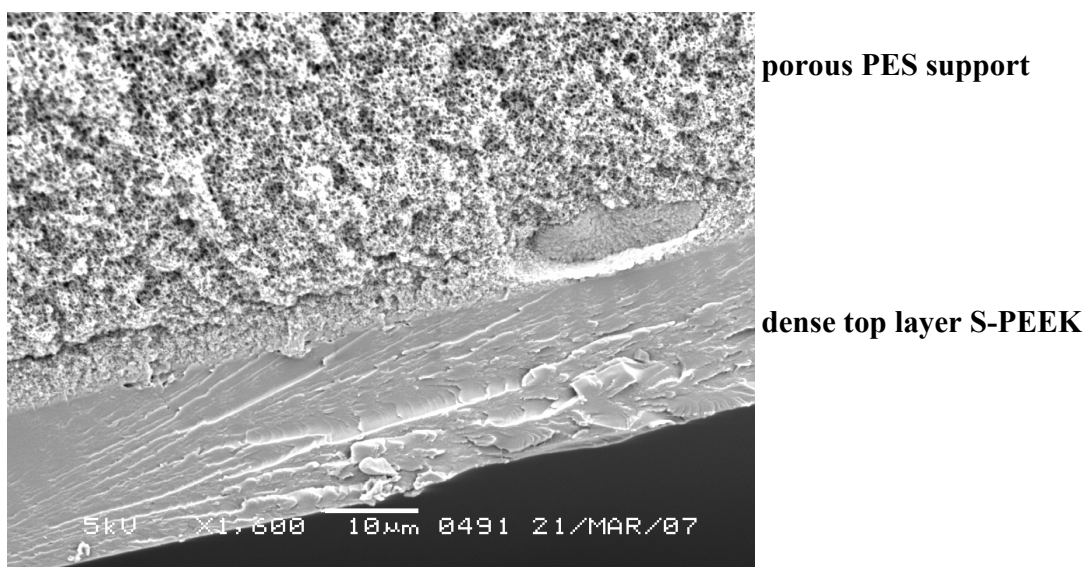


porous PES support

dense top layer S-PEEK

**Figure 2:** SEM picture of the prepared composite hollow fiber membrane with a top layer of sulfonated poly ether ether ketone.

*Experimental set-up for controlled humidification*

Gas humidification experiments were performed with one single fiber, coated with a dense layer of S-PEEK. The fiber had a length of 20 cm and both ends were potted into PE tubes. The potted ends were squeezed with rubber rings into a glass module. The experimental set up is schematically presented in Figure 3.
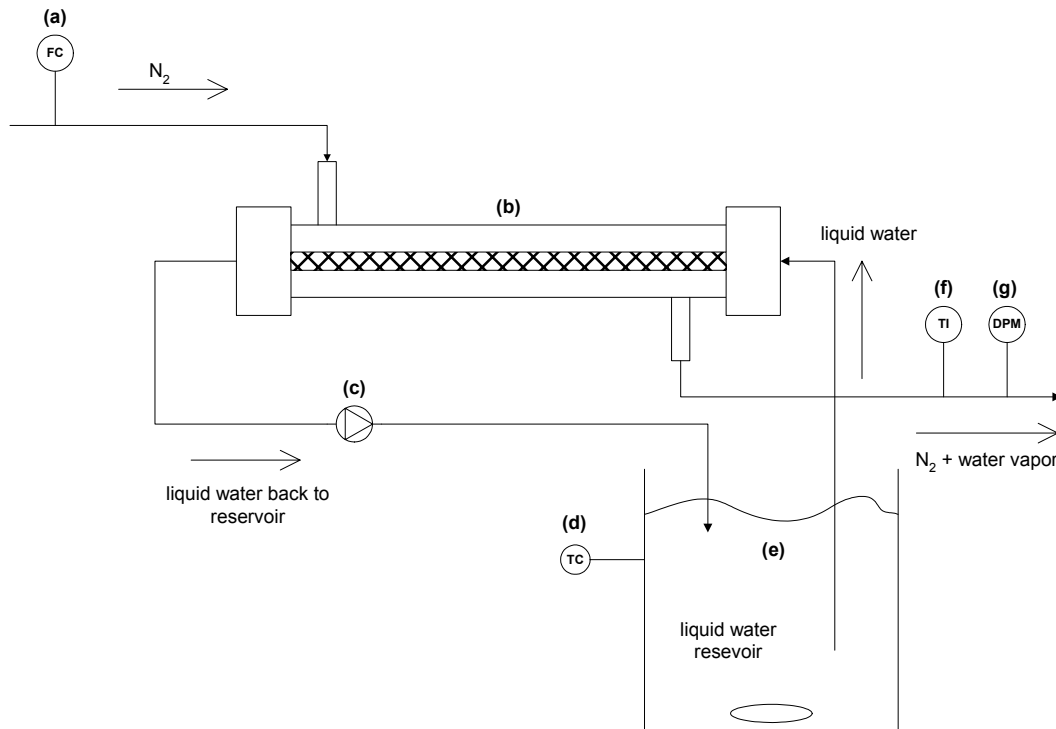


**Figure 3:** Set up for humidification experiments. (a) Flow controller, (b) membrane module, (c) hose pump, (d) temperature controller, (e) temperature controlled water reservoir (f) temperature indicator and (g) dew point mirror.

Liquid water was pumped with a hose pump (c, Watson Marlow 330) through the inside of the membrane and the water temperature inside the membrane was assumed to be the same as the temperature of the liquid water reservoir, because of the use of isolated tubes and the high flow rate of the liquid water.

The dry nitrogen stream flowed in counter current direction to the liquid and the velocity of the nitrogen stream was controlled using a flow controller (a, Brooks 5850E). The dew point and the temperature of the nitrogen flow leaving the membrane module were analyzed by means of a dew point mirror (g, Dewmet Cooled Mirror dew point meter,

Michell Instruments BV) and a temperature indicator (f). The dew point temperature of the nitrogen flow was correlated to its water vapour pressure by the Antoine equation and based on this information the water vapour flux through the membrane could be calculated according to the method earlier described [1, 11]. Despite the higher temperatures of the liquid water, the temperature of the gas stream leaving the membrane after humidification is almost constant at 21-23°C.

The water vapor flux through the membrane at a water bath temperature of 30, 40, 50, 60 and 70°C was determined and the influence of the nitrogen flow rate on the transport behavior was determined varying the nitrogen flow rate between 70 and 700 l/h.

### Relative humidity

The performance of the membrane assisted humidification process was expressed as the relative humidity of the nitrogen stream.

In air climate systems, humidity is often expressed as relative humidity. The relative humidity (RH, %), is defined as the ratio of the partial vapor pressure and the vapor pressure of the liquid of the pure component ($H_2O$) at the specific temperature.

$$RH = 100 \cdot \frac{p_A}{p^{\circ}_A} \tag{1}$$

Where $p_A$ is the partial pressure of water vapor in the humidified gas stream (bar) and $p^{\circ}_A$ is the vapor pressure of the pure liquid (bar). A relative humidity of 100% represents a water saturated gas, whereas 0% relative humidity represents a dry gas stream.

### Resistance to mass transfer

The transfer of water from the liquid water side to the gas side is determined by several resistances in series: the resistance at the feed and that at the permeate side of the membrane and the resistance of the membrane itself. These resistances can be

mathematically represented by the resistance in series model and each resistance can be represented by its mass transfer coefficient k [11]:

$$\frac{1}{k_{ov}} = \frac{1}{k_f} + \frac{1}{k_m} + \frac{1}{k_p} \qquad (2)$$

where $k_{ov}$, $k_f$, $k_m$ and $k_p$ are the mass transfer coefficients [m/s] of the overall system, the feed side, the membrane and the permeate side, respectively. The resistance of the liquid feed phase is assumed to be much smaller than the membrane resistance and the resistance at the permeate side. However, to not exclude the possible resistance at the feed-membrane interface where dissolution of water into the dense coating layer occurs, this resistance is included in the membrane resistance as well, resulting in an overall membrane resistance which thus also includes possible effects at the feed-membrane interface. Hence the overall resistance can be calculated as the sum of the overall membrane resistance and the permeate resistance.

The overall mass transfer coefficient of the complete system, $k_{ov}$, can be calculated from the water vapor flux $J_{H2O}$ [mol/ m$^2$·s] and the driving force for permeation (the difference in concentration between feed and permeate side, $c_f$ and $c_p$ [mol/m$^3$] , with $c_p$ the average concentration in the fiber, calculated as $(c_{p,in}+c_{p,out})/2$ according to Equation 3 [11]:

$$J_{H_2O} = k_{ov} \cdot \left( c_f - c_p \right) \qquad (3)$$

The concentration of water at the feed side can be easily calculated from its temperature dependent density and the molecular weight of water (18 g/mol). The concentration of water vapor at the permeate side can be extracted form the dew point of the vapor, using the Antoine equation.

The mass transfer coefficient at the permeate side depends on the geometry of the system and the hydrodynamic conditions and is described by Sherwood relations [11]. In the present work, we use one single membrane fiber and the flow of nitrogen is parallel to the fiber. Asimakopoulou et al. [12] derived an equation which is valid for mass transfer of a

flow parallel to a fiber at small fiber packing density, which we also used in our work. First, the fiber fraction φ [-] is calculated via Equation 4:

$$\varphi = N \cdot \left( \frac{d_{out}}{d_{module}} \right)^2 \tag{4}$$

where N is the number of fibers, $d_{out}$ the outer diameter of the fiber [m] and $d_{module}$ the inner diameter of the membrane module [m].

The average velocity at the permeate side $u_{permeate,average}$ [m/s] can be calculated from Equation 5.

$$u_{permeate,average} = \frac{Q_{permeate}}{S_{permeate} \cdot (1 - \varphi)} \tag{5}$$

where $Q_{permeate}$ is the volume flow at the permeate side [m³/s] and $S_{permeate}$ is the cross sectional area of the module [m²].

The Reynolds and Schmidt number can now be calculated (Equation 6 and 7) to determine the Sherwood relation:

$$Re_p = \frac{u_{permeate,average} \cdot d_{out} \cdot \rho}{\eta} \tag{6}$$

$$Sc_p = \frac{\eta}{\rho \cdot D} \tag{7}$$

where ρ is the density of the gas at the permeate side [kg/m³], η is the viscosity of the gas at the permeate side [Pa·s] and D is the diffusion coefficient of water vapor in the gas mixture [m²/s]. The diffusion coefficient of water vapor in nitrogen D [m²/s] can be estimated from an empirical relation derived by Massman [13]:

$$D = D_0 \cdot \left(\frac{p_0}{p}\right) \cdot \left(\frac{T}{T_0}\right)^{1.81} \qquad (8)$$

where $D_0$ is the diffusion coefficient of water in nitrogen at $10^5$ Pa [1 bar] and 273.15 K [$D_0 = 2.19 \cdot 10^{-5}$ m$^2$/s] [11], $p_0 = 1.013 \cdot 10^5$ Pa [1.013 bar], p is the pressure [bar], T is the absolute temperature [K] and $T_0 = 273.15$ K.

The Sherwood relation for the permeate side as proposed by Asimakopoulou *et al.* [12] can now be applied to calculate the mass transfer coefficient at the permeate side:

$$Sh_p = \frac{k_p \cdot d_{out}}{D} = 1.45 \cdot \left(Re_p \cdot Sc_p \cdot \frac{d_{out}}{l}\right) \qquad (9)$$

where l is the length of the fiber [m].

Because the overall mass transfer coefficient of the process can be directly calculated from the obtained water flux from the feed side through the membrane to the permeate side and the mass transfer coefficient at the permeate side can be obtained from the Sherwood relation described above, the overall mass transfer coefficient of the membrane can be calculated as well, using Equation 2.

## Results and discussion

### *Relative humidity and water vapor flux*

Variation of a single parameter to tune the relative humidity for the specific application is preferred to keep the system simple. On the other hand, control over a wide range of relative humidities is required to create flexibility in the process. In the present work we use the temperature and/or the gas flow rate as tools to tune and control this relative humidity of the gas phase. Figure 4 shows the experimentally obtained relative humidity (RH) of the gas stream as a function of the nitrogen flow rate and the temperature of the liquid water.
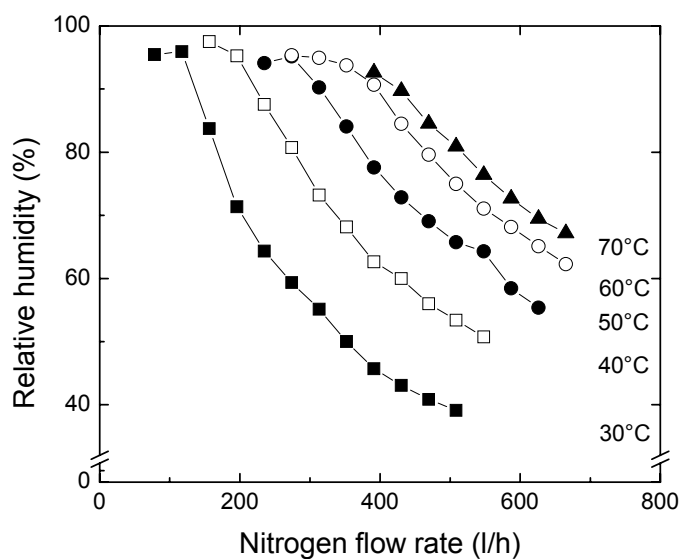
**Figure 4:** Relative humidity of the gas stream as a function of the nitrogen flow rate and the liquid water temperature.

Relative humidities ranging from 40 up to 100% can be realized with a single hollow fiber membrane coated with a dense layer of S-PEEK. Although the maximum relative humidity that can be reached is 100%, the experimentally obtained value is slightly lower than 100%. This is due limitations in the experimental system where we can only determine the temperature of the humidified gas stream a short distance after it leaves the membrane module, which leads to some additional cooling of the gas stream. The relative humidity decreases with increasing nitrogen flow rate, except for a few values close to complete saturation (100% relative humidity). This inconsistency at extremely high relative humidities is due to limitations in the supply of dry nitrogen (too low nitrogen flow rate). The relative humidity obtained at a certain nitrogen flow rate increases with increasing temperature, probably due to the increased transport rate of water vapor at higher temperatures.

Figure 5 shows the water flux from the feed side, through the membrane to the permeate side as a function of the nitrogen flow rate and the temperature.
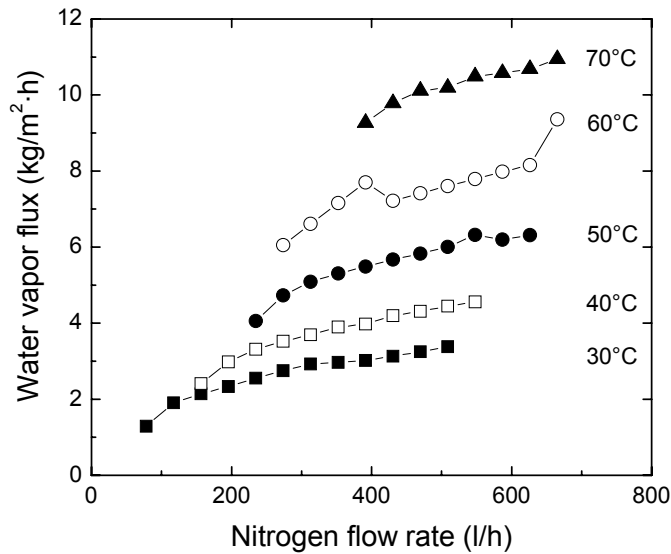
**Figure 5:** Water vapor flux as a function of the nitrogen flow rate and the liquid water temperature.

The water vapor flux increases with both increasing nitrogen flow rate and increasing liquid water temperature. At a liquid water temperature of 70 °C and a nitrogen flow rate of approximately 700 l/h more than 11 kg/m$^2$·h water vapor is transported through the membrane. The increase in water vapor flux with increasing nitrogen flow rate is especially at higher flow rates due to a decrease in permeate boundary layer resistance with increasing nitrogen flow rate. At lower flow rates, the supply of dry nitrogen limits the humidification process and only part of the membrane area is required to humidify this gas stream. Increase in nitrogen flow rate thus results in more effective use of the total length of the membrane and an increase in water flux though the membrane. So in addition to the decrease of the boundary layer resistance at low flow rates also this effect contributes to an increase in water flux through the membrane with increasing flow rate. This is also reflected in the more steep increase in the water flux at lower flow rates than at higher flow rates.

The increase in water flux with increasing temperature is most probably due to the increased transport rate of water vapor at higher temperatures.

Kneifel *et al.* [14] report water vapor fluxes in membrane humidifiers using porous poly ether imide membranes (PEI) coated with a dense top layer of poly dimethyl siloxane (PDMS) to prevent leakage of liquid water into the gas stream. Transport of liquid water through the membrane disturbs the control of the relative humidity and at the same time allows pollutants present in the water to reach the clean air side as well. For the PDMS coated membranes, Kneifel *et al.* [14] report water vapor fluxes up to 0.7 kg/m$^2$·h. The membranes used in the present work have a highly hydrophilic dense membrane layer instead of the more hydrophobic PDMS layer, resulting in water vapor fluxes that are more than 15 times higher than the ones reported by Kneifel *et al.* [14]. The membranes used in the present work thus combine the advantage of a dense membrane (no water leakage) with the advantage of a porous, highly permeable membrane (high water vapor flux).

### *Resistance to mass transfer*

As described earlier, the water vapor that permeates from the feed side, through the membrane to the permeate side experiences three different resistances in series. If we assume that the resistance of the liquid phase is negligible compared to the other two resistances, the overall membrane resistance and the permeate resistance determine the total water flux. Figure 6 shows the resistance at the permeate side calculated with the approach of Asimakopoulou *et al.* [12] as a function of the nitrogen flow rate and the temperature of the liquid water. The left side of the Figure represents the lower temperatures, whereas the resistances at the higher temperatures are located at the right side of the plot. As mentioned earlier, although the temperature of the liquid water was varied, the temperature of the humidified gas stream was almost constant at 21–23 °C.
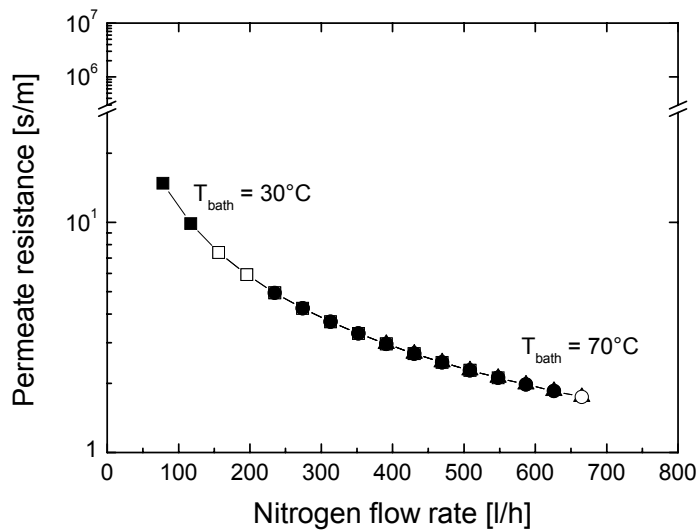
**Figure 6:** Permeate side resistance versus nitrogen flow rate at a liquid water temperature of 30, 40, 50, 60 and 70°C. Although the temperature of the liquid water was varied, the temperature of the humidified gas stream was almost constant at 21–23 °C.

The resistance to mass transfer at the permeate side decreases with increasing nitrogen flow rate from approximately 15 s/m to 1.5 s/m, due to a decrease in gas phase boundary layer resistance with increasing nitrogen flow rate [11]. At each specific nitrogen flow rate, the resistance to mass transfer at the permeate side is independent of the temperature of the liquid water. As mentioned earlier, although the temperature of the liquid water varies significantly, the temperature of the humidified gas stream is almost constant at 21–23 °C, which explains the independency of this gas phase boundary layer resistance to the temperature.

Figure 7 shows the overall membrane resistance as a function of the temperature of the liquid water and the nitrogen flow rate.
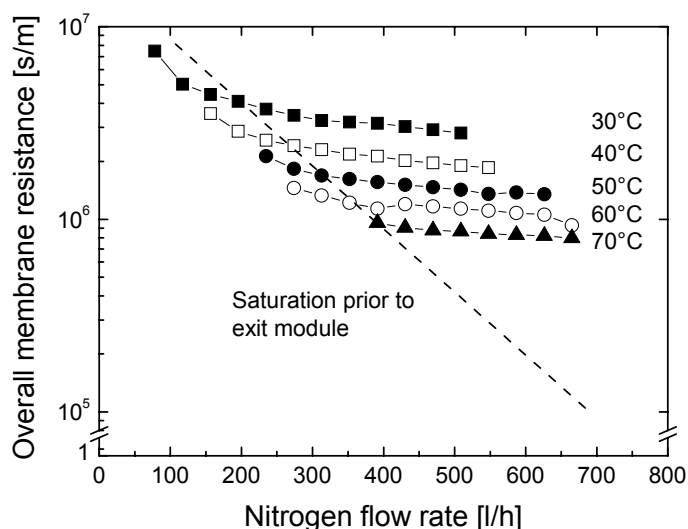
**Figure 7:** Overall membrane resistance as a function of the nitrogen flow rate and the temperature of liquid water.

The overall membrane resistance is five orders of magnitude higher than the resistance at the permeate side. It determines thus to a very large extend the water vapor flux from the liquid water side, through the membrane, to the gas side. The overall membrane resistance decreases with increasing temperature due to an increased transport rate at higher temperatures.

Figure 7 seems to pretend that the membrane resistance initially decreases with increasing nitrogen flow rate, although the membrane resistance is supposed to be independent of the nitrogen flow rate. At low nitrogen flow rates, the supply of fresh, dry nitrogen gas limits the water vapor flux through the membrane, resulting in only partial use of the total membrane area. With increasing nitrogen flow rate, the membrane area required for humidification on the total nitrogen stream increases. This is reflected in the decrease in calculated membrane resistance at low flow rates but in fact is due to the limitation in nitrogen supply. To verify this, we recalculated the membrane resistance at lower liquid flow rates for smaller membrane areas assuming that only part of the total membrane area is used for permeation. This indeed resulted in a constant value, independent of the nitrogen flow rate, for the overall membrane resistance. At higher

liquid flow rates, the membrane resistance dominates the water transport and determines the water flux.

The transition between the area where the nitrogen flow limits the process (saturation of nitrogen stream prior to exit membrane module) and the area where the membrane determines the water vapor flux is represented by the dotted line in Figure 7. Mass transport in the area below the dotted line is determined by the supply of nitrogen and the stream is saturated before it leaves the membrane, whereas mass transport above the dotted line is governed by the overall membrane resistance.

# Conclusions

The present work investigates the potential of hydrophilic membranes based on sulfonated poly (ether ether ketone) for the controlled humidification of gas streams. The temperature and gas flow rate are used as tools to tune and control the relative humidity. The proposed membrane material allows the passage of water only, while most of the contaminations are retained. Membrane assisted gas humidification thus integrates purification and humidification in one single step.

Water vapor fluxes up to 11 kg/m$^2$·h could be obtained and relative humidities ranging from 40 up to 100% could be realized with a single hollow fiber membrane coated with a dense layer of S-PEEK.

The relative humidity decreases with increasing nitrogen flow rate and increasing temperature of liquid water. The water vapor flux increases with increasing nitrogen flow rate due to a decrease in gas phase boundary layer, and increasing liquid water temperature due to the increased transport rate of water vapor. At lower flow rates, the supply of dry nitrogen limits the humidification process, whereas at higher nitrogen flow rates, mass transport through the membrane is the limiting factor that governs the humidification process. The overall membrane resistance is five orders of magnitude higher than the resistance at the permeate side. The results prove that membrane assisted gas humidification is a promising alternative for conventional humidification methods.

# References

1.  H. Sijbesma, K. Nymeijer, R. van Marwijk, R. Heijboer, J. Potreck, M. Wessling, Flue gas dehydration using polymer membranes, Journal of Membrane Science 313 (2008) 263-276.

2.  S.P. Giordano, E.L. Holland, A performance comparison of disposable humidifiers, Respiratory Therapy 3 (1973) 49-51.

3.  Z. Zhao, Experimental study of sprayers in air-washer spraying chambers, Journal of Textile Research, China Textile Engineering Society 12 (1991) 222-225.

4.  S. Neidhardt, Rotating spray humidifiers in hospital air conditioning systems: Hygienic and technical problems (Umlaufsprühbefeuchter in Krankenhausklimaanlagen - Ein hygienisch-technischer Problemfall), Forum Städte-Hygiene 37 (1986) 62-64.

5.  G.H. Guvelioglu, H.G. Stenger, Flow rate and humidification effects on a PEM fuel cell performance and operation, Journal of Power Sources 163 (2007) 882-891.

6.  M.M. Saleh, T. Okajima, M. Hayase, F. Kitamura, T. Ohsaka, Exploring the effects of symmetrical and asymmetrical relative humidity on the performance of $H_2$/air PEM fuel cell at different temperatures, Journal of Power Sources 164 (2007) 503-509.

7.  H. Abe, H. Iwamoto, T. Toshima, T. Iino, G.W. Gale, Novel photoresist stripping technology using ozone/vaporized water mixture, IEEE Transactions on Semiconductor Manufacturing 16 (2003) 401-408.

8.  E.D. Olson, C.A. Reaux, W.C. Ma, J.W. Butterbaugh, Alternatives to standard wet cleans, Semiconductor International 23 (2000) 70-72, 74, 76.

9.  C.A. Balaras, E. Dascalaki, A. Gaglia, HVAC and indoor thermal conditions in hospital operating rooms, Energy and Buildings 39 (2007) 454-470.

10. E.N. Komkova, M. Wessling, J. Krol, H. Strathmann, N.P. Berezina, Influence of the nature off polymer matrix and the degree of sulfonation on the properties of membranes, Polymer Science Series A 43 (2001) 300-307.

11.   S. Metz, W. van de Ven, J. Potreck, M. Mulder, M. Wessling, Transport of water vapor and inert gas mixtures through highly selective and highly permeable polymer membranes, Journal of Membrane Science 251 (2005) 29-41.

12.   A.G. Asimakopoulou, A.J. Karabelas, A study of mass transfer in hollow-fiber membrane contactors - The effect of fiber packing fraction, Journal of Membrane Science 282 (2006) 430-441.

13.   W.J. Massman, A review of the molecular diffusivities of $H_2O$, $CO_2$, $CH_4$, $CO$, $O_3$, $SO_2$, $NH_3$, $N_2O$, $NO$ and $NO_2$ in air, $O_2$ and $N_2$ near STP, Atmospheric Environment 32 (1998) 1111-1127.

14.   K. Kneifel, S. Nowak, W. Albrecht, R. Hilke, R. Just, K.V. Peinemann, Hollow fiber membrane contactor for air humidity control: Modules and membranes, Journal of Membrane Science 276 (2006) 241-251.

# Chapter 6

# Preparation of porous membrane morphologies from sulfonated poly ether ether ketone

## Abstract

The present work describes the preparation of porous membrane morphologies from the highly hydrophilic polymer sulfonated poly ether ether ketone. Coagulation of the polymer in common non-solvents such as water is impossible since the material does not solidify sufficiently, but forms a gel only. We discovered that concentrated electrolyte solutions however are very effective as precipitation medium. We present the effect of the type of non-solvent and the composition of the coagulation bath as a method to tune the morphology of these highly hydrophilic structures.

# Introduction

For the filtration of aqueous solutions, hydrophilic membranes are highly desirable. The general opinion is that an increased hydrohilicity of the membrane reduces its fouling tendency thus enhancing the membrane performance, and much research has been carried out on hydrophilization of membranes for especially micro and ultra filtration membranes [1-6]. Strategies to hydrophilize membranes include among others the blending of a hydrophobic polymer with a hydrophilic polymer. Roesink *et al.* investigated the fouling behavior of membranes prepared from a blend of a hydrophobic polymer (poly ether imide) and a hydrophilic additive (poly vinyl pyrrolidone) [7]. Other methods include the hydrophilization of hydrophobic membranes by means of surface modification. Pierraci *et al.* proposed a photochemical modification of poly ether sulfone membranes [8]. Major disadvantage of these methods is the increased complexity of the membrane production process and the increased costs.

Here, we propose another approach to prepare hydrophilic membranes based on the use of intrinsically hydrophilic polymers e.g. sulfonated poly ether ether ketone as polymer for the development of porous, hydrophilic membranes for e.g. micro and ultra filtration. Preparation of porous membranes based on this polymer in one single step may circumvent the above mentioned disadvantages. To the knowledge of the authors this approach has not been addressed in current literature for such a high degree of sulfonation.

Sulfonated poly ether ether ketone (S-PEEK) is a highly hydrophilic polymer prepared from the sulfonation of poly ether ether ketone. It is especially known from its use in (methanol) fuel cell applications because of its high proton conductivity combined with good mechanical stability [9-14], but also its use as membrane material for flue gas dehydration is recently reported [15]. Due to its highly hydrophilic nature, it is a potentially interesting membrane material for aqueous separations as well. The sulfonic acid groups in the polymer do not only increase the hydrophilicity of the membrane, but also introduce fixed negative charges, which influence the fouling behavior as well, e.g. by electrostatic repulsion of foulants with the same charge as the membrane [16, 17].

In the present work we investigate the potential of this polymer sulfonated poly ether ether ketone to form porous, highly hydrophilic membrane morphologies. The most often used method to produce porous polymeric structures is by phase inversion using the immersion precipitation process. Variation of especially the non-solvent is a strong tool to tune the membrane morphology. Wilhelm describes in his thesis the preparation of porous fibers from S-PEEK by phase inversion with water as a non-solvent [18], however the coagulation can only be done directly after the sulphonation reaction when the polymer is still in the concentrated sulfuric acid solution. The later makes the use of metal based spinnerets and casting knifes impossible due to corrosion of the fluidic channels. It is desirable to form the porous membrane morphology out of a solvent such as N-methyl-2-pyrrolidon. Commonly used non-solvents such as water or aliphatic alcohols do not work effectively since they only result in polymeric gels with insufficient mechanical strength. Here, we report for the first time the use of strong electrolyte solutions as precipitation media for very hydrophilic poly electrolytes.

This work investigates the effect of the type of non-solvent and the composition of the coagulation bath as a method to tune the morphology of porous, highly hydrophilic sulfonated poly ether ether ketone structures.

## Experimental

Sulfonated poly ether ether ketone (SPEEK, Figure 1) was prepared according to the method described in literature [19].
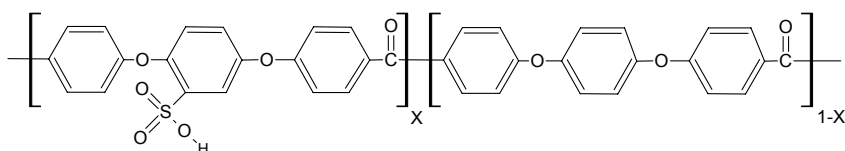


**Figure 1:** Chemical structure of sulfonated poly ether ether ketone (S-PEEK).

The polymer was used in its proton form. A 15 wt.% solution of the sulfonated polymer with a sulfonation degree of 72 % (x = 0.72) in N-methyl-2-pyrrolidon (NMP) was cast

on a glass plate using a 0.30 mm casting knife. Before use the glass plate was cleaned with acetone and ethanol to remove residuals. After casting, the film on the glass plate was placed in an acid or salt containing aqueous coagulation bath for a certain time for phase separation to occur. After phase separation, the film was washed in ultra pure water (Milli-Q, 18.2 MΩ·cm at 25°C) and removed from the glass plate. The film was dried over night at room temperature and additionally one night in a vacuum oven at 30°C. The structure and morphology of the prepared films were investigated using scanning electron microscopy (SEM, Jeol 5600 scanning electron microscope).

To investigate the effect of the non-solvent and the exchange time on the morphology of the prepared membranes, the solvent exchange time, the type of non-solvent and the composition of the coagulation bath were varied. The solvent exchange time was varied from 2 to 6 minutes. As non-solvents concentrated nitric acid (65 wt.%) or a saturated salt solution (NaCl) in water was used. To suppress the formation of macro voids, an approach proposed by Smolders et al. [20] to add solvent to the coagulation bath, was investigated. Weight ratios of 25/75, 50/50 and 75/25 solvent-non-solvent were used.

# Results and discussion

## *Introduction*

The most often used method to produce porous structures is by phase inversion using the so called immersion precipitation process, which starts from a thermodynamically stable polymer solution. By immersing this solution in a solvent which is a non-solvent for the polymer, de-mixing of the polymer-solvent system will occur from the point on where so much non-solvent is present in the polymer-solvent system that the solution becomes thermodynamically unstable. The composition of the ternary mixture polymer-solvent-non-solvent during immersion precipitation is often illustrated in ternary phase diagrams [21]. The corners of the triangle illustrate the pure components and a point between two corners, a mixture of the two components. Any point inside the triangle represents a specific composition of the three components. The binodal represents the composition of the mixture where it becomes thermodynamically instable and the solvent-polymer de-mixing begins [21]. In this region nucleation of the polymer lean phase starts consisting of solvent, non-solvent and very little polymer in droplet shape. These droplets continue growing until the polymer rich phase solidifies. Coalescence of the droplets before solidification results in an open porous structure [21]. Diffusion processes of solvent and non-solvent during membrane formation and de-mixing of solvent and polymer thus strongly influence the final morphology of the polymer structure.

## *Nitric acid as coagulant for S-PEEK*

To obtain porous structures of hydrophilic sulfonated poly ether ether ketone with a controlled and tunable porosity, an appropriate polymer-solvent-non-solvent system is required. NMP is used as solvent for S-PEEK, which requires the non-solvent to be miscible with NMP and simultaneously to be a non-solvent for S-PEEK. Because of its hydrophilic nature, S-PEEK swells in the most often used non-solvent, water. Phase separation of S-PEEK/NMP in water, results in a swollen gel and restricts the formation of a porous structure with a significant amount of solvent associated with the polymer.

It can be hypothesized that the interaction between NMP and the sulfonic acid group at the polymer backbone of S-PEEK is stronger than the interaction of water with NMP. Based on this assumption, a non-solvent with a higher affinity to the solvent than to the polymer is required to extract the solvent (NMP) from the sulfonic acid group and to exchange the solvent with a non-solvent to induce perform phase separation.

Sekizaki *et al.* suggested that 1-ethyl-2-pyrrolidone (which is comparable to the solvent used in our work (N-methyl-2-pyrrolidon (NMP)) undergoes oxygen protonation in the presence of acids, forming a hydrogen bond at the carbonyl oxygen [22]. We hypothesize that the interaction between the sulfonic acid group of the sulfonated polymer and NMP as a derivate of 1-ethyl-2-pyrrolidone, stems from the same protonation reaction. The sulfonic acid group, which is present as -$SO_3H$, can dissociate into -$SO_3^-$ and $H^+$ if a proton acceptor (NMP) is present. NMP has a mesomeric resonance structure with a negative oxygen ($O^-$) and a positive nitrogen atom ($N^+$), stabilized via a pi-binding of the free electron (Analog to polyvinyl pyrrolidone (PVP) [23]). When dissolved in NMP, the -$SO_3H$ group of the polymer dissociates and protonates the negatively charged oxygen of this mesomeric border structure, resulting in negative fixed charges at the polymer backbone, which experience electrostatic interactions with the positive $N^+$ atoms of NMP. The interaction between S-PEEK and NMP is based on a protonation reaction, and thus introduces ionic interactions between the solvent and the polymer, while the interaction of the non-solvent (water) with the solvent NMP is only based on dipole-dipole interactions. In general, ionic interactions are considered to be stronger than dipole-dipole interactions, which can explain why water is not a suitable solvent to push away the solvent: the interaction between NMP and the sulfonic acid groups at the polymer backbone of S-PEEK is stronger than the interaction of water with NMP.

If we assume that the protonation of NMP and the ionic interaction between $SO_3^-$ and $N^+$ of NMP are responsible for the strong interaction between SPEEK and the solvent NMP, a suitable non-solvent for the formation of porous structures of SPEEK, should be a stronger acid the sulfonic acid groups on the polymer backbone in order to keep the -$SO_3^-$ group protonated and to change the interactions from ionic to dipole-dipole, while the

interactions of NMP and the strong acid will be based on ionic interactions. Water is a weak acid (pKs = 14), while the $pK_s$ value of benzene sulfonic acid, as part of the repeating unit of S-PEEK, is 0.7 [24]. $HNO_3$ is a much stronger acid (pKs = -1.32 [25]), and as such able to keep the $SO_3^-$ group protonated and to break down the ionic interaction between the polymer and the solvent NMP. This reduces the solubility of SPEEK in the NMP/$HNO_3$ mixture and leads to phase separation and solidification of the polymer.

For this reason concentrated nitric acid (65% $HNO_3$) is used as a non-solvent for phase separation of S-PEEK. In this context it is worthwhile mentioning the concentrated nitric acid still contains 32 wt.% water. This characteristic will be revisited later on.

Figure 2 shows the cross section (a) and the air side surface (b) of a porous SPEEK structure after coagulation in 65 wt.-% concentrated nitric acid for 2 minutes.
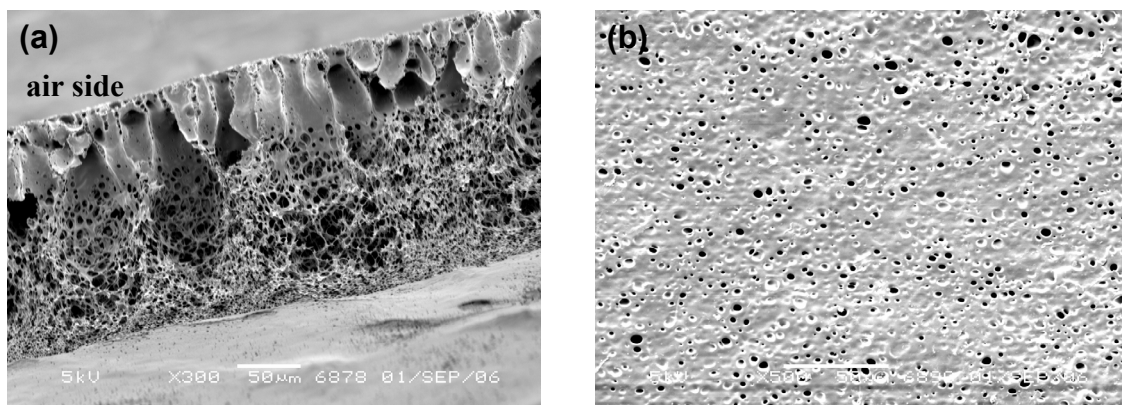


**Figure 2:** Porous S-PEEK structure obtained after coagulation in concentrated $HNO_3$; (a) cross section [magnification 300x]; (b) air side surface [magnification 500x].

Figure 2a shows the cross section of a porous S-PEEK film coagulated in concentrated nitric acid. The cross section shows a non homogenous porous structure with a porosity gradient. Three quarter of the cross section, seen from the glass side, shows a sponge like structure while one quarter, located at the air side, shows a finger like structure containing large macro voids. The pores are interconnected and open. Figure 2b shows

the air side surface of the same film. The air side surface is open and shows several pores with different sizes.

The effect of the coagulation time on the polymer structure is investigated and the coagulation time is varied from 2 to 6 minutes. Figure 3 shows the cross section of two films, coagulated for (a) 4 minutes and (b) 6 minutes in concentrated $HNO_3$. Figure 3 can be compared to Figure 2a (2 minutes exchange time).
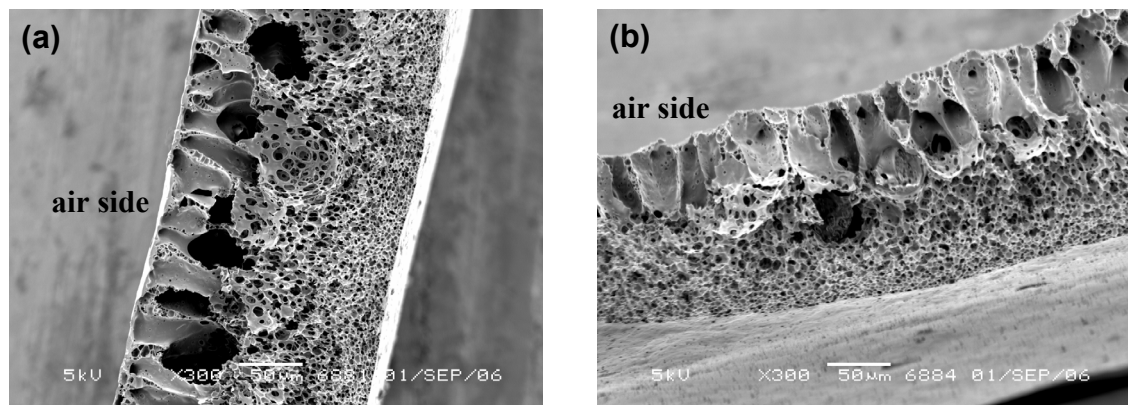


**Figure 3:** Porous S-PEEK structure obtained from coagulation in concentrated $HNO_3$; (a) 4 minutes exchange time [magnification 300x]; (b) 6 minutes exchange time [magnification 300x].

A porous structure of S-PEEK is formed but large macro voids close to the air side of the films are visible. No structural differences between the films prepared at different coagulation times are visible, suggesting that complete coagulation occurs in less then two minutes. In further experiments the coagulation time was kept at two minutes.

*Macrovoid suppression during coagulation of S-PEEK in nitric acid*

Wienk *et al.* [26] and Broens *et al.* [27] investigated the formation of macrovoids in membrane forming systems based on amorphous or semi-crystalline polymers. The diffusion of both solvent and non-solvent towards particular domains of the polymer-solvent system is the basis for macro void formation. They showed that the formation of macrovoids is caused by a faster growth rate of these voids relative to the solidification of the porous structure. This often goes also along with fast instantaneous demixing, as

opposed slow delayed demixing. Smolders *et al.* [20] showed that the addition of solvent to the coagulation bath induces a transition from this fast instantaneous demixing regime to a delayed demixing regime. Macro void formation does not occur in the delayed demixing regime because the rate of macro void formation is lower than the rate of solidification. It is generally accepted that macrovoid formation during phase separation is related to the penetration rate of the non-solvent into the casting solution and the kinetics of diffusion of solvent and non-solvent [28]. Termonia *et al.* [29] proofed the suppression of macro voids by adding solvent to the coagulation bath. In this case the coagulation becomes an utmost slow process controlled by the diffusion of the non-solvent [29]. Following this argumentation, coagulation of S-PEEK in 75/25 (Figure 4), 50/50 (Figure 5) and 25/75 (Figure 6) wt.% mixtures of $HNO_3$/NMP is performed.
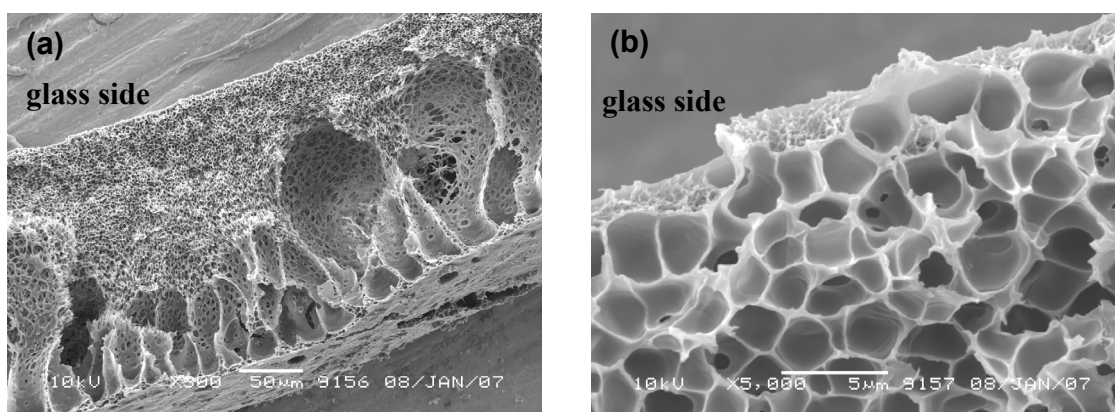


**Figure 4:** Porous S-PEEK structure obtained from coagulation in a 75/25 mixture of $HNO_3$/NMP; (a) cross section [magnification 300x]; (b) higher magnification of the cross section at the glass side [magnification 5.000x].

The polymeric structure formed after coagulation in a mixture of $HNO_3$/NMP (75/25 wt.%) still shows macro voids. Apparently, the addition of only 25 wt.% of solvent (NMP) to the coagulation bath ($HNO_3$) is not sufficient to suppress macro void formation.

Figure 5 shows the SEM-pictures of the porous S-PEEK structure obtained after coagulation in a 50/50 wt.% mixture of $HNO_3$/NMP.
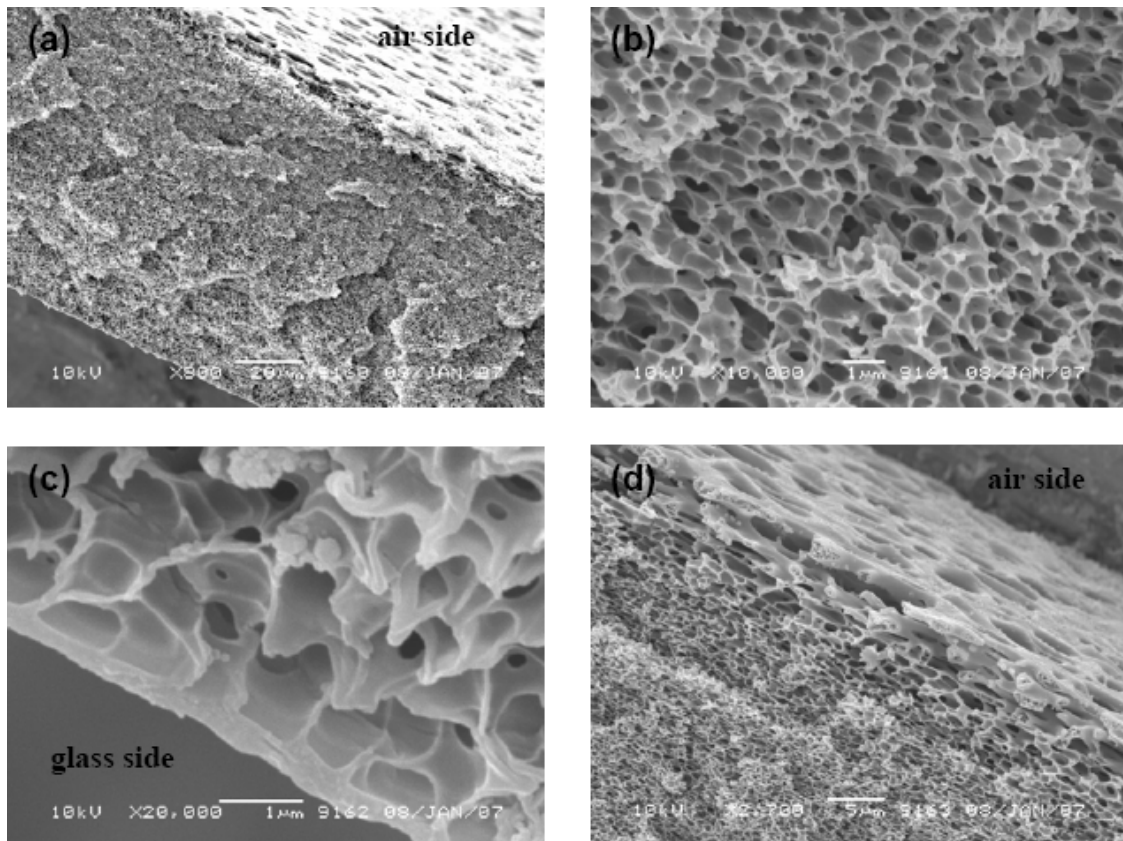
**Figure 5:** Porous S-PEEK structure obtained after coagulation in a 50/50 mixture of HNO₃/NMP; (a) cross section [magnification 800x]; (b) inner structure (cross section) [magnification 10.000x]; (c) higher magnification of the cross section at the glass side of the film [magnification 20.000x]; (d) higher magnification of the cross section at the air side of the film [magnification 2.700x].

Using a mixture of 50/50 HNO₃/NMP as coagulation bath leads to macro void free porous structures of S-PEEK. A cellular morphology is obtained, which is according to Stropnik *et al.* [30] due to phase separation by nucleation and growth of the polymer lean phase.

Figure 6 shows the SEM pictures of the morphology obtained after coagulation in HNO₃/NMP with a ratio of 25/75 wt.%. Again macro void free structures with a cellular structure are obtained. The structure seems to have a homogeneous uniform pore distribution with open, interconnected pores.
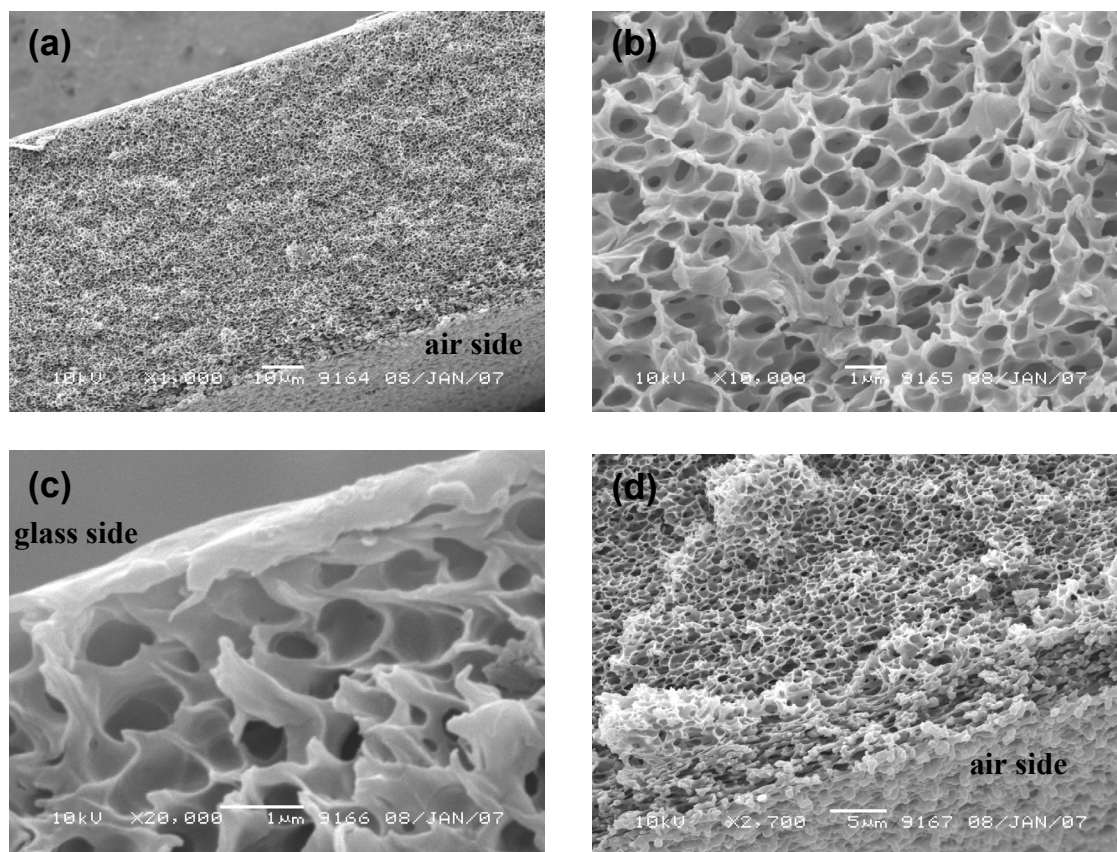
**Figure 6:** Porous S-PEEK structure obtained from coagulation in HNO$_3$/NMP (25/75) mixture;  (a) cross section [magnification 1.000x]; (b) middle structure of the film [magnification 10.000x]; (c) higher magnification of the cross section at the glass side of the film [magnification 20.000x]; (d) cross higher magnification of the cross section at the air side of the film [magnification 2.700x].

Visual differences in phase separation behavior of S-PEEK are observed depending on the composition of the coagulation bath. Coagulation of S-PEEK in a mixture of more than 75 wt.% HNO$_3$ (only 25 wt.% NMP) leads to a porous structure with macro voids (Figure 4). Coagulation bath mixtures containing at least 50 wt.% of NMP result in macro void free porous structures. Also in the phase separation process itself, differences between the films coagulating in a mixture containing only 25 wt.% NMP and those coagulating in bath mixtures containing at least 50 wt.% of NMP are observed. Phase separation into a coagulation bath that contains more than 75 wt.% HNO$_3$ (only 25 wt.% NMP) immediately results in a transition of the transparent film to an opaque film. During phase separation of the structures in 50/50 wt.% HNO$_3$/NMP or higher amounts

of NMP, the structure remains transparent until it finally contacts the washing water. With increasing NMP content and thus decreasing $HNO_3$ content, also the amount of water in the mixture decreases (actually, $HNO_3$ is present as a mixture of 65 wt.% $HNO_3$ and 35 wt.% water). Lower amounts of water thus slow down the protonation reaction, resulting in a delayed solidification process.

### *Influence of salt-ions on the coagulation process*

From water soluble poly electrolytes (polymers containing fixed charges) it is known that they can precipitate in highly concentrated salt solutions [31-33]. In solution with low ionic strength these polymers have a stretched configuration due to the repulsive electrostatic interactions between the fixed charges. The addition of high concentrations of ions shield the fixed charges of the polymer and decrease the electrostatic repulsion between the polymer segments [34, 35]. The polymer rearranges from a soluble configuration into an insoluble configuration and it precipitates [32]. Sulfonated poly (ether ether ketone) is a poly electrolyte with fixed negative charges and the use of a high ionic strength salt solution as coagulation medium can induce phase separation and precipitation of the polymer. To evaluate this effect we used a saturated salt solution (NaCl) as coagulant for SPEEK. The high charge density of the positive sodium ions compared to NMP shields the fixed charges of the polymer and induces precipitation of the polymer. Figure 7 shows SEM pictures of a porous S-PEEK structure after coagulation in this saturated NaCl solution.
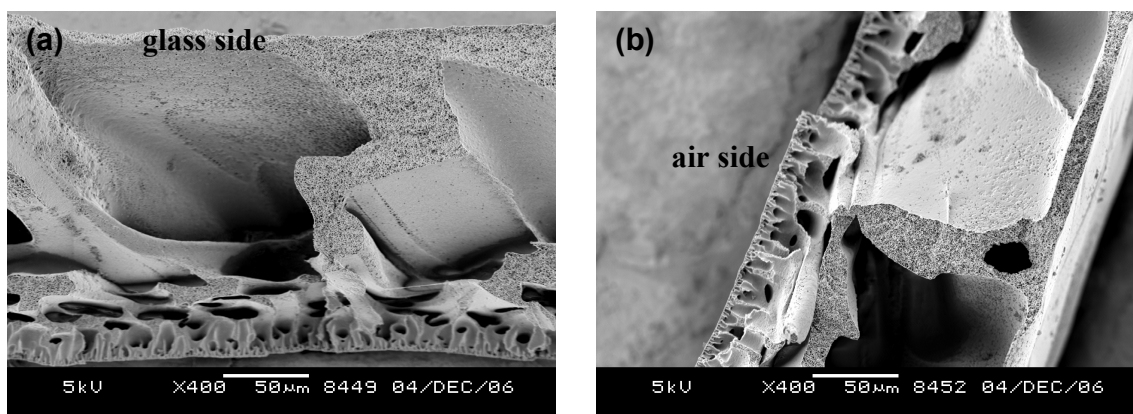
**Figure 7: Cross section of** porous S-PEEK structure obtained after coagulation in saturated NaCl solution; [both magnifications 400x].

The use of a saturated salt solution as coagulation medium for SPEEK indeed induces phase separation and results in a porous structure, unfortunately still containing large macro voids. Next to saturated NaCl solution we also used a saturated BaCl$_2$ solution as a coagulation medium, but did not find any influence on the difference in mono- (NaCl) or bivalent (BaCl$_2$) ions on the phase separation behavior of S-PEEK in NMP.

# Conclusions

This paper describes a method to prepare highly hydrophilic porous structures of sulfonated poly ether ether ketone (S-PEEK). The effect of the type of non-solvent and the composition of the coagulation bath as a method to tune the morphology of these highly hydrophilic structures is investigated. Porous structures could be obtained after coagulation of the polymer in concentrated $HNO_3$, which could be explained from the stronger protonating effect of $HNO_3$ than of the sulfonic acid group. Macro void formation was successfully suppressed by the addition of solvent (NMP) to the non-solvent ($HNO_3$), which delays the demixing of the polymer and the solvent and accelerates the solidification process. The use of a coagulating medium with a high ionic strength shields the fixed charges of the sulfonated polymer and induces phase separation as well. The preparation of the highly hydrophilic porous structures presented in this work offers a new direction for the production of low fouling membranes for e.g. micro and ultra filtration.

# References

1.  H.D.W. Roesink, Microfiltration: membrane development and module design. University of Twente, The Netherlands Enschede, 1989.

2.  D.L. Cho, J. Lee, Membrane fouling in microfiltration process and its control by surface modification of membrane, Polymer-Korea 21 (1997) 142-153.

3.  K.R. Kull, M.L. Steen, E.R. Fisher, Surface modification with nitrogen-containing plasmas to produce hydrophilic, low-fouling membranes, Journal of Membrane Science 246 (2005) 203-215.

4.  Y. Wang, J.H. Kim, K.H. Choo, Y.S. Lee, C.H. Lee, Hydrophilic modification of polypropylene microfiltration membranes by ozone-induced graft polymerization, Journal of Membrane Science 169 (2000) 269-276.

5.  D.S. Wavhal, E.R. Fisher, Hydrophilic modification of polyethersulfone membranes by low temperature plasma-induced graft polymerization, Journal of Membrane Science 209 (2002) 255-269.

6.  L.Q. Shen, Z.K. Xu, Z.M. Liu, Y.Y. Xu, Ultrafiltration hollow fiber membranes of sulfonated polyetherimide/polyetherimide blends: preparation, morphologies and anti-fouling porperties, Journal of Membrane Science 218 (2003) 279-293.

7.  H.D.W. Roesink, M.A.M. Beerlage, W. Potman, T. van den Boomgard, M.H.V. Mulder, C.A. Smolders, Characterization of new membrane materials by means of fouling experiments; Adsorption of BSA on poly ether imide-poly vinyl pyrrolidone membranes, Colloids Surfaces 55 (1991) 231-243.

8.  J. Pierraci, J.V. Crivello, G. Belfort, Photochemical modification of 10 kDa polyethersulfone ultrafiltration membranes for reduction of biofouling, Journal of Membrane Science 156 (1999) 223-240.

9.  A. Basile, L. Paturzo, A. Iulianelli, I. Gatto, E. Passalacqua, Sulfonated PEEK-WC membranes for proton-exchange membrane fuel cell: effect of the increasing level of sulfonation on electrochemical performances, Journal of Membrane Science 281 (2006) 377-385.

10. M. Gil, X.L. Ji, X.F. Li, H. Na, J.E. Hampsey, Y.F. Lu, Direct synthesis of sulfonated aromatic poly(ether ether ketone) proton exchange membranes for fuel cell applications, Journal of Membrane Science 234 (2004) 75-81.

11. L. Grosmaire, S. Castagnoni, P. Huguet, P. Sistat, M. Boucher, P. Bouchard, P. Bebin, S. Deabate, Probing proton dissociation in ionic polymers by means of in situ ATR-FTIR spectroscopy, Physical Chemistry Chemical Physics 10 (2008) 1577-1583.

12. H.Y. Jung, K.Y. Cho, K.A. Sung, W.K. Kim, J.K. Park, The effect of sulfonated poly(ether ether ketone) as an electrode binder for direct methanol fuel cell (DMFC), Journal of Power Sources 163 (2006) 56-59.

13. D.W. Kim, J.M. Ko, W.J. Kim, J.H. Kim, Study on the electrochemical characteristics of quasi-solid-state electric double layer capacitors assembled with sulfonated poly(ether ether ketone), Journal of Power Sources 163 (2006) 300-303.

14. L. Paturzo, A. Basile, A. Iulianelli, J.C. Jansen, I. Gatto, E. Passalacqua, High temperature proton exchange membrane fuel cell using a sulfonated membrane obtained via $H_2SO_4$ treatment of PEEK-WC, Catalysis Today 104 (2005) 213-218.

15. H. Sijbesma, K. Nymeijer, R. van Marwijk, R. Heijboer, J. Potreck, M. Wessling, Flue gas dehydration using polymer membranes, Journal of Membrane Science 313 (2008) 263-276.

16. J.F. Blanco, J. Sublet, Q.T. Nguyen, P. Schaetzel, Formation and morphology studies of different polysulfones-based membranes made by wet phase inversion process, Journal of Membrane Science 283 (2006) 27-37.

17. G.N.B. Barona, B.J. Cha, B. Jung, Negatively charged poly(vinylidene fluoride) microfiltration membranes by sulfonation, Journal of Membrane Science 290 (2007) 46-54.

18. F.G. Wilhelm, Bipolar membrane electrodialysis: membrane development and transport characteristics. University of Twente, The Netherlands Enschede, 2001.

19. E.N. Komkova, M. Wessling, J. Krol, H. Strathmann, N.P. Berezina, Influence of the nature off polymer matrix and the degree of sulfonation on the properties of membranes, Polymer Science Series A 43 (2001) 300-307.

20. C.A. Smolders, A.J. Reuvers, R.M. Boom, I.M. Wienk, Microstructures in phase-inversion membranes. 1. Formation of macrovoids, Journal of Membrane Science 73 (1992) 259-275.

21. M.H.V. Mulder, Basic principles of membrane technology, Kluwer Academic Publishers Dordrecht, 1996.

22. H. Sekizaki, K. Danjo, H. Eguchi, Y. Yonezawa, H. Sunada, A. Otsuka, Solid-state interaction of ibuprofen with polyvinylpyrrolidone, Chemical Pharmaceutical Bulletin 43 (1995) 988-993.

23. http://archive.tu-chemnitz.de/pub/2004/0019, Figure 12, 12.08.2008.

24. H. Römpp, E. Ühlein, Chemie Lexikon, Franckh´sche Verlagshandlung Stuttgart, 1966.

25. G. Schulze, J. Simon, Jander·Jahr Maßanalyse, Walter de Gruyter Berlin, 1989.

26. I.M. Wienk, R.M. Boom, M.A.M. Beerlage, A.M.W. Bulte, M. Smolders, H. Strathmann, Recent advances in the formation of phase inversion membranes made from amorphous semi-crystalline polymers, Journal of Membrane Science 113 (1996) 361-371.

27. L. Broens, F.W. Altena, C.A. Smolders, D.M. Koenhen, Asymmetric membrane structures as a result of phase separation phenomena, Desalination 32 (1980) 33-45.

28. H. Strathmann, K. Kock, Formation mechanism of phase inversion membranes, Desalination 21 (1977) 241-255.

29. Y. Termonia, Molecular modeling of phase-inversion membranes - effect of additives in the coagulant, Journal of Membrane Science 104 (1995) 173-179.

30. C. Stropnik, A. Car, Some aspects of polymeric asymmetric porous membranes formation by wet-phase separation method, Desalination 199 (2006) 130-132.

31. L. Burlamacchi, M.F. Ottaviani, E.M. Ceresa, M. Visca, Stability of colloidal TiO$_2$ in the presence of polyelectrolytes and divalent metal ions, Colloids and Surfaces 7 (1983) 165-182.

32. V.A. Izumrudov, M.Y. Gorshkova, I.F. Volkova, Controlled phase separations in solutions of soluble polyelectrolyte complex of DIVEMA (copolymer of divinyl ether and maleic anhydride), European Polymer Journal 41 (2005) 1251-1259.

33. K.S. Khairou, W.M. Al-Gethami, R.M. Hassan, Kinetics and mechanism of sol-gel transformation between sodium alginate polyelectrolyte and some heavy divalent metal ions with formation of capillary structure polymembranes ionotropic gels, Journal of Membrane Science 209 (2002) 445-456.

34. P.C. Hiemenz, R. Rajagopalan, Principle of colloid and surface chemistry, Marcel Dekker New York, US, 1997.

35. J. Lyklema, Fundamentals of interface and colloid science, Academic Press Inc. Burlington, US, 1991.

# Chapter 7

## Conclusions and outlook

The aim of the work described in this thesis is the development of hydrophilic membranes and the fundamental understanding of water vapor and gas transport through these membranes. In this last chapter the main conclusions of the work are summarized and an outlook on further research, especially focused on the simultaneous removal of water and the capture of $CO_2$ is presented.

## *Conclusions*

**Chapter 2** of this thesis presents an analysis of the sorption kinetics of water vapor and liquid water in the glassy polymer sulfonated poly ether ether ketone (S-PEEK). Analysis of the sorption isotherms and determination of the sorption kinetics proof the occurrence of both Fickian sorption behavior and relaxational phenomena already at very low water concentrations in the polymer. With increasing water concentration, the relative importance of relaxation phenomena increases, whereas the relative contribution of Fickian diffusion decreases.

Based on the water vapor sorption kinetics only, the Fickian diffusion coefficient increases over two orders of magnitude with increasing water vapor concentration. Taking also the diffusion kinetics from liquid water sorption experiments into account reveals a change of even three orders of magnitude of the Fickian diffusion coefficient when the water concentration in the polymer increases.

**Chapter 3** presents the sorption thermodynamics of water vapor in two hydrophilic polymers (sulfonated poly ether ether ketone (S-PEEK) and a poly ethylene oxide-poly amide block copolymer (PEBAX® 1074)). The thermodynamic approach presented offers a strong method to distinguish between enthalpic and entropic contributions of water vapor sorption. It allows to explain the nature of water sorption in both polymers and to address the state of water in the polymer.

Analysis of water vapor sorption in S-PEEK and PEBAX$^{®}$ shows that the Gibbs energy of sorption has a negative value in both polymers. For PEBAX$^{®}$ water vapor sorption becomes thermodynamically more favorable at higher water vapor activities, whereas for S-PEEK the free energy shows a maximum. In all cases, the enthalpy of water sorption is negative, i.e. the sorption process is exothermic and heat is released. Especially at higher water vapor activities, the heat of water sorption in PEBAX$^{®}$ equals the heat required to solvate a water molecule from the equilibrium vapor phase into pure liquid water, suggesting that additional sorbed water molecules experience a water-like environment. This is supported by data obtained from cluster analysis which confirm the formation of water clusters in the polymer matrix over the full activity range. In S-PEEK the polymer-water interactions prevail, especially at lower water vapor activities, most probably stemming from the hydration of the ionogenic sulfon groups present in the sulfonated polymer.

The entropy of water sorption for both polymers is negative over the full range of water vapor activities (sorption is entropically unfavorable). For PEBAX$^{®}$ the entropy decreases with increasing water vapor activity over almost the full activity range due to the formation of water clusters which introduces an additional level of organization. For SPEEK the entropy increases (less negative) with increasing sorption due to the increased degree of freedom and the increase in swelling degree.

The thermodynamic analysis shows that for both polymers water sorption is driven by a favorable water sorption enthalpy, whereas the sorption entropy is intrinsically unfavorable. For S-PEEK, water sorption is governed by enthalpy-entropy compensation (with increasing activity the enthalpy and the entropy become less negative). In the case of PEBAX$^{®}$ enthalpy-entropy compensation is observed only at lower activities (with increasing activity, the enthalpy and the entropy become more negative). At higher water vapor activities, the more favorable Gibbs energy of water sorption in PEBAX$^{®}$ is driven by the entropy.

The transport behavior of a hydrophilic, highly permeable type of PEO based block copolymer (PEBAX$^{®}$ 1074) as membrane material for the removal of water vapor from light gasses is presented in **Chapter 4**. Water vapor sorption isotherms in PEBAX$^{®}$ 1074

represent Flory-Huggins type of sorption and the highly hydrophilic nature of the block copolymer results in high amounts of absorbed water (up to 0.4 g of water per gram of dry polymer at 20°C). When taking into account the swelling of the polymer due to water vapor sorption, the Fickian diffusion coefficient increases over the full activity range and changes over two orders of magnitude. As determined from measurements with binary gas mixtures, the water vapor permeability increases exponentially with increasing water vapor activity whereas the nitrogen permeability slightly decreases with increasing water vapor activity. Consequently, the water over nitrogen selectivity increases with increasing water vapor activity. The results not only show the high potential of hydrophilic PEO-based block copolymers for dehydration purposes (e.g. the dehydration of flue gasses, natural gas dew pointing or the humidification of air). Because of the interaction of $CO_2$ with the polar ether linkages in PEO based block copolymers, these polymers also offer attractive routes to the integration of dehydration and $CO_2$ capture using membrane technology.

The potential of membrane technology for the controlled humidification of gas streams is described in **Chapter 5**. It investigates the potential of hydrophilic membranes based on sulfonated poly (ether ether ketone) for the controlled humidification of gas streams using the temperature and gas flow rate as tools to tune and control the relative humidity. Membrane assisted gas humidification integrates purification and humidification in one single step. The proposed membrane material allows the passage of water only, while most of the contaminations are retained.

Water vapor fluxes up to 11 kg/m$^2$·h could be obtained and relative humidities ranging from 40 up to 100% could be realized with a single hollow fiber membrane coated with a dense layer of S-PEEK. The water vapor flux increases with increasing nitrogen flow rate and increasing temperature of the liquid water. The overall membrane resistance is five orders of magnitude higher than the resistance at the permeate side and mainly governs the humidification process. The results proof that membrane assisted gas humidification is a promising alternative for conventional humidification methods.

**Chapter 6** finally, investigates the potential of the highly hydrophilic polymer sulfonated poly (ether ether ketone) to form porous morphologies. The effect of the type of non-solvent and the composition of the coagulation bath as a method to tune the morphology of these highly hydrophilic structures is investigated. The preparation of these highly hydrophilic porous structures offers an important tool for the production of low fouling membranes for e.g. drinking water applications.

## *Outlook*

# Simultaneous flue gas dehydration and carbon dioxide (CO$_2$) capture

Jens Potreck, Jeroen Jansen, Joop van der Linden, Kitty Nijmeijer, Matthias Wessling

## Introduction

The capture of CO$_2$ from large emission sources is a tremendous scientific and technological challenge, which since Kyoto receives significant attention from scientists [1, 2], the industry, policy makers and the society [3-6]. The current worldwide emission of CO$_2$ is estimated to be more than $20 \cdot 10^9$ tonnes per year and a further increase is foreseen for the next decades (Figure 1) [3, 7].
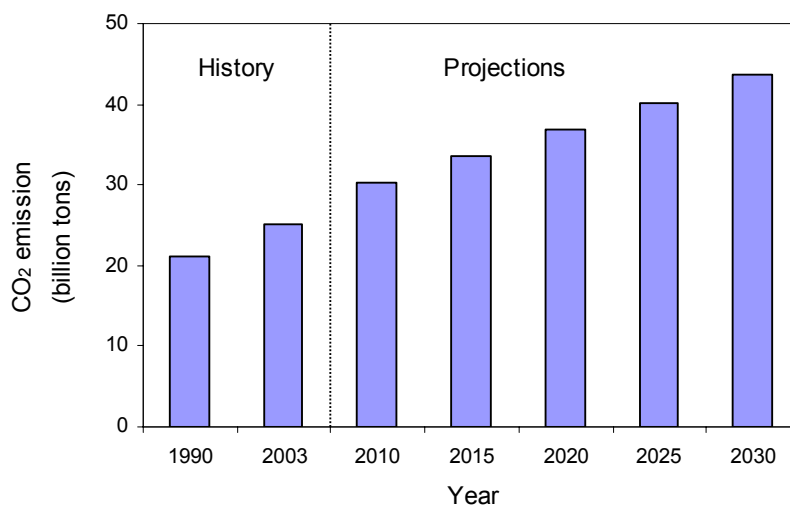


**Figure 1**: (Expected) total worldwide carbon dioxide emissions [7].

Carbon dioxide is one of the most important greenhouse gases in the atmosphere and as such supposed to be one of the main contributors to global warming and climate change. The industrial emission of large amounts of CO$_2$ is considered as one of the major sources for that. Most of the human emissions of carbon dioxide result primarily from the

combustion of (fossil) fuels for energy. Another important source of $CO_2$ can be found in the exploration of natural gas fields, making the capture of $CO_2$ from natural gas an important separation as well. Together the power and industry sectors dominate the current global $CO_2$ emission and together account for approximately 60% of the total $CO_2$ emissions [3].

To limit the effect of $CO_2$, national governments and international organizations have set stringent targets for $CO_2$ emission in the near future. The European Union sets a target of 20% reduction of $CO_2$ emissions in 2020 [5], whereas the Dutch government even aims to reduce the national $CO_2$ emissions with at least 30% in 2020 [6].

Fossil fuels are currently the dominant source of energy (86%) and are expected to dominate the global energy market in the near future as well [7]. One of the disadvantages of the use of fossil fuels to produce electricity is the generation of tremendous amounts of flue gasses. These gasses consist mostly of nitrogen (72 vol.%), but also contain significant amounts of carbon dioxide (14 vol.%) and water vapor (11 vol.%) [8].

Traditional methods to remove $CO_2$ from gas streams frequently use ad- or absorption processes mostly based on amine technology. Although applied on a very large industrial scale worldwide, amine technology has several disadvantages which mainly include the low oxidative stability of the amine based absorption liquid and the regeneration step (desorption), which consumes tremendous amounts of energy and results in high losses of the absorption liquid due to evaporation. Amine technology is currently mostly used for the treatment of natural gas streams with general higher concentrations of $CO_2$. Currently no cost effective technology applied on an industrial scale for the removal of $CO_2$ from flue gases from fossil fuel fired power plants exists. Membrane technology is a very attractive alternative for the removal of $CO_2$ from flue gases:  it is an energy efficient process, it has a small footprint, it is easy to scale up, to implement and to operate, and it is reliable (no moving parts). Recently, we presented the technical feasibility of flue gas dehydration [8]: composite membranes with a selective layer of S-PEEK operated for about a year in a flue gas stack. This technical demonstration makes the vision of membranes operating in flue gas for carbon dioxide capture viable. In the following, the

performance of the two materials studied in this thesis will also be analyzed with respect to their $CO_2/N_2$ separation performance.

## Segmented block-copolymer PEBAX

PEBAX® as membrane material has an extremely high water vapor permeability, but has a high potential for the removal of $CO_2$ as well, due to the high affinity of the soft PEO segments in PEBAX® for $CO_2$, as already described in literature [9-13].
To further improve its performance for $CO_2$ capture, additives that enhance the transport of $CO_2$ and/or the selectivity of the process could be added resulting in mixed matrix membranes with improved performance for $CO_2$ capture. This outlook focuses primarily on the simultaneous removal of water vapor and carbon dioxide from flue gases with PEBAX® based membranes and evaluates the potential of aminated dendrimeric additive (PAMAM) and multi wall carbon nano tubes as additive to enhance the carbon dioxide permeability and increase the carbon dioxide over nitrogen selectivity of the membranes.

The matrix membrane material used in this outlook is PEBAX® 1074, a commercially available, hydrophilic, PEO based block copolymer described in detail in Chapter 4 of this thesis. 1 wt.% multi wall carbon nano tubes (MWNT) or 1 wt.% PAMAM, a hyper branched dendrimeric structure is used as additive to increase the $CO_2$ capture ability of the polymer. The nano tubes, presented schematically in Figure 2, are produced by catalytic carbon vapor deposition with a catalyst containing 2.5 wt.% iron and 2.5 wt.% cobalt on an alumina support and are kindly provided by Facultés Universitaires Notre Dame de la Paix, Namur, Belgium. The dendrimeric polymer PAMAM (poly amido amine) is a hyper branched poly amide polymer purchased from Aldrich, Germany. The structure of PAMAM is schematically depicted in Figure 3.
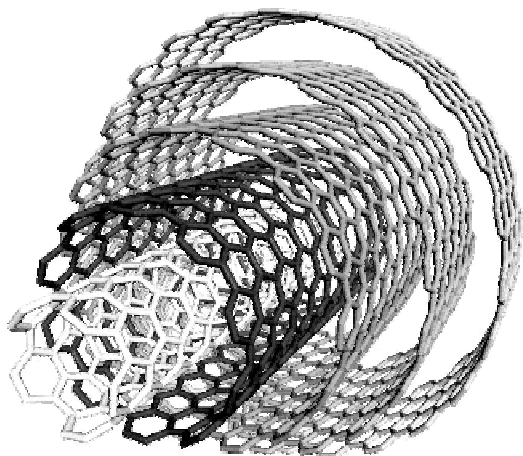
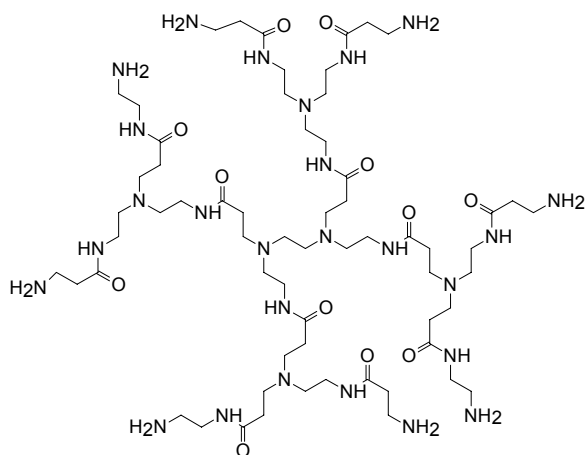**Figure 2:** Schematical representation of a multi wall carbon nano tube [14].



**Figure 3:** Structure of the dendrimeric polymer PAMAM [15].

## Experimental

PEBAX® 1074 was used as matrix membrane material for membrane preparation. To prepare the membranes, 7 wt.-% of PEBAX® 1074 was dissolved in N-methyl-2-pyrrolidone (NMP, purchased from Acros Organics) at 100°C. After dissolution of the polymer, 1 wt.% of either PAMAM or MWNT was added. PAMAM dissolved in hot NMP while the MWNT formed a dispersion with the dissolved PEBAX® and the NMP. Both solutions were stirred extensively to dispense the additives in the solution. The hot solution was cast on a preheated glass plate (80°C) with a 0.47-mm casting knife. The solvent was evaporated under nitrogen atmosphere and subsequently the membranes were

placed in a nitrogen oven at 80°C for one week to remove any residual solvent. After that the membranes were removed from the glass plate with water and subsequently washed with water for another three days. Finally, the membranes were stored in a vacuum oven at 30°C. Membranes were used when no further mass decrease in time was observed (~14 days). The thickness of the membranes with 1 wt.% PAMAM was 46 μm, while the membranes with 1 wt.% MWNT had a thickness of 51 μm.

The gas and water vapor permeabilities were all measured at 50°C and water vapor activities in the range of 0.4-0.98, according to the procedure earlier described in literature [8, 16, 17]. The measured data are obtained from binary mixtures of either water vapor and nitrogen or water vapor and carbon dioxide resulting in mixed gas selectivities for water vapor over nitrogen or carbon dioxide, but ideal selectivities of carbon dioxide over nitrogen.

Figure 4 shows the water vapor permeability as a function of the water vapor activity measured at 50°C of the PEBAX® membranes without additive and the corresponding values for the membranes with 1 wt.% PAMAM or 1 wt.% MWNT as additive.
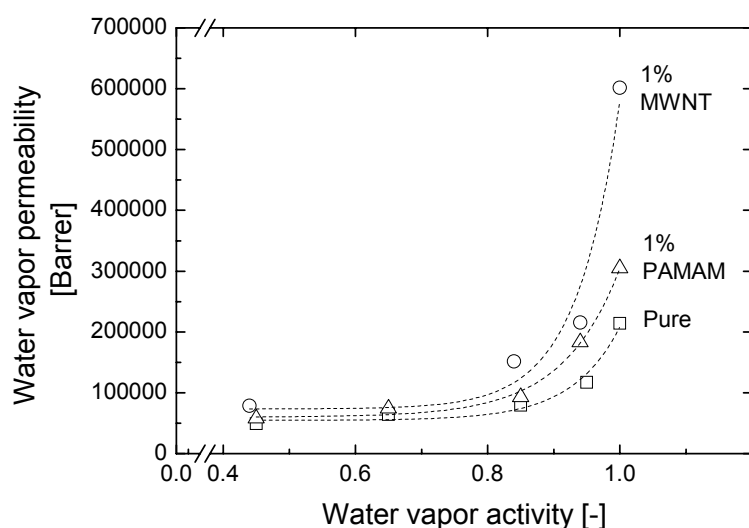


**Figure 4:** Water vapor permeability versus the water vapor activity at 50°C for pristine PEBAX® membranes and for PEBAX® membranes containing 1 wt.% MWNT or 1 wt.% PAMAM as additive.

The water vapor permeability increases exponentially for all three membranes with increasing water vapor activity, due to the increase in water vapor solubility with increasing water vapor activity as shown in Chapter 4 of this thesis.

Both modified membranes show higher water vapor permeabilities than the pure PEBAX® membranes. PEBAX® with PAMAM shows an increase in permeability to 300.000 Barrer while PEBAX® with MWNT shows a tremendous increase in permeability up to a value of 600.000 Barrer for a water vapor activity of 0.98. We hypothesize that the increase in permeability can be attributed to an increase in hydrophilicity or a decrease in crystallinity of PEBAX® due to the addition of the additives, but this requires further research to understand the fundamentals behind it.

The carbon dioxide permeability as a function of the water vapor activity for the three membranes is shown in Figure 5.
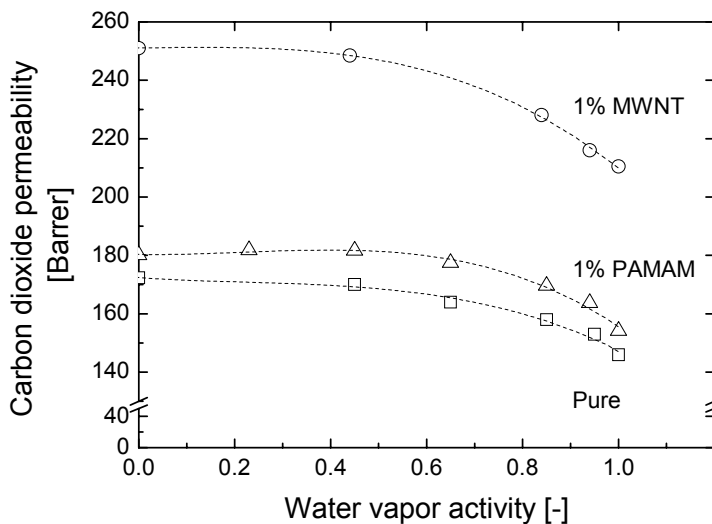


**Figure 5:** Carbon dioxide permeability as a function of the water vapor activity at 50°C for pristine PEBAX® membranes and membranes with 1 wt.% MWNT or PAMAM as additive.

The carbon dioxide permeability decreases with increasing water vapor activity (similar behavior was found for $N_2$) most probably due to a lower solubility of the gas in the

water swollen polymer than in the dry polymer as described earlier in Chapter 4 of this thesis. The carbon dioxide permeability increases slightly when 1 wt.% PAMAM is used as additive. A reason could be a slight contribution of facilitated transport of carbon dioxide through the presence of the amine groups in PAMAM, as also reported in literature [18-20]. The addition of MWNT on the other hand results in a significant increase in $CO_2$ permeability. This may be due to a decrease in crystallinity in PEBAX$^{®}$ because the permeability of all components in the feed mixture is increased by the addition of MWNT, but this requires further research for verification and to fully understand the changes in transport behavior shown here. Focus should be mainly on increasing the amount of amine groups either by increasing the amount of PAMAM or by using other generations of PAMAM with higher amine densities to enhance facilitated transport of $CO_2$.

Figure 6a shows the ideal $CO_2$ over $N_2$ selectivity as calculated from the binary measurements ($H_2O$-$CO_2$ and $H_2O$-$N_2$) and Figure 6b presents the real, mixed gas $H_2O$ over $N_2$ selectivity as calculated from a binary feed mixture for pristine PEBAX$^{®}$ membranes and for membranes with 1 wt.% MWNT or PAMAM as additive.
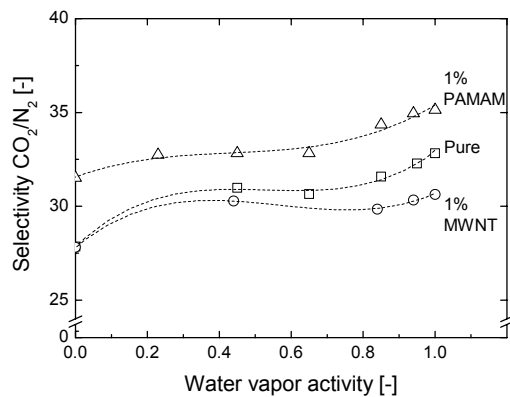
**Figure 6a:** Ideal $CO_2$ over $N_2$ selectivity as calculated from the binary measurements ($H_2O$-$CO_2$ and $H_2O$-$N_2$) as a function of the water vapor activity at 50°C for pristine PEBAX® membranes and for membranes with 1 wt.% MWNT or PAMAM as additive.

**Figure 6b:** Mixed gas $H_2O$ over $N_2$ selectivity as calculated from a binary feed mixture as a function of the water vapor activity at 50°C for pristine PEBAX® membranes and for membranes with 1 wt.% MWNT or PAMAM as additive
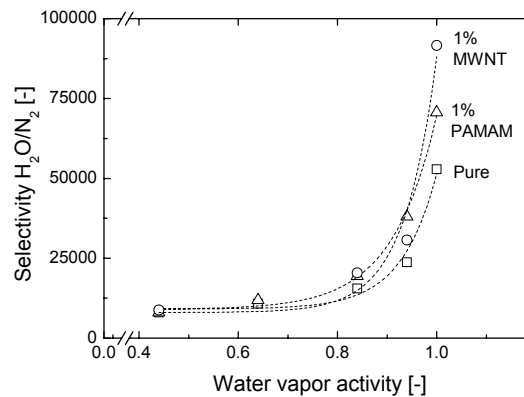
Compared to the pure PEBAX® membranes, the carbon dioxide over nitrogen selectivity increases for PEBAX® with PAMAM as additive, while it decreases for PEBAX® with MWNT. The increase in carbon dioxide over nitrogen selectivity for PEBAX with PAMAM is caused by its higher carbon dioxide permeability, most probably due to the occurrence of facilitated transport for carbon dioxide only [19] while the transport of nitrogen is not influenced. MWNT as additive to PEBAX® decrease the selectivity of carbon dioxide over nitrogen due to the non selective increase in the permeability of all gases upon addition of MWNT.

The water vapor over nitrogen selectivity increases with increasing water vapor activity due to an increase in water vapor permeability and only a slight decrease in nitrogen permeability with increasing water vapor activity. This increase in selectivity is even more pronounced for the membranes with the additives due to the even stronger increase in water vapor permeability in these materials.

# Sulfonated poly ether ether ketone (S-PEEK)

So far all measurements were performed for binary systems (e.g. $N_2$ and water vapor or $CO_2$ and water vapor), whereas flue gas contains significant amounts of all three components, i.e. ~ 72 vol.% nitrogen, ~11 vol.% of water vapor and ~14 vol.% carbon dioxide [8]. The presence of one component in a gas mixture can have a significant effect on the permeation behavior of the other components. Performance results extracted from binary systems do not always resemble the performance obtained with ternary systems, and significant differences between the corresponding values for permeability and selectivity can exist.

To investigate the effect of the presence of a third component on the performance of sulfonated poly (ether ether ketone) membranes, both binary and ternary gas mixtures were used and the results are compared. Measurements were performed using the same system and procedure as described earlier in this chapter for PEBAX membranes. Binary mixtures containing either $N_2$/water vapor or $CO_2$/water vapor and ternary mixtures containing $CO_2$ (10 vol.%)/ $N_2$ (90 vol.%)/water vapor were used as feed mixtures.

Table 1 compares the nitrogen and carbon dioxide permeability as obtained from binary and ternary gas mixtures for dense sulfonated poly ether ether ketone membranes as a function of the water vapor activity (only values for a = 0.9 and 0.98 are presented). Also the ideal, hypothetical $CO_2/N_2$ selectivities as calculated from the measurements with binary systems and the real, experimentally determined selectivities for ternary mixtures are presented.

**Table 1:** Nitrogen and carbon dioxide permeability, carbon dioxide over nitrogen selectivity for S-PEEK measured using a binary ($N_2$/$H_2O$, $CO_2$/$H_2O$) gas/water vapor mixture and a ternary ($CO_2$ (10 vol.%)/$N_2$ (90 vol.%)/$H_2O$) gas/water vapor mixture at 50° and 2.5 bar for a water vapor activity of 0.9 and 0.98.

| | | Binary mixture | Ternary mixture | Water vapor activity |
|---|---|---|---|---|
| Permeability (Barrer) | $N_2$ | 0.04 | 0.21 | 0.9 |
| | | 0.06 | 0.48 | 0.98 |
| | $CO_2$ | 11.49 | 11.99 | 0.9 |
| | | 19.89 | 23.47 | 0.98 |
| Selectivity (-) | $CO_2$/$N_2$ | 287 | 57 | 0.9 |
| | | 332 | 49 | 0.98 |

Especially the nitrogen permeability is significantly influenced by the presence of $CO_2$. The ternary permeability values are 6 to 8 times higher than the values obtained for binary systems. The $CO_2$ permeability is only very slightly changed due to the presence of the other components. As a result, the ideal, hypothetical $CO_2$/$N_2$ selectivity is much higher than the real, experimentally determined selectivity obtained for the ternary system. Based on binary mixtures, extremely high $CO_2$/$N_2$ selectivities would have been predicted, while in practice, $CO_2$/$N_2$ selectivities of ~50 at water vapor activities of 0.9-0.98 can be obtained for ternary mixtures. Results from binary systems could be falsely interpreted in terms of performance for ternary systems. Nevertheless, the selectivity obtained for ternary mixtures is in this case still reasonable high, which shows the strong potential of sulfonated poly ether ether ketone as membrane material for both the dehydration of flue gases and the capture of $CO_2$, and opens many new directions for further research.

# References

1.      E. Favre, Carbon dioxide recovery from post-combustion processes: Can gas permeation membranes compete with absorption? Journal of Membrane Science 294 (2007) 50-59.

2.      C.E. Powell, G.G. Qiao, Polymeric $CO_2/N_2$ gas separation membranes for the capture of carbon dioxide from power plant flue gases, Journal of Membrane Science 279 (2006) 1-49.

3.      O. Davidson, B. Metz Special report on carbon dioxide capture and storage; Intergovernmental Panel on Climate Change: Geneva, Switzerland, (2005); www.ipcc.ch.

4.      A. Gore, An inconvenient truth, Rodale Press, USA (2006).

5.      www.europa.eu.

6.      www.vrom.nl.

7.      Energy Information Administration, International Energy Outlook 2006.

8.      H. Sijbesma, K. Nymeijer, R. van Marwijk, R. Heijboer, J. Potreck, M. Wessling, Flue gas dehydration using polymer membranes, Journal of Membrane Science 313 (2008) 263-276.

9.      V. Barbi, S.S. Funari, R. Gehrke, N. Scharnagl, N. Stribeck, SAXS and the gas transport in polyether-block-polyamide copolymer membranes, Macromolecules 36 (2003) 749-758.

10.     V.I. Bondar, B.D. Freeman, I. Pinnau, Gas sorption and characterization of poly(ether-b-amide) segmented block copolymers, Journal of Polymer Science Part B-Polymer Physics 37 (1999) 2463-2475.

11.     V.I. Bondar, B.D. Freeman, I. Pinnau, Gas transport properties of poly(ether-b-amide) segmented block copolymers, Journal of Polymer Science Part B-Polymer Physics 38 (2000) 2051-2062.

12.     J.H. Kim, S.Y. Ha, Y.M. Lee, Gas permeation of poly(amide-6-b-ethylene oxide) copolymer, Journal of Membrane Science 190 (2001) 179-193.

13.     J.H. Kim, Y.M. Lee, Gas permeation properties of poly(amide-6-b-ethylene oxide)-silica hybrid membranes, Journal of Membrane Science 193 (2001) 209-255.

145

14.   www.ulb.ac.be/sciences/cpmct/researches.htm.

15.   www.aldrich.com.

16.   S. Metz, W. van de Ven, J. Potreck, M. Mulder, M. Wessling, Transport of water vapor and inert gas mixtures through highly selective and highly permeable polymer membranes, Journal of Membrane Science 251 (2005) 29-41.

17.   S.J. Metz, W.J.C. van de Ven, M.H.V. Mulder, M. Wessling, Mixed gas water vapor/$N_2$ transport in poly(ethylene oxide) poly(butylene terephthalate) block copolymers, Journal of Membrane Science 266 (2005) 51-61.

18.   L. Deng, T. Kim, M. Hägg, PVA/PVAm blend FSC membrane for $CO_2$-capture, Desalination 199 (2006) 523-524.

19.   T. Kim, B. Li, M. Hägg, Novel fixed-site-carrier polyvinylamine membrane for carbon dioxide capture, Journal of Polymer Science Part B-Polymer Physics 42 (2004) 4326-4336.

20.   J. Shen, L. Wu, D. Wang, C. Gao, Sorption behavior and separation performance of novel facilitated transport membranes for $CO_2/CH_4$ mixtures, Desalination 223 (2008) 425-437.

# Summary

Fossil fuel fired power plants produce electricity and in addition to that large volume flows of flue gas, which mainly contain $N_2$, $O_2$, and $CO_2$, but also large quantities of water vapor. To prevent condensation of the water vapor present in this flue gas stream, water needs to be removed before emission to the atmosphere. Commercial dehydration processes such as the use of a condenser or a desiccant system have several disadvantages and membrane technology is an attractive, energy efficient alternative for dehydration of gas streams.

The work presented in this thesis focuses on the characterization of the molecular gas and water vapor transport properties of two different types of polymeric membranes. The fundamental understanding of water vapor and gas transport phenomena through these materials is particularly interesting since both materials are different in their chemistry and physical state:

- PEBAX$^®$ is a block copolymer which shows molecular transport through the soft polyethylene oxide based rubbery phase.
- S-PEEK (sulfonated poly ether ether ketone) shows molecular transport through an amorphous glassy phase with ionic groups present which will preferentially be hydrated over the apolar matrix.

The two polymeric systems vary strongly in relation to polymer/vapor interactions, relaxation phenomena, and separation performance of the membranes.

Because it is known that the sorption of penetrant molecules in a glassy polymer can induce strong plasticization effects, the first part of this thesis analyzes the kinetic sorption behavior of water vapor in S-PEEK films. Sorption isotherms are determined experimentally using a gravimetric sorption balance and the relative contributions of Fickian diffusion and relaxational phenomena are quantified as a function of the water concentration in the polymer using the model of Hopfenberg and Berens. Both, Fickian diffusion on a short time scale, and also long time relaxations can be observed already at

very low water vapor concentrations. Penetrant sorption induces a depression of the glass transition temperature of the polymer. The diffusion coefficient increases over two orders of magnitude with increasing water vapor concentration. Taking also the diffusion coefficient for liquid water into account, it reveals a change of even three orders of magnitude.

The second part of this work presents a thermodynamic analysis of the sorption of water vapor in the two polymers as a function of the temperature. The thermodynamic approach presented offers a strong method to distinguish between enthalpic and entropic contributions of water vapor sorption. It allows to explain the nature of water sorption in both polymers and to address the state of water in the polymer. The results are discussed in relation to water clustering phenomena and the thermodynamics of water vapor sorption in liquid water (self-solvation of water).

Analysis of water vapor sorption in the two polymers shows that the Gibbs energy and the enthalpy of water sorption are negative, i.e. the sorption process is exothermic. The results suggest that in PEBAX$^®$ additional sorbed water molecules experience a water-like environment, whereas in S-PEEK the polymer-water interactions prevail. The entropy of water sorption for both polymers is negative over the full range of water vapor activities (sorption is entropically unfavorable). For S-PEEK, water sorption is governed by enthalpy-entropy compensation. In the case of PEBAX$^®$ enthalpy-entropy compensation is observed at lower activities only. At higher water vapor activities, the more favorable Gibbs energy of water sorption in PEBAX$^®$ is driven by the entropy.


In the next part of this thesis the transport of water vapor and gas through the rubbery polymer PEBAX$^®$ membrane is investigated to evaluate the potential of PEBAX$^®$ as a candidate for flue gas dehydration of coal fired thermal power plants. The permeability of water vapor and gas through PEBAX$^®$ is measured simultaneously (binary nitrogen/water vapor feed) as a function of the temperature to investigate the effect of the presence of water vapor on the transport of gas. The water vapor permeability increases exponentially with increasing water vapor activity whereas the nitrogen permeability slightly decreases with increasing water vapor activity. Consequently, the water over nitrogen selectivity increases with increasing water vapor activity. Water vapor sorption isotherms in

PEBAX[®] represent Flory-Huggins type of sorption and the highly hydrophilic nature of the block copolymer results in high amounts of absorbed water. When taking into account the swelling of the polymer due to water vapor sorption, the Fickian diffusion coefficient increases over the full activity range and changes over two orders of magnitude. The results not only show the high potential for PEBAX[®] as dehydration membranes, but offers attractive routes to the integration of simultaneous dehydration and $CO_2$ capture, because of a high affinity of PEBAX[®] with $CO_2$.

Hydrophilic polymers are not only attractive for the dehydration of gas streams but also have potential as membrane material for the opposite process, i.e. the controlled humidification of gas streams, where the temperature and gas flow rate can be used as tools to tune and control the relative humidity. The proposed membrane material (S-PEEK) allows the passage of water only, while most of the contaminations are retained. As such, membrane assisted gas humidification integrates purification and humidification in one single step. Relative humidities ranging from 40 up to 100% could be realized with a single hollow fiber membrane coated with a dense layer of S-PEEK. The water vapor flux increases with increasing nitrogen flow rate and increasing temperature of the liquid water. The overall membrane resistance is five orders of magnitude higher than the resistance at the permeate side and mainly governs the humidification process. The results prove that membrane assisted gas humidification is a promising alternative for conventional humidification methods.

At the end of this work a method to create porous morphologies from S-PEEK is presented. Coagulation of the polymer in common non-solvents such as water is impossible since the material does not solidify sufficiently, but forms a gel. We discovered that concentrated electrolyte solutions however are very effective as precipitation medium. Porous structures could be obtained after coagulation of the polymer in concentrated $HNO_3$, which could be explained from the stronger protonating effect of $HNO_3$ than of the sulfonic acid group. Macro void formation was successfully suppressed by the addition of solvent (NMP) to the non-solvent ($HNO_3$), which delays the demixing of the polymer and the solvent. The use of a coagulating medium with a high ionic strength shields the fixed charges of the sulfonated polymer and induces phase separation as well. The preparation of the highly hydrophilic porous structures presented

in this work offers a new direction for the production of low fouling membranes for e.g. micro and ultra filtration.

Finally the use of additives (dendrimers and carbon nano tubes) in the two hydrophilic polymers (S-PEEK and PEBAX$^{®}$) as a route to enhance the performance of the membranes for the simultaneous removal of water vapor and the capture of $CO_2$ from flue gases is explored. The results show that the water vapor permeability and the water vapor over gas selectivity can be even further increased by the addition of only small amounts specific additives. For S-PEEK membranes also the performance using ternary (water vapor/$CO_2$(10 vol.%)/$N_2$(90 vol.%)) instead of binary (water vapor/$CO_2$ or water vapor/$N_2$) gas mixtures is investigated. These measurements show that the $CO_2$ permeability is only very slightly influenced by the presence of the other components, while the nitrogen permeability for the ternary system is much higher. As a result, the selectivity obtained for the ternary system is significantly lower than the ideal, hypothetical $CO_2/N_2$ selectivity as calculated from binary measurements. Nevertheless the results show the strong potential of sulfonated poly ether ether ketone as membrane material for both, the dehydration of flue gases and the capture of $CO_2$, and opens many new directions for further research.

# Samenvatting

Energiecentrales die gebruik maken van fossiele brandstoffen produceren naast electriciteit ook grote volumes rookgas die voornamelijk bestaat uit $N_2$, $O_2$ en $CO_2$, maar ook grote hoeveelheden waterdamp. Om te voorkomen dat de aanwezige waterdamp in de rookgasstroom condenseert, moet deze verwijderd worden voordat het in contact komt met de atmosfeer. Commerciële ontwateringsprocessen, zoals het gebruik van een condenser, hebben zwaarwegende nadelen. Membraantechnologie daarentegen is een aantrekkelijk, energie-efficiënt alternatief voor gasstromen.

Het werk gepresenteerd in dit proefschrift is gericht op de karakterisatie van moleculair gas- en watertransport eigenschappen van twee verschillende types polymeer membranen. Het fundamentele begrip van waterdamp en gastransport fenomenen door deze materialen zijn vooral interessant omdat de chemie en fysische staat van beide materialen anders zijn:

- PEBAX® is een blok-copolymeer waarbij transport plaatsvindt door de zachte polyetheenoxide-gebaseerde rubberfase
- S-PEEK (gesulfoneerde poly ether ether keton) laat transport zien door een amorfe glasachtige fase met ionische groepen: deze zullen eerder gehydrateerd worden dan de apolaire matrix.

De polymeer/damp interacties, relaxatie fenomenen en scheidingsprestaties van de membranen variëren sterk tussen de twee polymeersystemen.

Omdat het bekend is dat de sorptie van de penetrerende moleculen in een glasachtig polymeer sterke plasticerende effecten tot gevolg kunnen hebben, wordt in het eerste deel van dit proefschrift een onderzoek beschreven naar het kinetisch sorptie gedrag van waterdamp in S-PEEK films. Sorptie isothermen zijn experimenteel bepaald gebruik makend van een gravimetrische sorptie balans. De relatieve bijdragen van Fick's diffusie en relaxatie fenomenen zijn gekwantificeerd als functie van water concentratie in het polymeer door het model van Hopfenberg en Berens te gebruiken. Zowel Fick's diffusie

op korte tijdsschaal en lange termijn relaxaties werden waargenomen bij erg lage waterdampconcentraties. Sorptie van een penetrant veroorzaakt een depressie in de glasovergangtemperatuur van het polymeer. De diffusiecoëfficiënt stijgt met twee orders van grootte bij toenemende waterdampconcentratie. Als de diffusiecoëfficiënt voor vloeistoffen in water ook wordt beschouwd, blijkt er zelfs een verandering van drie orders van grootte te zijn.

Het tweede deel van dit werk presenteert een thermodynamische analyse van waterdamp sorptie in de twee polymeren als functie van de temperatuur. De gepresenteerde thermodynamische benadering bleek een sterke methode om de enthalpische en entropische bijdragen van waterdamp sorptie te onderscheiden. Het is in staat om de aard van water sorptie in beide polymeren te verklaren en om de staat van water in het polymeer te benoemen. De resultaten worden bediscussieerd in relatie tot water clustering fenomenen en de thermodynamica van waterdamp sorptie in vloeibaar water (self-solvation van water).

Analyse van waterdamp sorptie in de twee polymeren laat zien dat de Gibbs energie en enthalpie van water sorptie negatief zijn. Dit wil zeggen dat het sorptie process exotherm is. De resultaten suggereren dat in PEBAX® extra geabsorbeerd water een waterachtige omgeving waarneemt, terwijl in S-PEEK de polymeer-water interacties overheersen. De water sorptie entropie voor beide polymeren is negatief voor de hele reeks van waterdamp activiteiten (sorptie is entropisch ongunstig). Voor S-PEEK wordt water sorptie beheerst door enthalpie-entropie compensatie. In het geval van PEBAX® wordt alleen bij lagere activiteit enthalpie-entropie compensatie waargenomen. Bij hogere activiteiten wordt de gunstige Gibbs energie voor water sorptie veroorzaakt door de entropie.

In het volgende deel van dit proefschrift is het transport van waterdamp en gas door het rubberachtige PEBAX® membraan onderzocht om het potentieel van PEBAX® als kandidaat te onderzoeken voor ontwatering van rookgas van koolgestookte thermische energiecentrales. Om het effect van de aanwezigheid van water op het transportgedrag van gas te onderzoeken, is de permeabiliteit van waterdamp en gas door PEBAX® tegelijkertijd gemeten als functie van de temperatuur (de voeding is een mengsel van

stikstof en waterdamp). De waterdamp permeabiliteit stijgt exponentieel bij toenemende waterdamp activiteit terwijl de stikstof permeabiliteit slechts lichtelijk afneemt bij toenemende waterdamp activiteit. Hierdoor stijgt de selectiviteit van water ten opzichte van stikstof bij toenemende waterdamp activiteit. De waterdamp sorptie isothermen in PEBAX® laten een Flory-Huggins-achtige sorptie zien en de zeer hydrofiele aard van het blok-copolymeer resulteert in grote hoeveelheden geabsorbeerd water. Als de zwelling van het polymeer door waterdamp sorptie wordt meegenomen, stijgt de Fick's diffusie coëfficiënt voor het gehele activiteit bereik en het verandert twee orders van grootte. De resultaten laten niet alleen de grote potentie zien van PEBAX® als ontwateringsmembranen, maar bieden ook aantrekkelijke routes naar de integratie van gelijktijdige ontwatering en $CO_2$ afvang, door de hoge affiniteit van PEBAX® met $CO_2$.

Hydrofiele polymeren zijn niet alleen aantrekkelijk voor ontwateren van gasstromen, maar hebben ook potentieel als membraanmateriaal voor het omgekeerde proces, het gecontroleerde bevochtiging van gasstromen, waarbij de temperatuur en gasstroomsnelheid gebruikt kunnen worden om de relatieve vochtigheid te regelen en te controleren. Het voorgestelde membraanmateriaal (S-PEEK) staat alleen het passeren van water toe, terwijl de meeste verontreinigingen tegengehouden worden. Zodoende wordt membraan geassisteerde gasbevochtiging geïntegreerd met purificatie in één enkele stap. Relatieve vochtigheden, variërend van 40 tot 100%, kunnen gerealiseerd worden met een enkele holle vezel membraan gecoat met een dichte laag S-PEEK. De waterdamp flux stijgt met toenemende stikstof stroomsnelheid en toenemende temperatuur van het vloeibare water. De overall membraanweerstand is vijf orders van grootte hoger dan de weerstand aan de permeaat zijde en bepaalt voornamelijk het bevochtigingsproces. De resultaten bewijzen dat membraan geassisteerde gasbevochtiging een veelbelovend alternatief is voor conventionele bevochtigingsmethoden.

Aan het eind van dit werk wordt een methode gepresenteerd om poreuze morfologiën te maken van S-PEEK. Coagulatie van het polymeer in gebruikelijke niet-oplosmiddelen zoals water is onmogelijk omdat het materiaal niet voldoende solidificeert, maar een gel vormt. Wij ontdekten echter dat geconcentreerde electrolietoplossingen erg effectief zijn als precipitatie media. Poreuze structuren konden verkregen worden na coagulatie in geconcentreerd $HNO_3$. Dit kan verklaard worden door een sterker protonerend effect van

$HNO_3$ in vergelijking tot de sulfonzuurgroep. Macrovoid vorming kon succesvol onderdrukt worden door een oplosmiddel (NMP) bij het niet-oplosmiddel ($HNO_3$) te voegen, waardoor het ontmengen van het polymeer en het oplosmiddel vertraagd werd. Het gebruik van een coagulatiemedium met een hoge ionische sterkte schermt de gefixeerde lading af van het gesulfoneerde polymeer en veroorzaakt tevens fasescheiding. De bereiding van de zeer hydrofiele poreuze structuren gepresenteerd in dit werk biedt een nieuwe richting aan voor de productie van 'low-fouling' membranen voor bijvoorbeeld micro- en ultrafiltratie.

Als laatste is het gebruik van additieven (dendrimeren en carbon-nanotubes) onderzocht in de twee hydrofiele polymeren (S-PEEK en PEBAX®) als een route om de prestatie van de membranen voor gelijktijdige verwijdering van waterdamp en $CO_2$ van rookgassen. De resultaten laten zien dat de waterdamp permeabiliteit en de waterdamp tot gas selectiviteit verder kan toenemen door de toevoeging van slechts kleine hoeveelheden specifieke additieven. Voor S-PEEK membranen is ook de prestatie onderzocht voor ternaire (waterdamp/$CO_2$ (10 vol.%)/$N_2$ (90 vol.%)) in plaats van binaire (waterdamp/$CO_2$ of waterdamp/$N_2$) gasmengsels. Deze metingen laten zien dat de $CO_2$ permeabiliteit slechts in beperkte mate beïnvloedt wordt door de aanwezigheid van andere componenten, terwijl de stikstof permeabiliteit voor het ternaire systeem veel hoger is. Hierdoor is een selectiviteit verkregen voor het ternaire systeem die significant lager is dan de ideale, hypothetische $CO_2/N_2$ selectiviteit die berekend is uit binaire metingen. Desondanks laten de resultaten zien dat gesulfoneerd poly ether ether keton een veelbelovend membraan materiaal is voor zowel ontwatering van rookgassen als ook de afvang van $CO_2$. Ook opent het vele nieuwe richtingen voor verder onderzoek.

# Danksagung

Now, after four and a half year working on my doctoral thesis it is time to say Thank You to a lot of people, who participated in this interesting but often not easy period of my life. I know it is always a problem to name people personally, because for sure I will forget some people who also attended this work. That is why first I want to thank everybody who participated in the last 4.5 years in any content to this doctoral thesis.

I want to say thanks first to Prof. Dr. Ing. Matthias Wessling. Matthias, thanks a lot for your trust in my work and for offering me this interesting and encouraging project to write my doctoral thesis.

Furthermore, I want to say thank you to my direct supervisors. The first half of my Ph.D. thesis was supervised by Dr. Dimitris Stamatialis, while the second part was supervised by my assistend promoter Dr. Kitty Nijmeijer. Dimitris, thank you for guiding me through the first two years of my Ph.D. thesis, thank you for all the fruitful and nice discussions about transport phenomena of mostly water vapor in membranes. Kitty, this work would surely not have been finished without your support. Thanks a lot for your supporting and encouraging help, for the nice words and for the scientific discussions, which leaded this work to success. I will never forget your words: Jens, alles komt goed aan het eind. I was not always sure, that everything will be fine at the end, but you were sure and this helped me a lot to finish this work.

One other extremely helpful and friendly colleague which I want to thank is Greet, the secretary of the Membrane Technology Group. Greet, you always made time, even if time was very rare, for the problems I had to solve during my Ph.D. thesis. All the paper work and the organization things went so perfectly because of your encouragement. Thanks a lot, Greet!

Many people were involved in the work of my Ph.D. thesis. First of all I want to mention Sybrand Metz, who convinced me, that Membrane Technology is a wonderful field to write my Ph.D. thesis. I want to thank my project colleagues Hylke Sijbesma and Sander Reijerkerk for the scientific as well as for the collegial cooperation. Thanks especially to Sander for the great planning of the NanoGLOWA trips.

Furthermore, a lot of students helped me with this work and without their help many things could not have been realized.

I want to thank Fuat Uyar, who wrote his Master thesis in our project. Fuat thanks a lot for the interesting results in water vapor sorption kinetics and S-PEEK production mainly shown in Chapter 2 of this work.

I want to thank Thomas Kosinski, who did his "Praxissemester" in our project. Thomas thanks a lot for the work on simultaneous water vapor and nitrogen permeation described in Chapter 4 of this thesis and the wonderful porous morphologies from S-PEEK described in Chapter 6 of this thesis.

Also I want to thank Willem-Jan van Dijk, who did his Bachelor thesis in our project. Willem-Jan, although your work is not explicitly mentioned in the chapters of this thesis, building the simultaneous permeation set up was extremely helpful for my Ph.D. thesis. Without building the set up and testing it, all the simultaneous permeation data could not have been measured.

I want to thank Marcel ten Hove, who did his Bachelor thesis in our project. Marcel thanks a lot for the preparation of the composite S-PEEK/PES membranes and the very interesting results on membrane assisted gas humidification presented in Chapter 5 of this thesis.

Last but not least I want to thank Jeroen Jansen and Joop van der Linden, who did their Bachelor thesis in our project. The work on the simultaneous permeation of water vapor and $CO_2$ is presented in the Outlook of this thesis and has to be further investigated.

The research project for my Ph.D. thesis was financed with a grant of the Dutch EET program and in addition it was financed by the European Union as part of the FP6 project NanoGLOWA (NMP 3-CT-1007-026735). I want to thank Rob Heijboer and Rob van Marwijk from KEMA for the fruitful discussions and for providing technical information about power plants during the EET project. And I want to thank Paul Raats from KEMA for the excellent project coordination of the NanoGLOWA project. Furthermore, I want to thank all the partners of both mentioned projects for the fruitful cooperation.

I also want to thank all my commission members: Prof. Favre, Prof. Engbersen and Dr. Brilman, but especially Dr. Nico van der Vegt for the support in Chapter 3 of this thesis and for the interesting and enthusiastic discussion about thermodynamics.

Working on my Ph.D. thesis did not only bring a deeper scientific background in membrane science for me, but as well new good friends. These friends came always together during the coffee- and lunch breaks mainly opened by somebody who called 'Rauchen'. Thank you guys for the funny, refreshing and wonderful time we had during 'Rauchen' breaks. Especially I want to name here Maik, Jutta, Hakan, Joao, Matias, Katja and Can as the core members of the 'Rauchen' gang but also thanks to Dana and Jörg for their help and the nice discussions we had. I will never forget this wonderful time.

What would a Ph.D. work be without wonderful office colleagues? Nothing I would say. In the old days in Langezijds our office was unique I guess, because we were the only office with a wonderful theme. '1330, dat is prettig', indeed it was a nice time we had in Langezijds, thanks for that to Laura, Alisia, Bernke and Sander. Also thanks to my office colleagues in Meander: Paul, Sander and David. I think we had an enjoyable time.

Furthermore I want to thank John, Lydia and Marcel and all the other members of the Membrane Technology Group for their help and their friendship. The nice social events we had were always a great pleasure for me and will keep in my mind for ever, one example I want to state here was the men-trip to Düsseldorf, thanks to all the participants for this wonderful event.

Great thanks also to Dr. Erik Roesink, who gave me all the freedom to finish this doctoral thesis while starting already a new job at Norit/X-Flow. Also thanks to my new colleagues at Norit/X-Flow for the wonderful working atmosphere and the easy integration into the group. Wilco en Joris, bedankt voor het helpen met de Nederlandse samenvatting.

Auch möchte ich meinen Freunden außerhalb der Universität danken, die immer Zeit und ein offenes Ohr für mich hatten und auch Verständnis hatten, wenn ich selbst mal keine Zeit hatte. Obwohl es gefährlich ist hier Namen zu nennen, möchte ich es trotzdem tun aber bitte verzeiht mir, wenn ich jemanden vergesse. Danke an Ralf, Martina, Elisabeth, Sandra B., Sandra O. und meinen Kumpels vom Stammtisch Powerpils (Wolfgang, Daniel, Andre, Benedikt, Christian W., Christian U., Thomas, Tobias und Martin) sowie meinen Kollegen von Pfarrgemeinderat und Musikverein Alstätte. Ihr hattet immer Verständnis, wenn ich keine Zeit hatte, da ich am Schreibtisch saß um meine

# Curriculum vitae

Jens Potreck was born on 4th of September 1978 in Gronau/Westfalen Germany. He finished the Alexander-Hegius-Gymnasium Ahaus in 1998. After the civil service he started studying chemical engineering on the University of Applied Sciences Münster/Steinfurt in 1999 and finished his study in 2003 with a diploma in polymer technology. He did his diploma work at the company Profilan in Legden/Germany on the modification of high molecular weight polyethylene. After the graduation in 2003 he started at the University of Twente in the Membrane Technology Group as a technician. In 2004 he started as a Ph.D. student in the field of gas separation membranes for flue gas treatment in the Membrane Technology Group at the University of Twente. Since August 2008 he works at Norit/X-Flow in the R&D department.